Université du Québec
École de technologie supérieure

GREPCI

MODELING AND CONTROL OF THREE-PHASE RECTIFIERS, OPERATING WITH HIGH EFFICIENCY AND LOW HARMONIC DISTORSION: APPLICATION TO THE VIENNA RECTIFIER

Ph. D. SENTENCE PRESENTATION

By: Nesrine BelHadj Youssef, Ph. D. student

OUTLINE

1. AC/DC CONVERSION : HISTORY AND APPLICATIONS
2. POWER QUALITY: HARMONICS PROBLEMS
3. THREE-PHASE POWER FACTOR CORRECTION SWITCHED MODE RECTIFIERS
4. INTRODICTION OF THE VIENNA TOPOLOGY
5. MAIN SCOPES OF RESEARCH
   - **GENERAL METHODOLOGY OF DESIGN**
   - **MODELING AND EXPERIMENTAL MODEL VERIFICATION**
   - **POWER CONTROL OF THE RECTIFIER**
6. SYNTHESIS OF THE PROPOSED CONTROL TECHNIQUES
7. SENSORLESS CONTROL USING A NONLINEAR OBSERVER
8. CONCLUSION AND CONTRIBUTIONS

INTRODUCTION

- 60% of the electric energy, produced in Canada and the USA, transites by static power converters [Hess, 1998].

- AC/DC converters ensure the interface and the adaptation of the energy between the electric grid and the CC loads.

AC/DC CONVERTERS: HISTORY (1)

- Until the XXth century: use of electromechanical rectifier, particularly for the railway electrification systems and the variable speed DC motor drives.

- Those rectifiers are characterized by a low efficiency and a high usure rate.

Nottingham Express Transit

AC/DC CONVERTERS: HISTORY (2)

- During the 70s: use of thyristors and diodes as input stage in the DC/DC and DC/AC converters.

- During the next years, developpement of power bipolar transistors, thus favorizing the apparition of low and medium power conversion electronics.

- At the earliest 80s: the apparition of transistor-based devices limits the use of the thyristors to the very high power applications.

AC/DC CONVERTERS: HISTORY (3)

- Since 1985: The use of IGBTs in medium power knows a large extension during 10 ans.
- In 1997: The apparition of IGCTs for voltages higher than 6 kV, risks, at long term, to put an end to the GTO thyristors.
- In 2002: apparition of silicium carbure based components (SiC).
- Since 2004: studies about diamond based components, allowing operation with much higher blocking and thermal abilities.

AC/DC CONVERTERS: APPLICATIONS

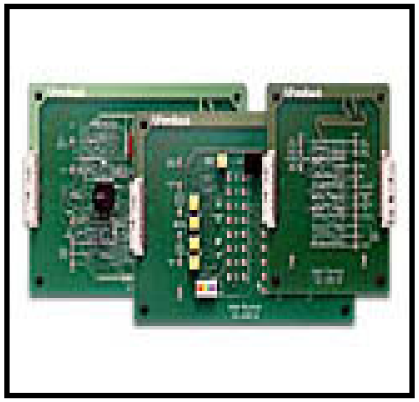

POWER QUALITY: HARMONICS PROBLEMS

ELECTRIC WAVEFORM DISTORSION

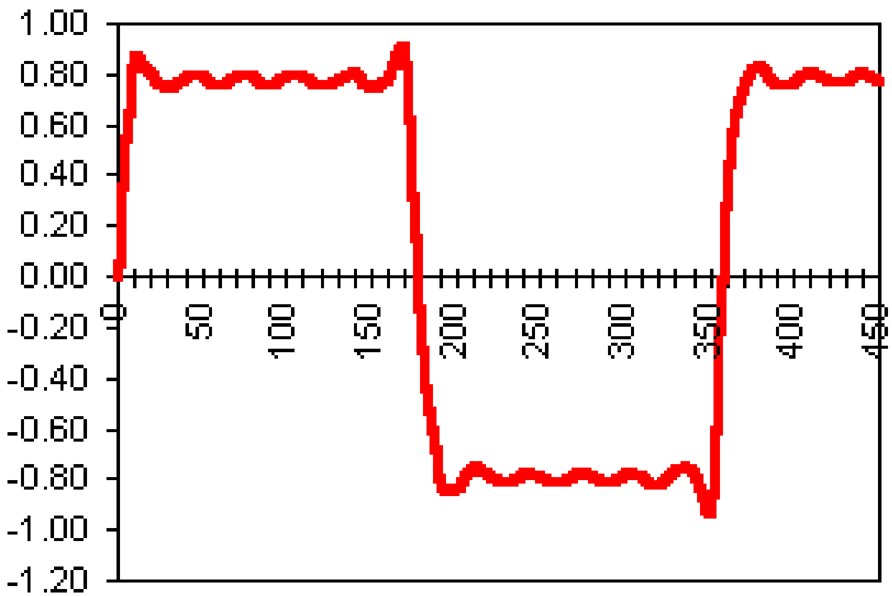

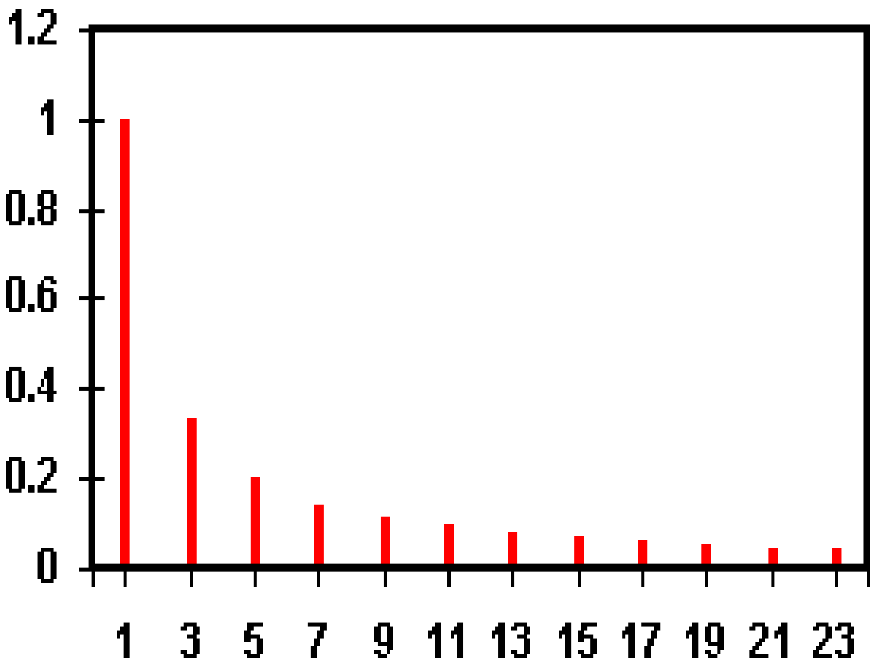

HARMONICS EFFECTS (1)

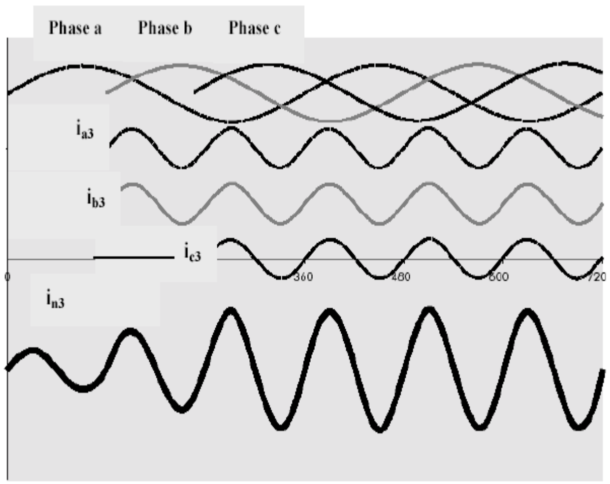

NEUTRAL OVERLOAD

Effects on the transformers

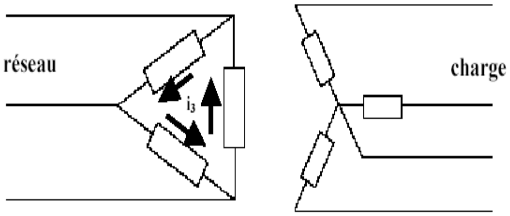

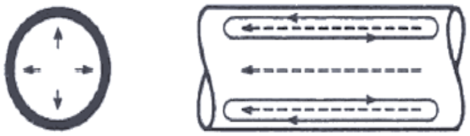

triple N harmonics

Eddy currents

Harmonics effects (2)

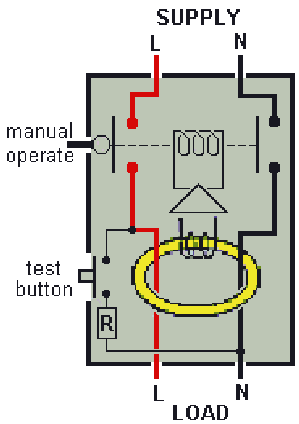

Differential current breakers

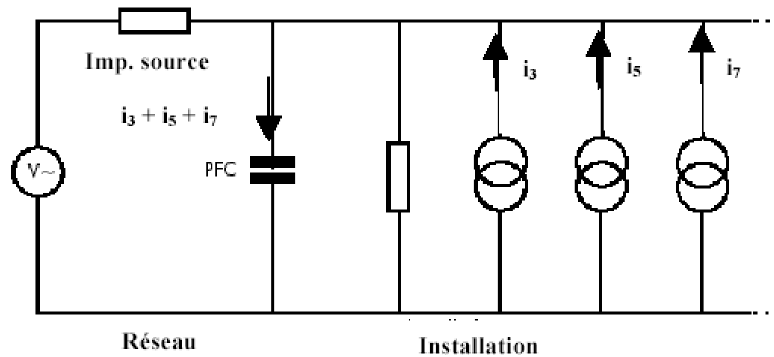

Constraints on the PFCC

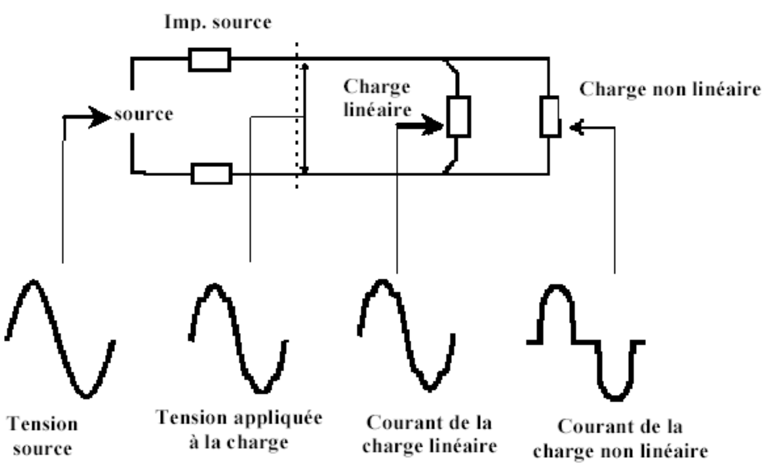

Voltage distorsion at the PCC

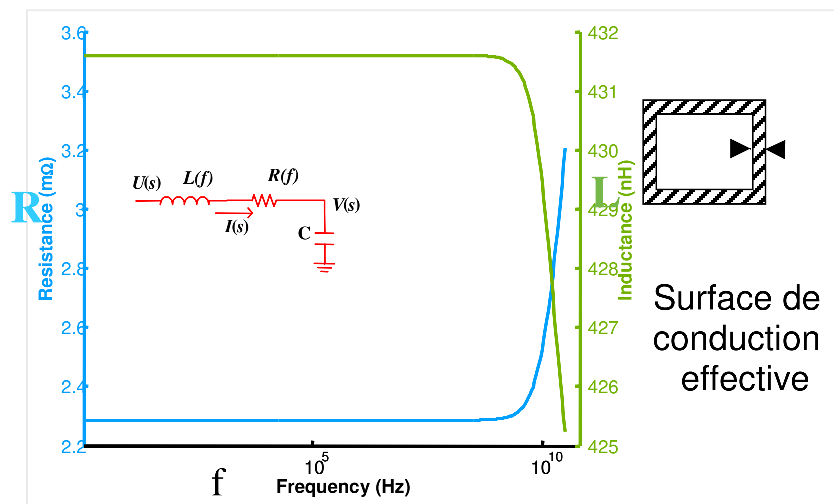

Skin effects

COSTS (1)

- ***Direct*:**
  - Equipments failure
  - Loss of production
  - Loss of salaries during improductive periods
  - Restarting costs

- ***Indirect*:**
  - Production delays
  - Loss of contracts

COSTS (2)

- The failure of two transformers in a glass factory in Europe may cause a loss of about 600 000 € and of 3 days of production [De Keulenaer, 2003].

- A fire, generated by the overheat of the neutral, may cost until 1 million € [De Keulenaer, 2003].

- The loss of power supply in a telecom edifice may cost the amount of 30 000 € [De Keulenaer, 2003].

COSTS (3)

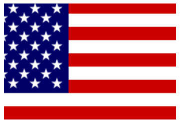

- Power quality: 120 billions $ US/year
- Costs related to harmonics: 50-67%

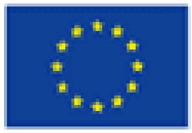

- 10 billions €/year

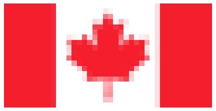

- 1.2 billions $/year

Harmonic Emission Limits in QUEBEC (Inspired from the IEC-61000-4-7)

	n impairs								n pairs				
Scc/Sr \ n	3	5	7	9	11, 13	[17,23[	[23,35[	[35,∞[	2	4	6	8	≥10
< 20	1	1.2	.8	.5	.5	.4	.3	.2	.75	.5	.3	.2	.15
≥20 et <50	1.5	2	1.5	.75	1	.65	.45	.3	1.1	.75	.45	.3	.25
≥50 et < 200	2	3	2	1	1.5	1	.7	.5	1.5	1	.6	.4	.3
≥ 200	3	4	3	1.25	2	1.5	1	.7	2.2	1.5	1	.6	.4

S_{cc}/S_r	TDDc
< 20	1.7
≥20 et <50	3
≥50 et < 200	4.5
≥ 200	6

Tableau 1: Limites d'émission des harmoniques (I_n/I_r %)

THREE-PHASE PFC/SMR: CLASSIFICATION

- Commutation type: spontaneous / forced,
- Line currents control: active/ passive / hybrid,
- Isolation (or not) of the output stage,
- Power flow: unidirectionnal / bidirectionnal,
- Conduction mode: continuous / discontinuous

THREE-PHASE PFC/SMR: ChARACTERISTICS

- Sinusoidal current absorption,
- Resistive characteristics of the mains fundamental,
- Possibility of regulation on the DC side,
- High power density,

THREE-PHASE PFC/SMR: TOPOLOGIES

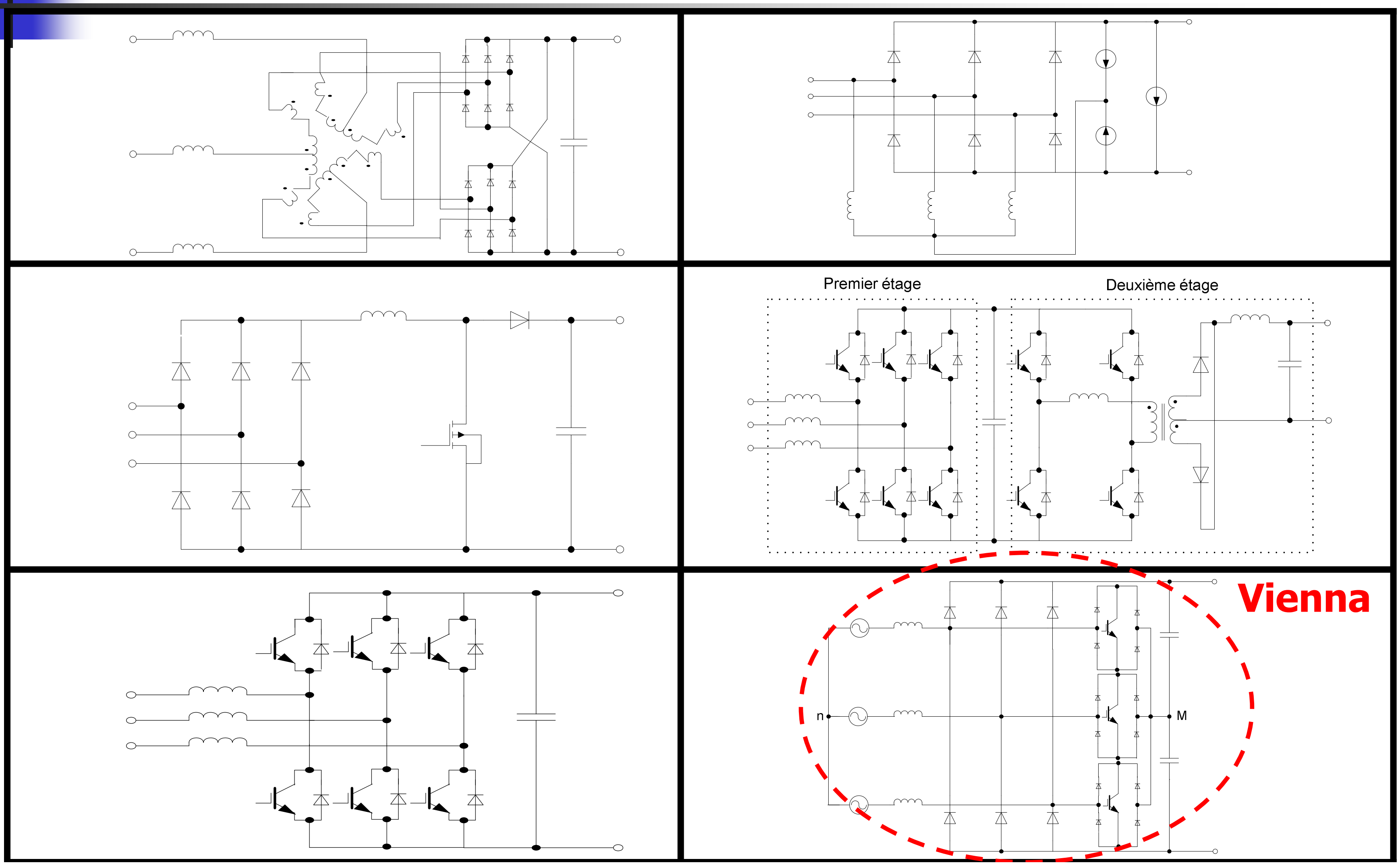

INTRODUCTION OF THE VIENNA TOPOLOGY

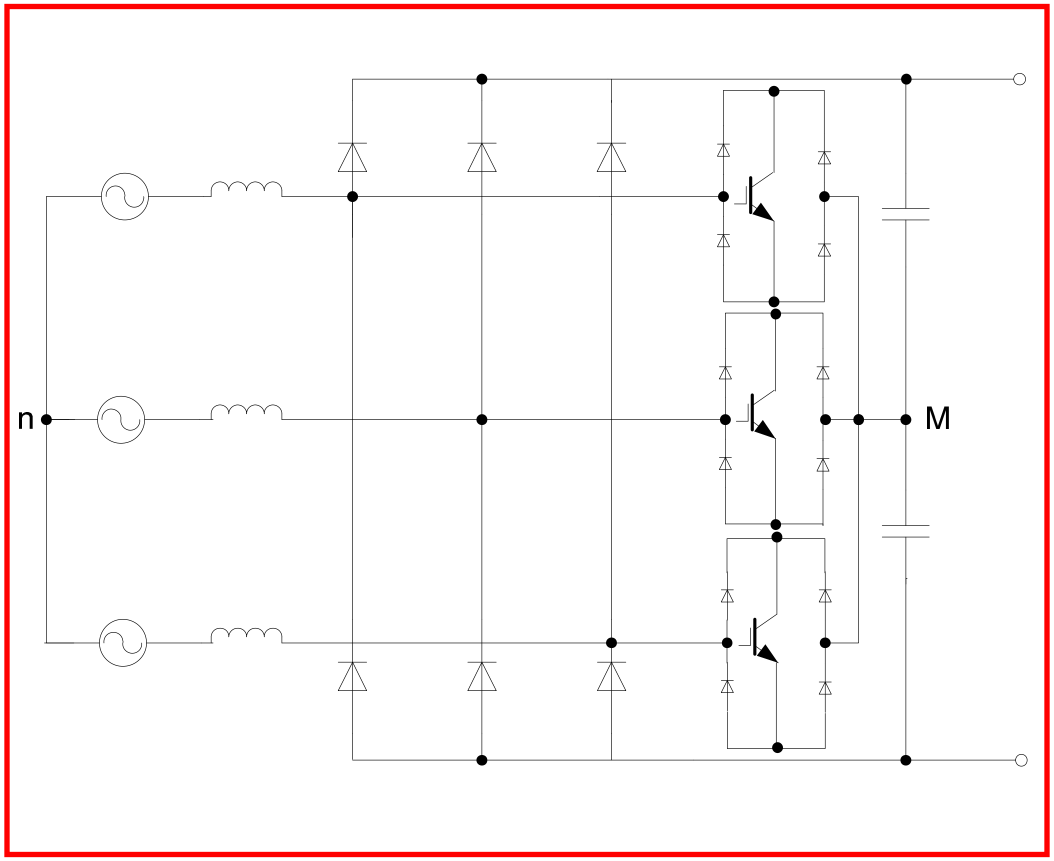

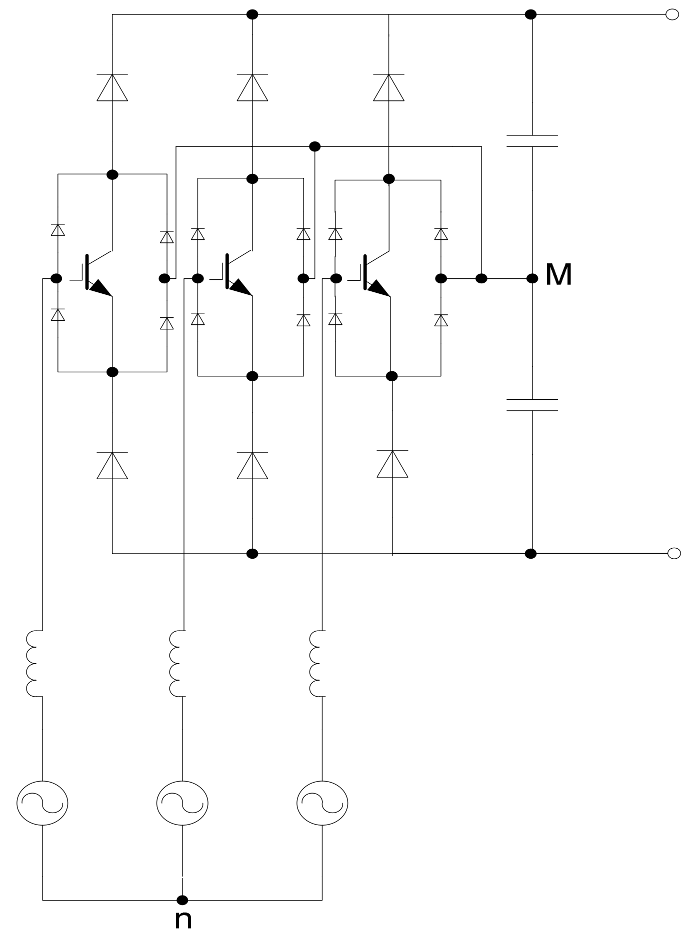

CARACTERISTICS

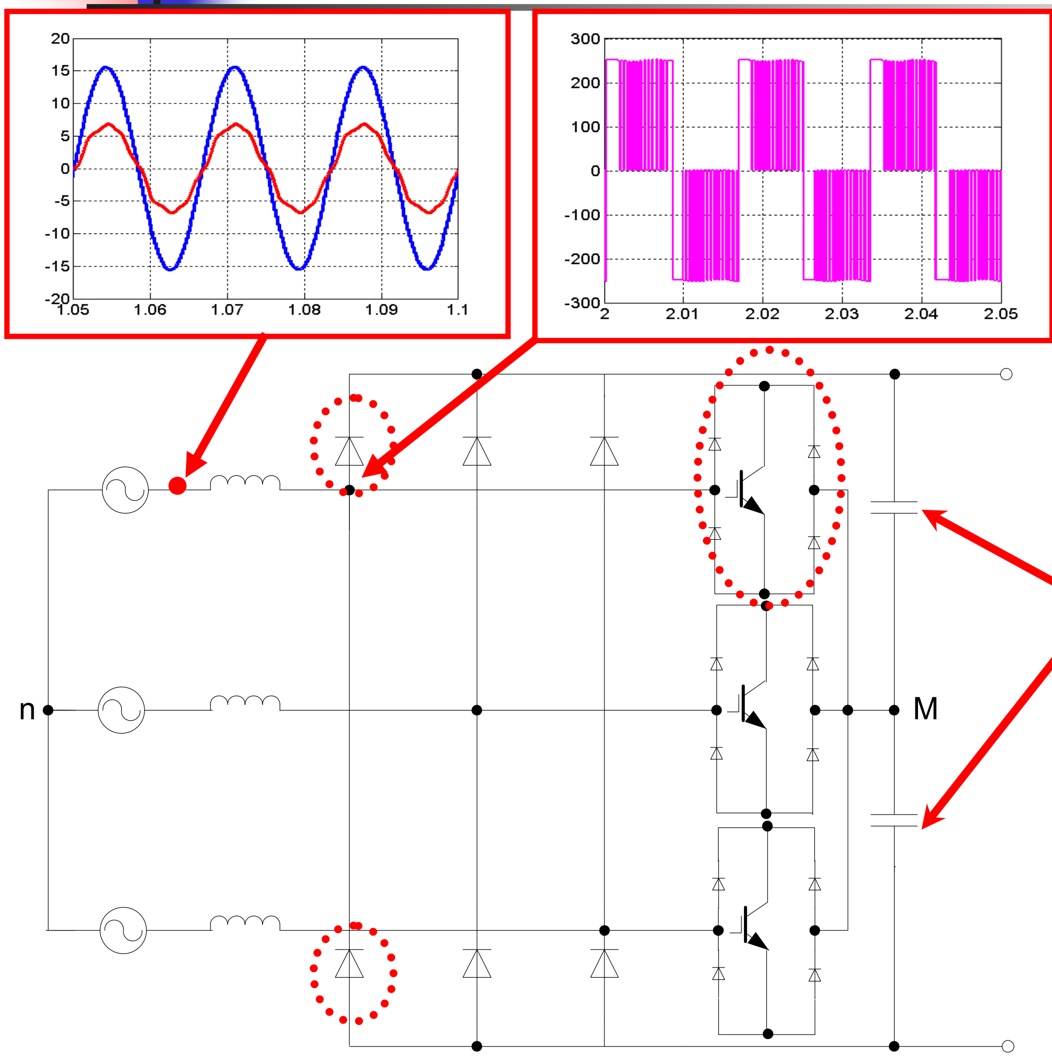

- Current/voltage phase angl
Between ± 30°

- Three-level input voltage

- Reduced ratings of the
Reactive components

- Two regulated and equal
DC power supplies

- Immunity against control
errors

- High efficiency

APPLICATIONS

Battery chargers

UPS

Integrated motors

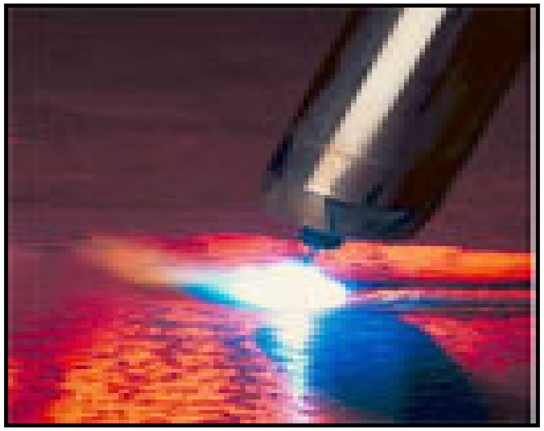

Welding units

Air conditioning

Aeronautics and maritime

VARIANTES

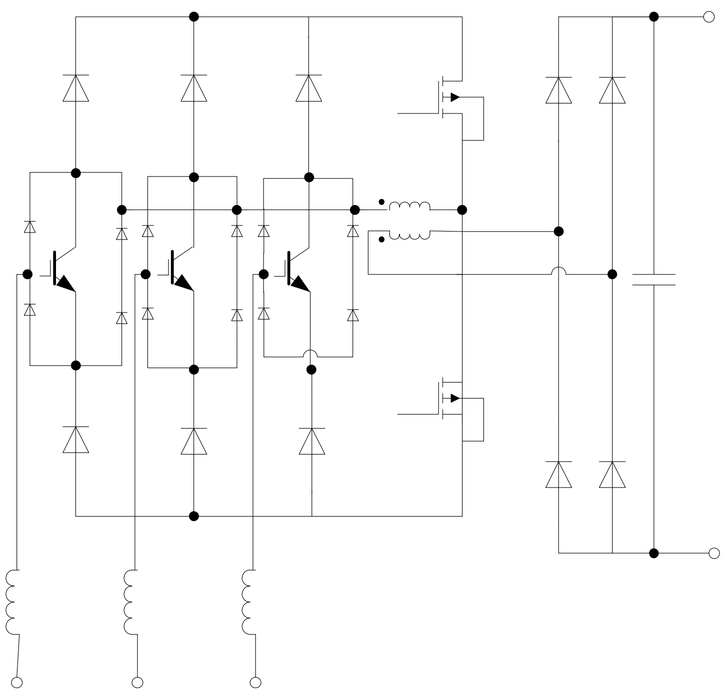

Vienna II

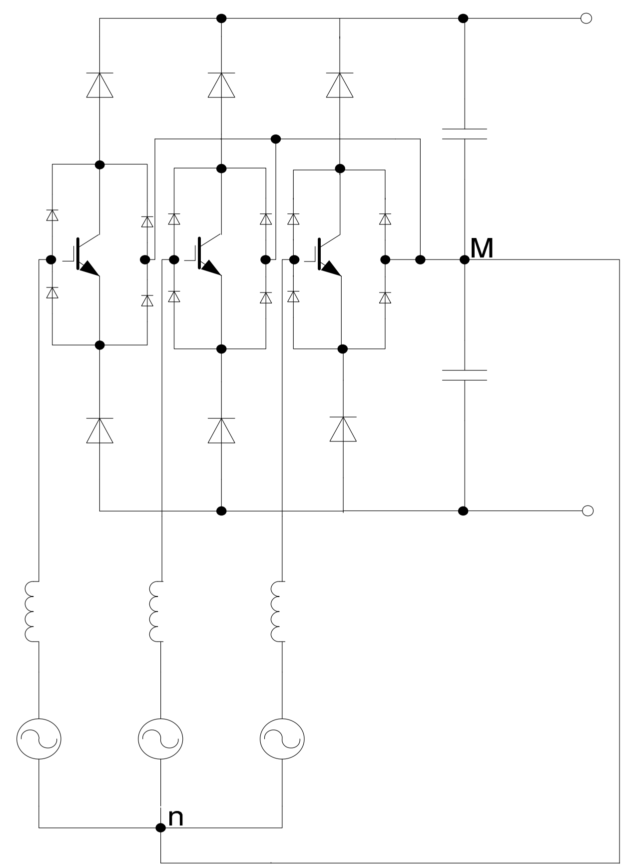

Vienna IV

MAIN RESEARCH OBJECTIVES

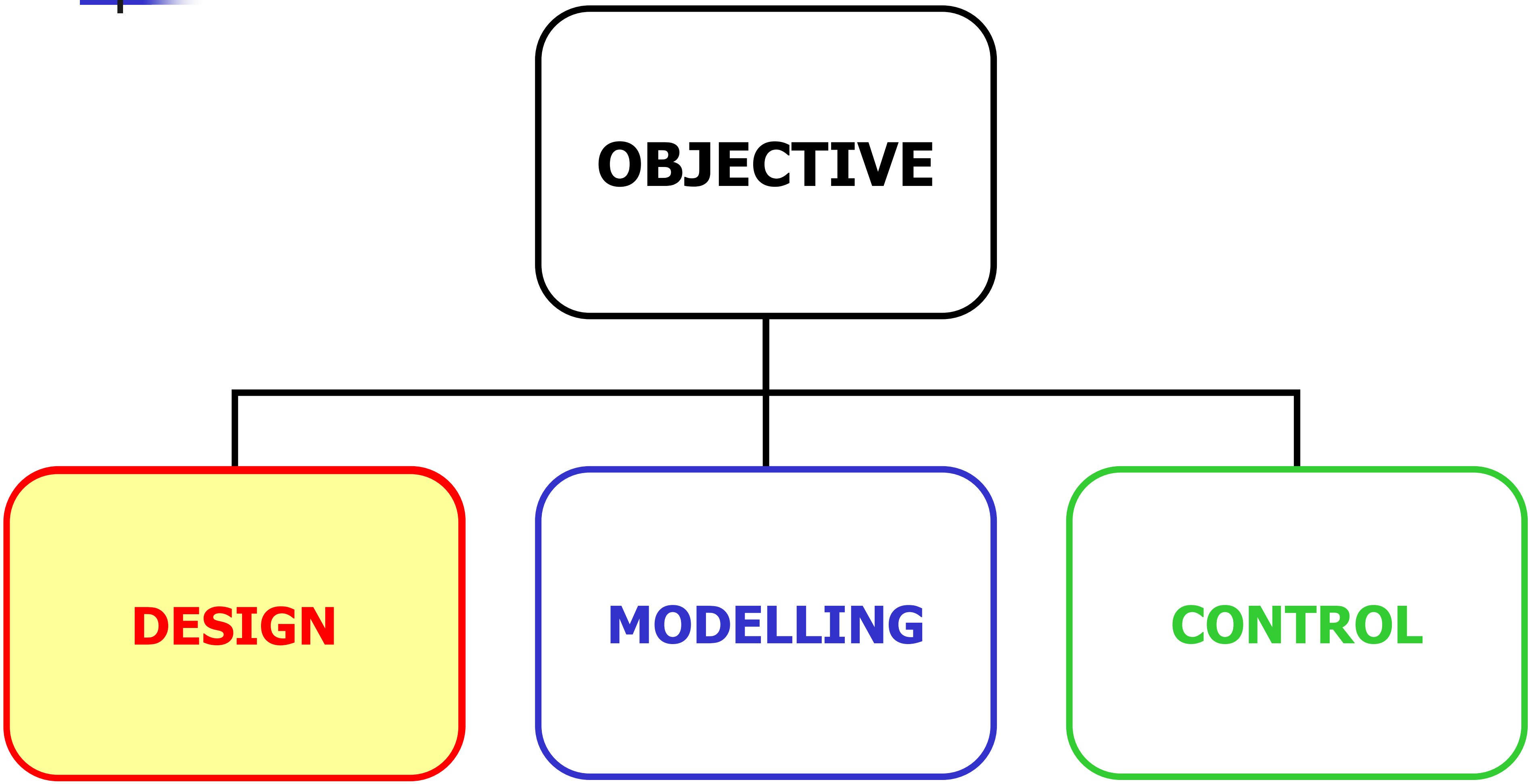

DESIGN

- To propose a general design methodology for the Vienna converter.
- To construct a 1.5 kVA prototype for the experimental validations.

Design elements

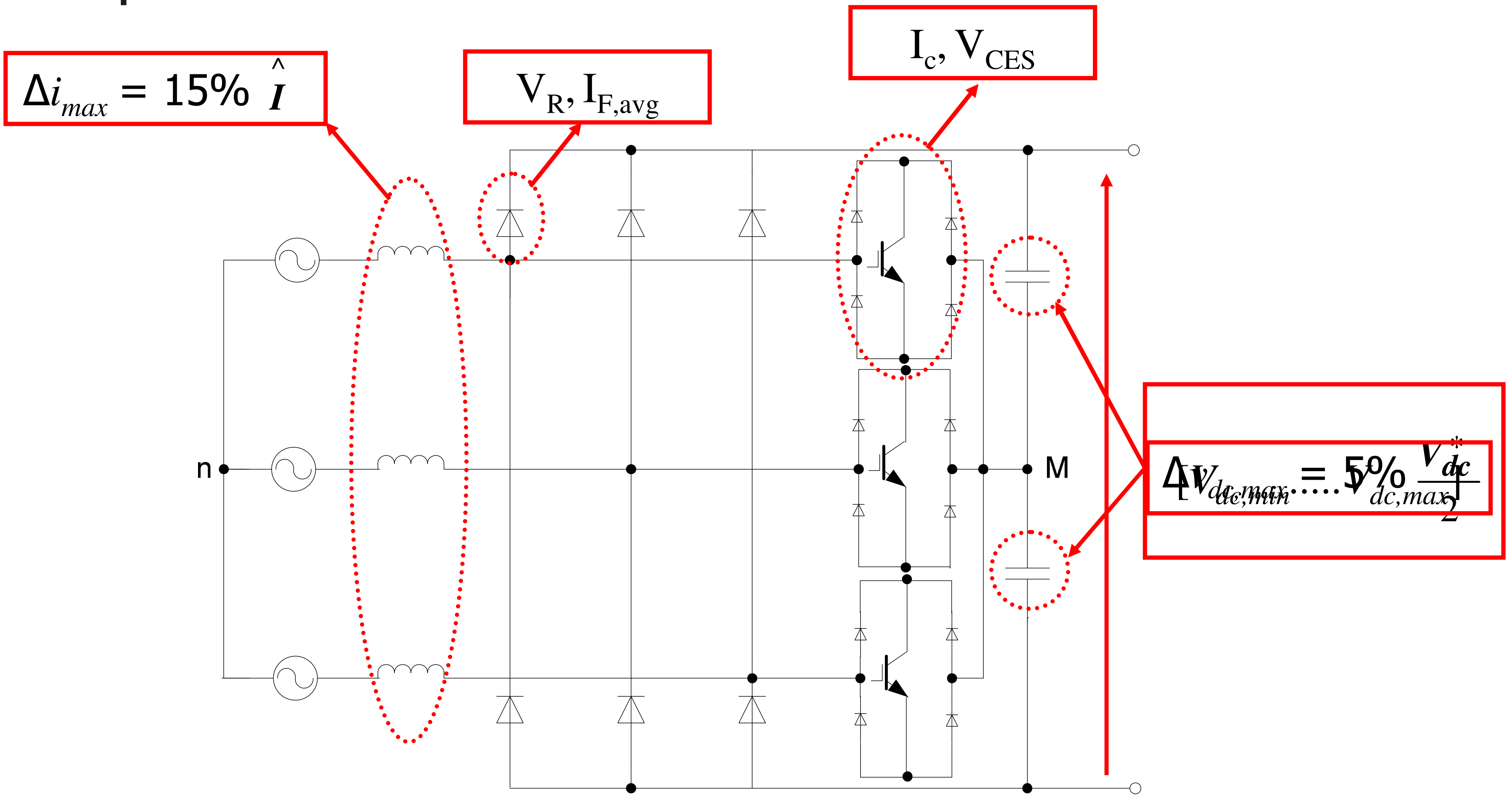

SPECIFICATIONS

NOMINAL POWER	1.5 kVA
POWER FACTOR	> 0.97
THREE-PHASE SUPPLY	110 V RMS
TOTAL DC BUS VOLTAGE	500 V
MAXIMUM CURRENT RIPPLE	15%
MAXIMUM VOLTAGE RIPPLE	± 5%
MAXIMUM CURRENT	10 A peak
THD	< 7%
SWITCHING FREQUENCY	constant

Prevalent switching sequences

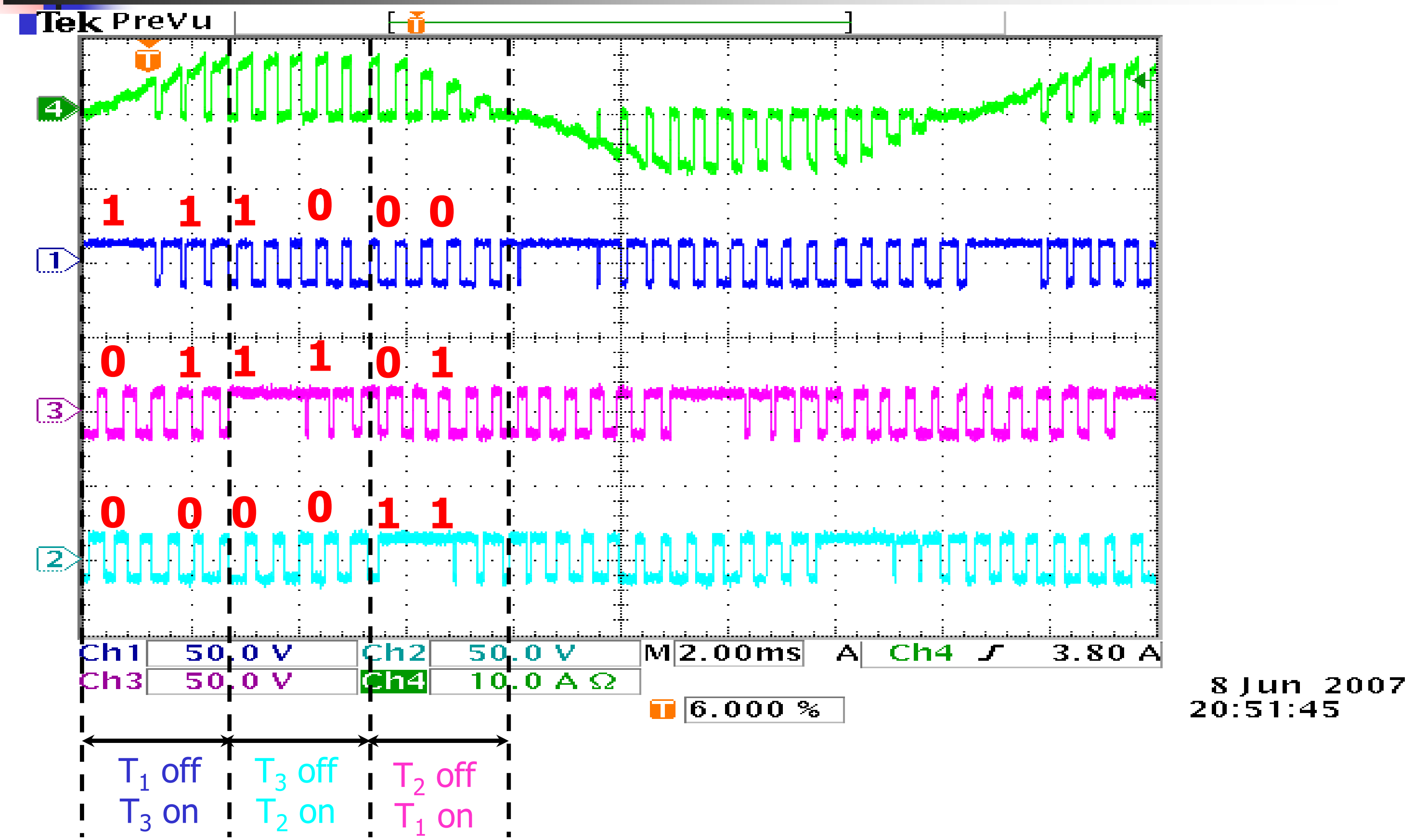

Line currents controllability

$i_k > 0$

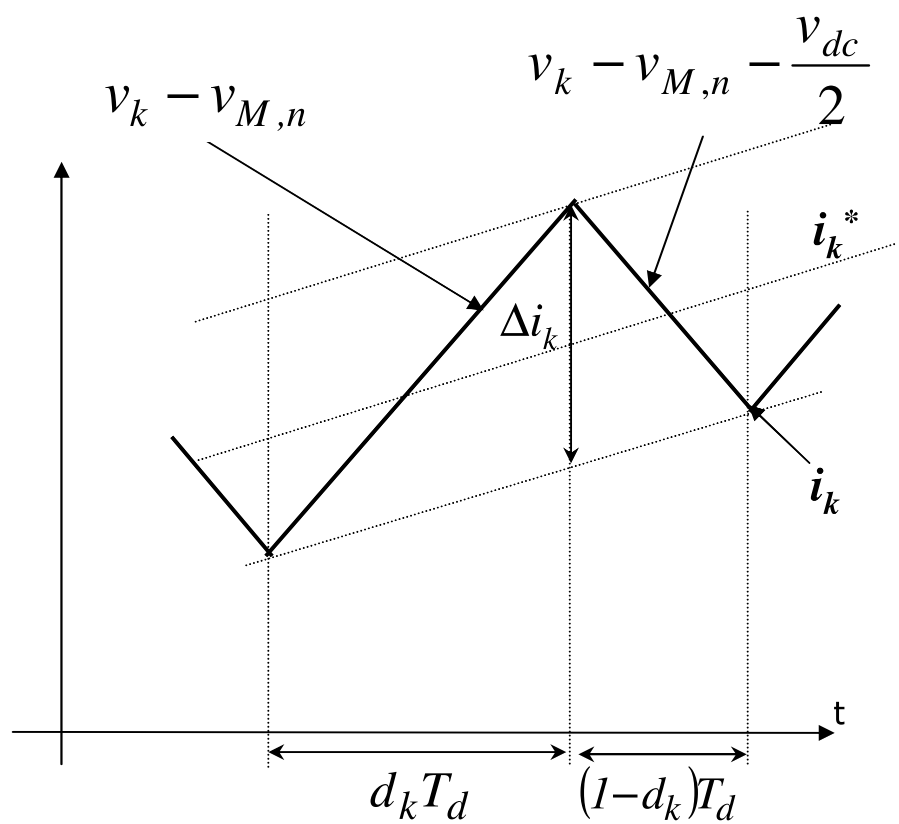

$i_k < 0$

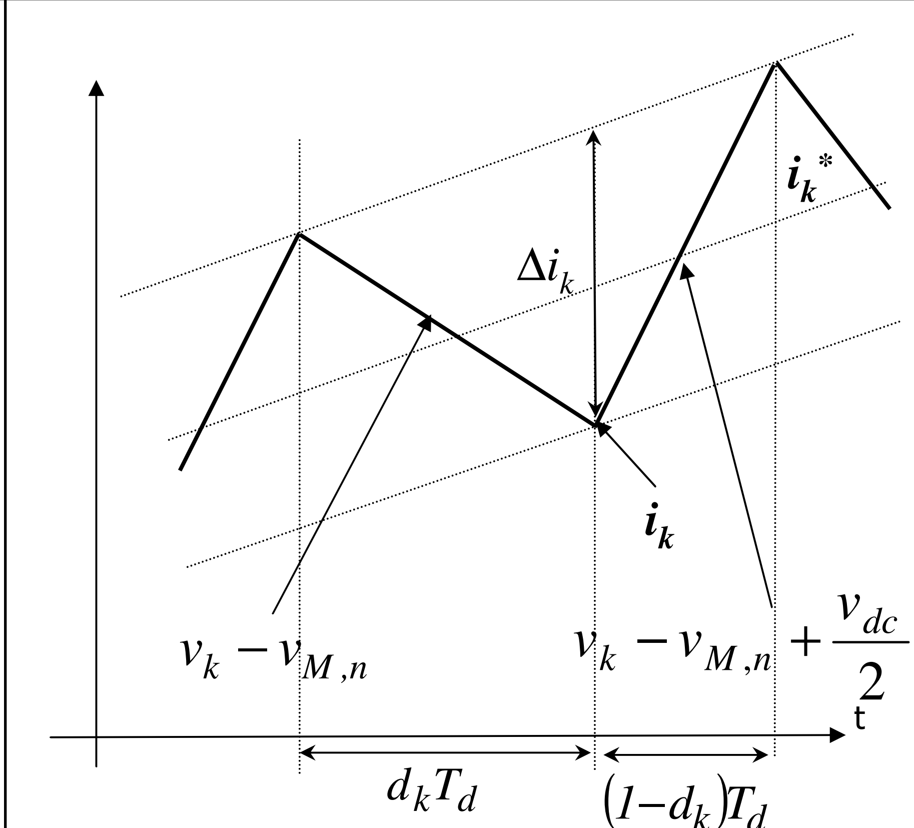

Circuit losses evaluation

conduction losses

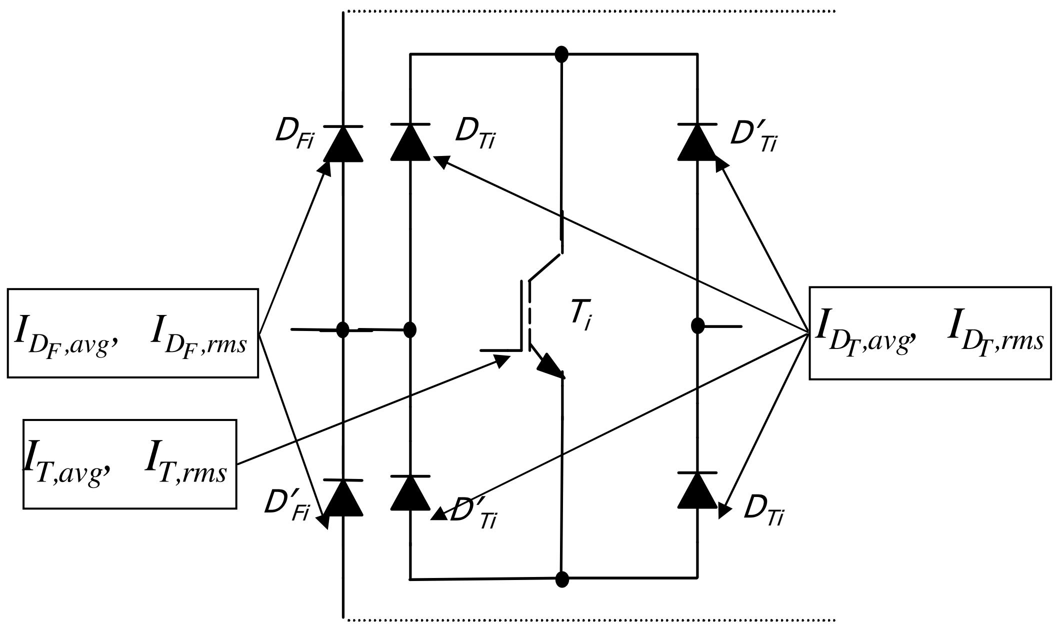

Switching losses

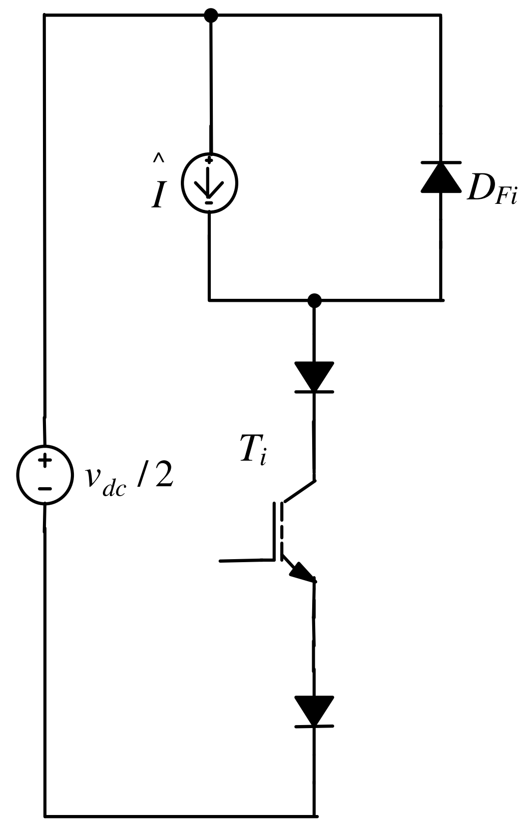

RMS/Average currents

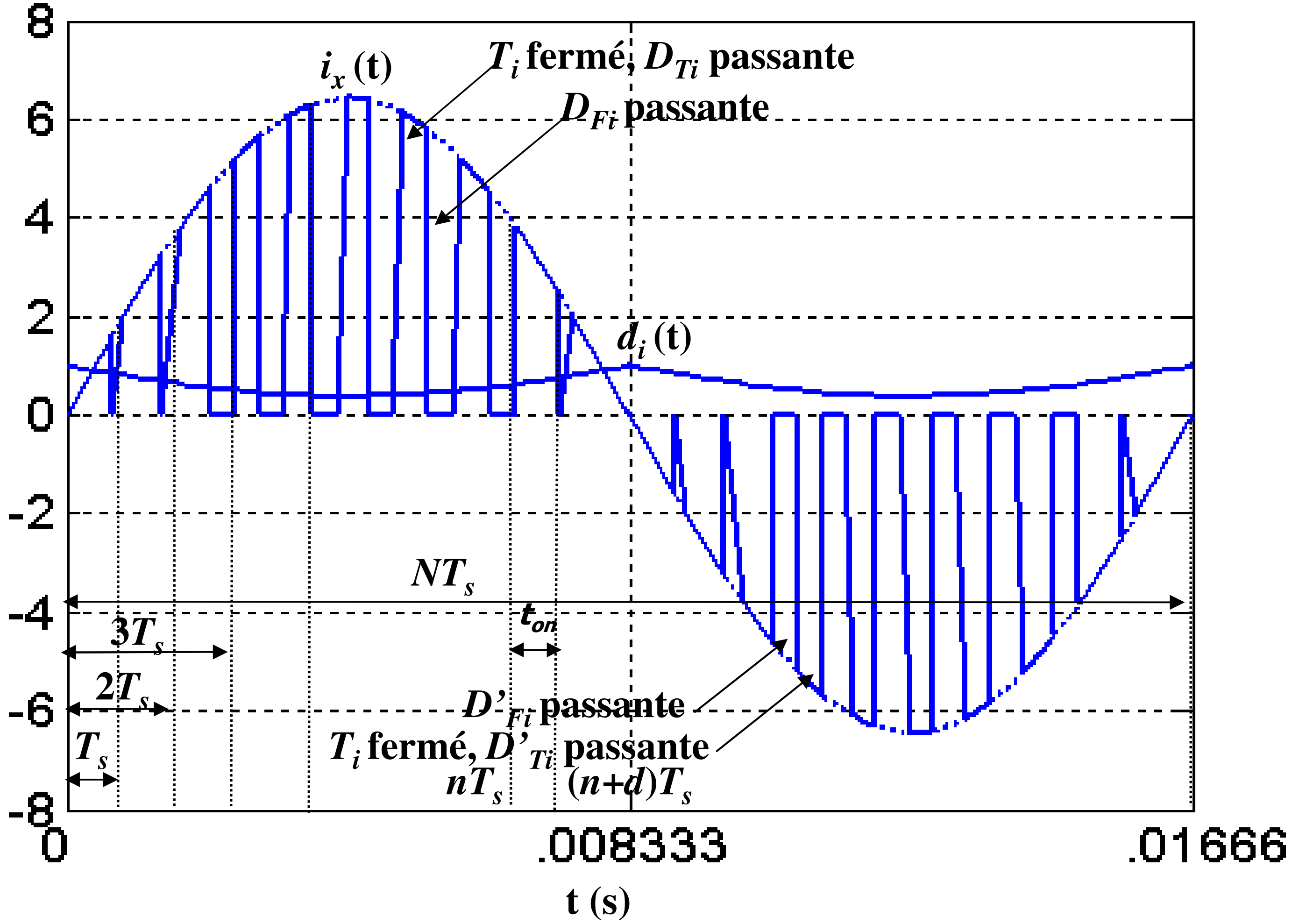

Power stage specifications

Components	Specifications
Boost inductors	L: (20 mH, 10A), r_L= 1.68 Ω
Filtering capacitors	C_{dc}: (470μF, 450V), L_c = 1.93mH, r_c = 183 mΩ
Decoupling capacitors	2.2 μF. 400V
(dv/dt) snubbers	R_{sv}: (50 kΩ, 1W), C_{sv}: (2.2 nF, 600V), D_{sv}: (15 A, 1200 V)
(di/dt) snubbers	R_{si}: (1 Ω, 1W), L_{si}: 1.3 μH, D_{si}: (15 A, 1200 V)
Four-quadrant switches	I_{c25} = 50A, V_{CES} = 1200V, $V_{CE(sat)typ.}$ = 2 V
Rectification diodes	V_R = 1200 V, $I_{F,avg}$ = 15 A

POWER CIRCUIT

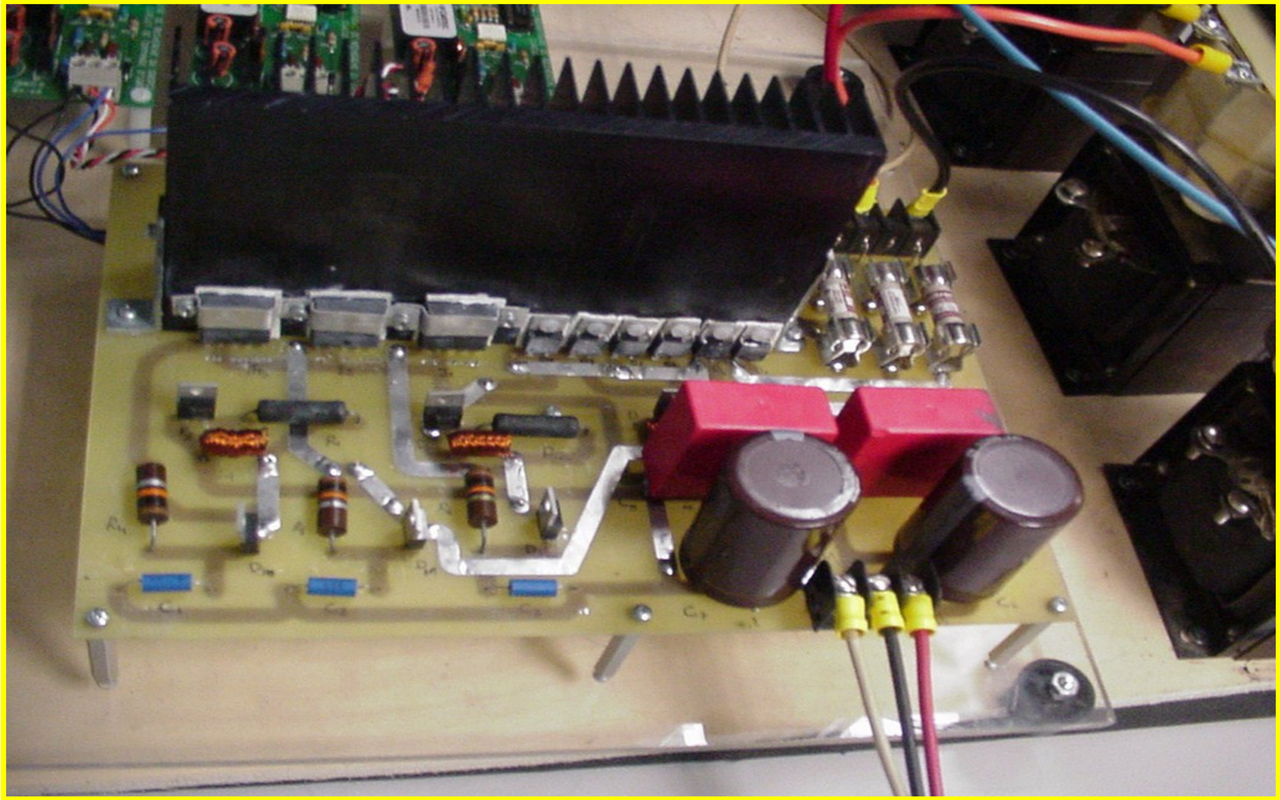

WAVEFORMS AT NOMINAL POWER

TDH = 37%
FP = .9

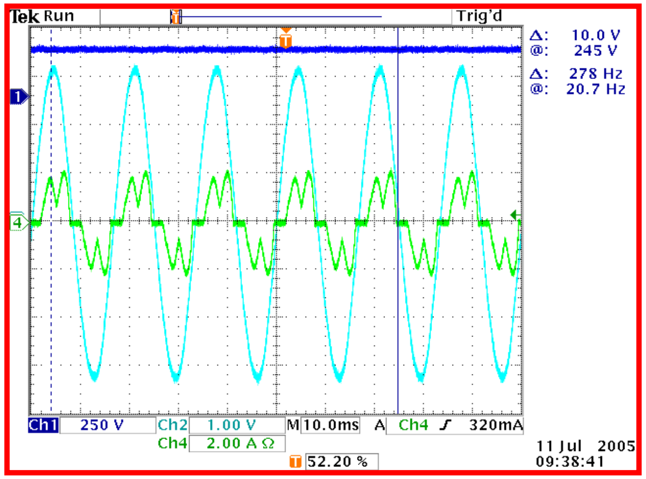

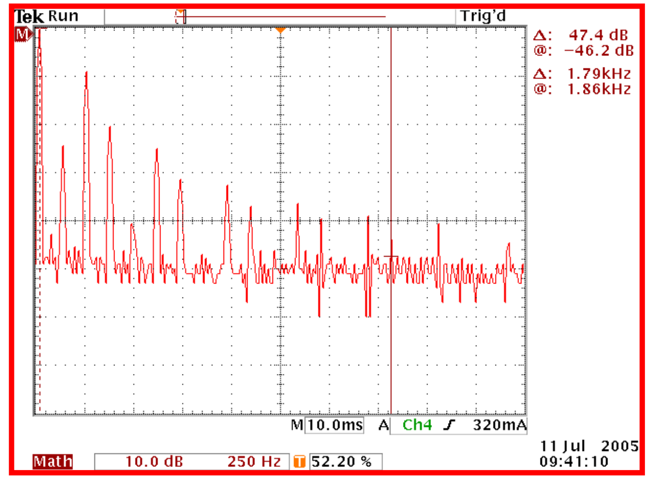

TDH = 5%
FP = .99

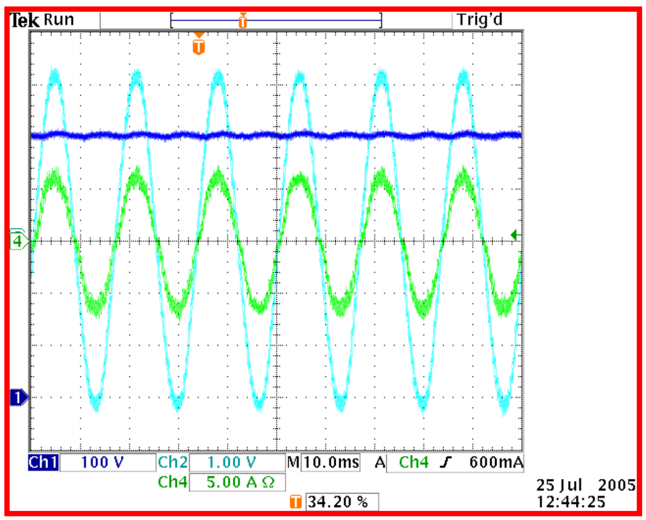

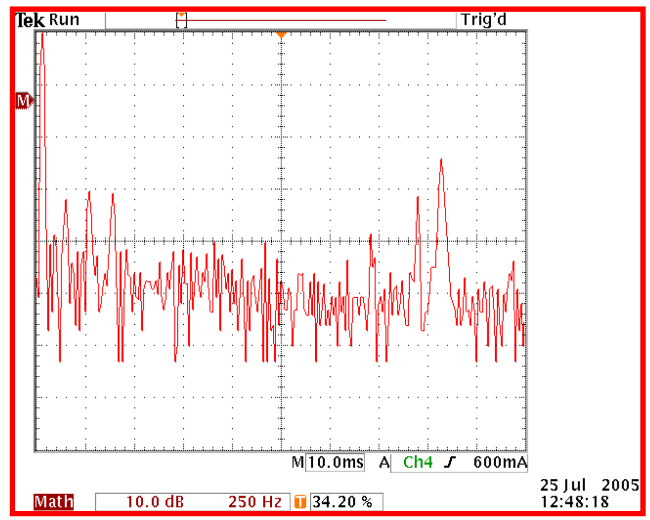

EXPERIMENTAL WAVEFORMS

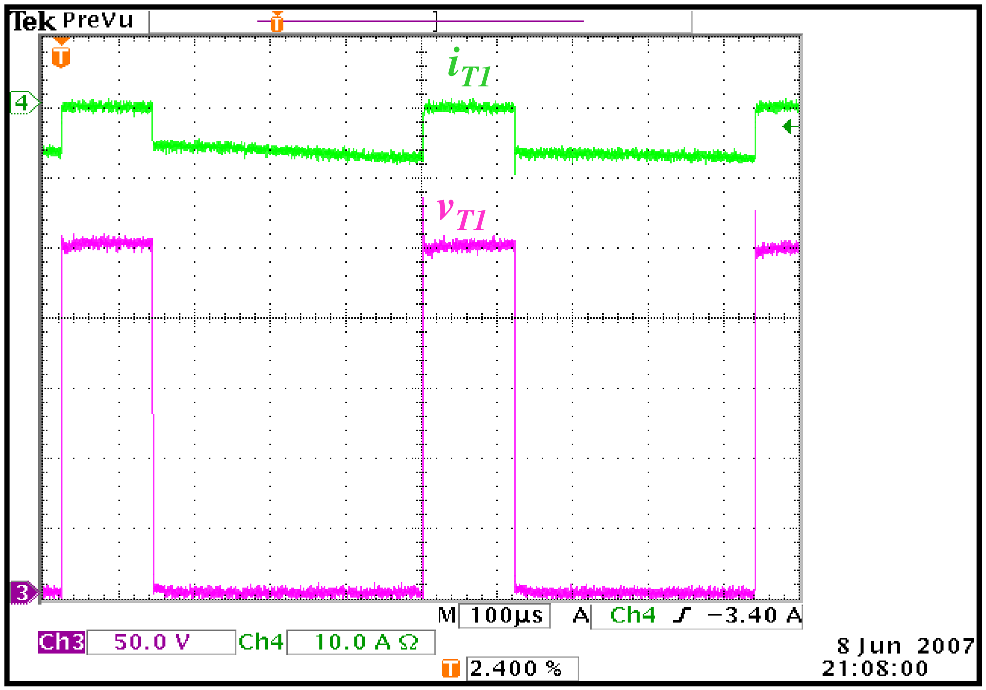

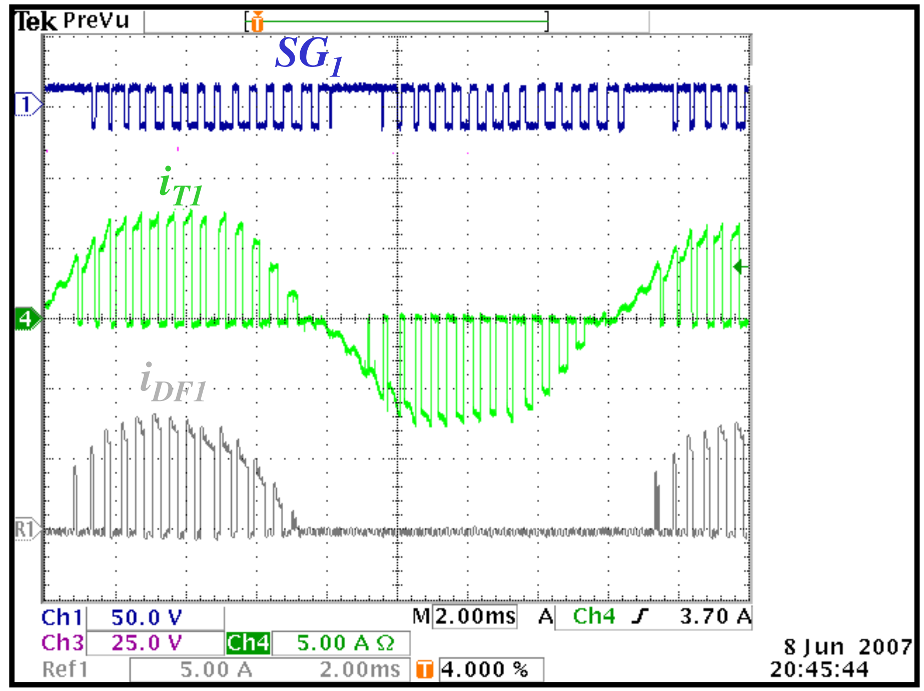

COMPUTED ENTITIES VS MEASURED ENTITIES

	COMPUTED VALUES	MEASURED VALUES
$I_{DF,avg}$ (A)	1.07	0.84
$I_{DF,rms}$ (A)	2.4	2.02
$I_{DT,avg}$ (A)	0.94	—
$I_{DT,rms}$ (A)	2.06	—
$I_{T,avg}$ (A)	0.8	0.75
$I_{T,rms}$ (A)	4	3.8
LOSSES (W)	34.5	51
EFFICIENCY (%)	97.7	96.6

AUXILIARY CIRCUITS

Transformers 120V/25V

Gate drives

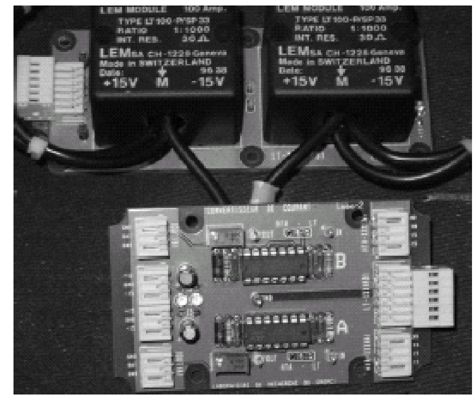

Sensors

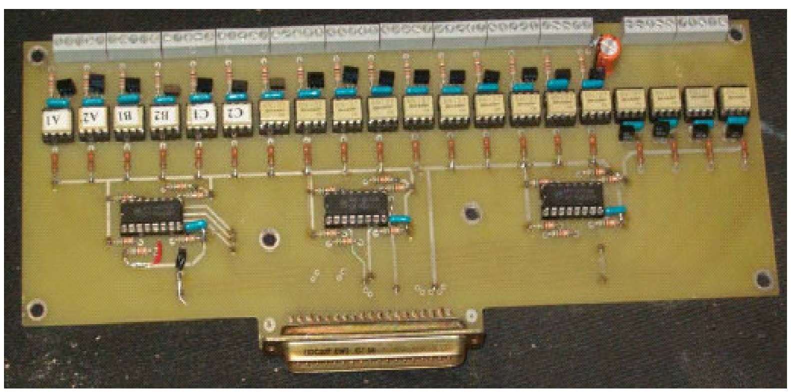

Opto-insulation board

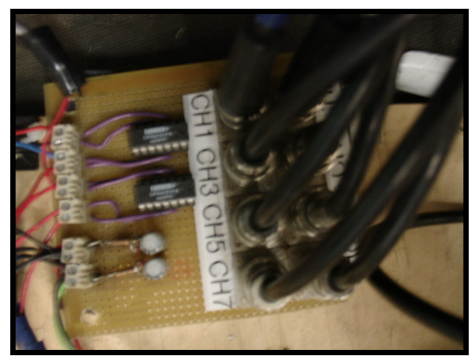

Protection circuit

EXPERIMENTAL SETUP

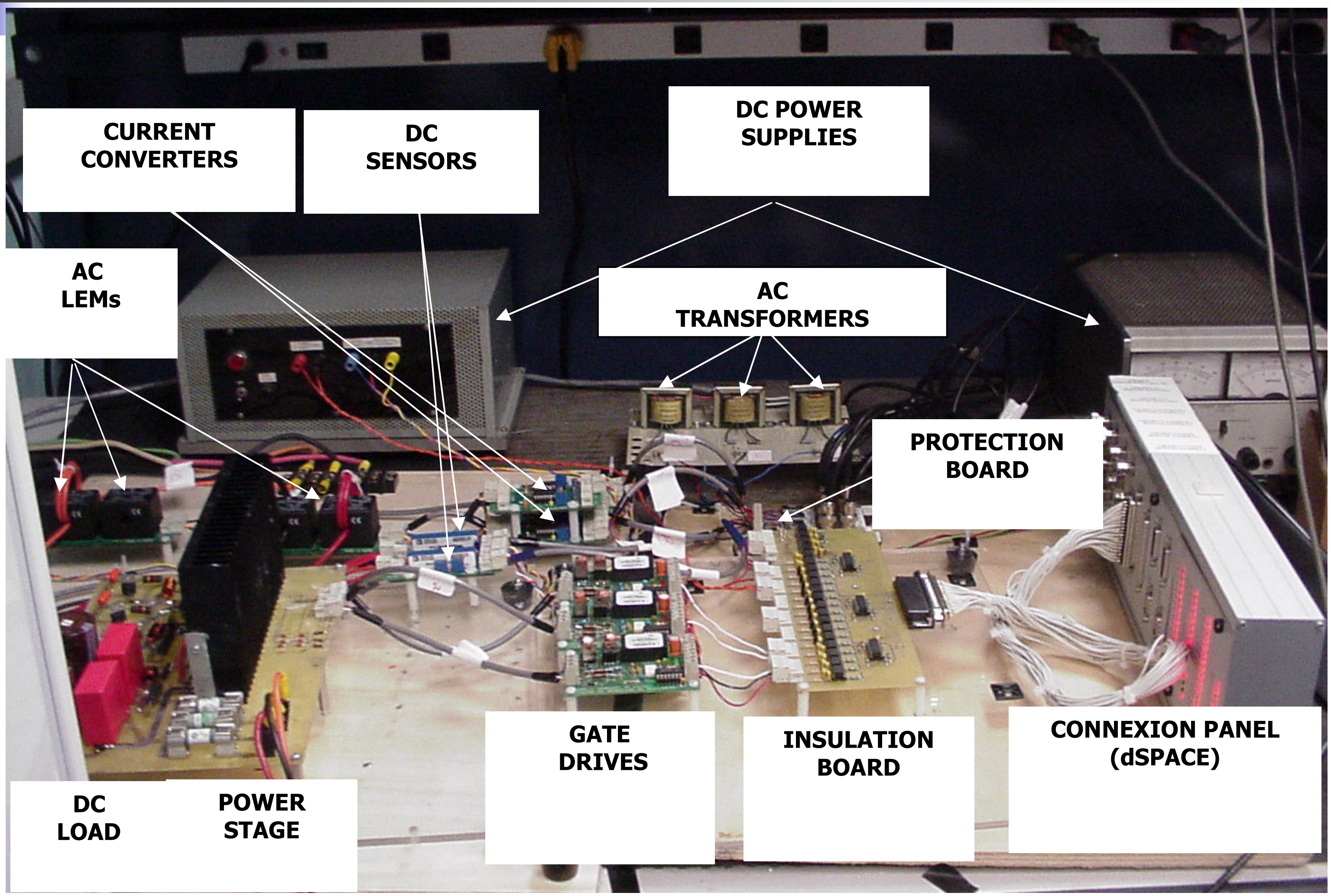

MAIN RESEARCH OBJECTIVES

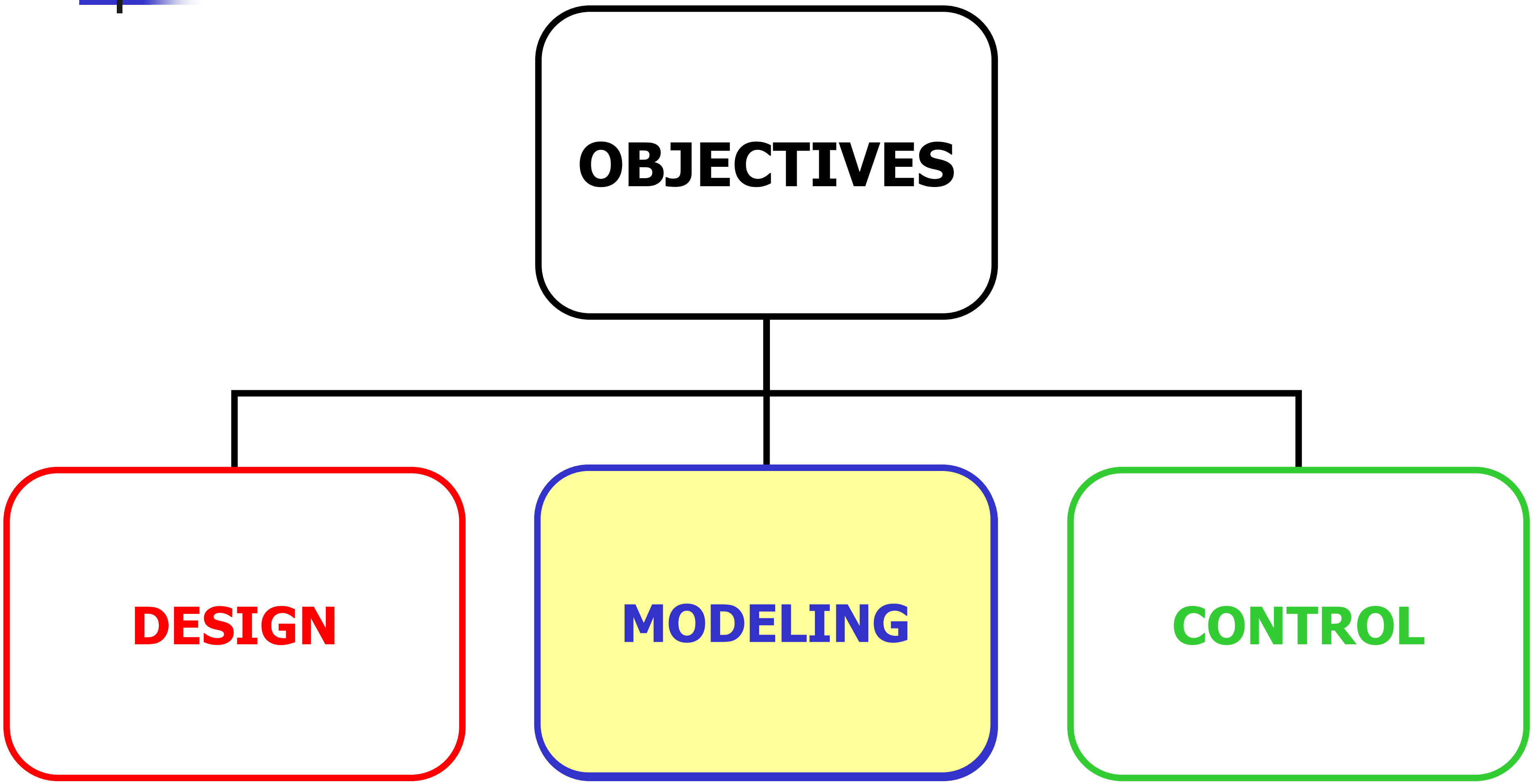

MODELING

- To propose reliable models for the Vienna topology, for dynamic analysis and control design aims.

- To experimentally validate the proposed, in order to conclude about their precision level.

MODELS TYPES

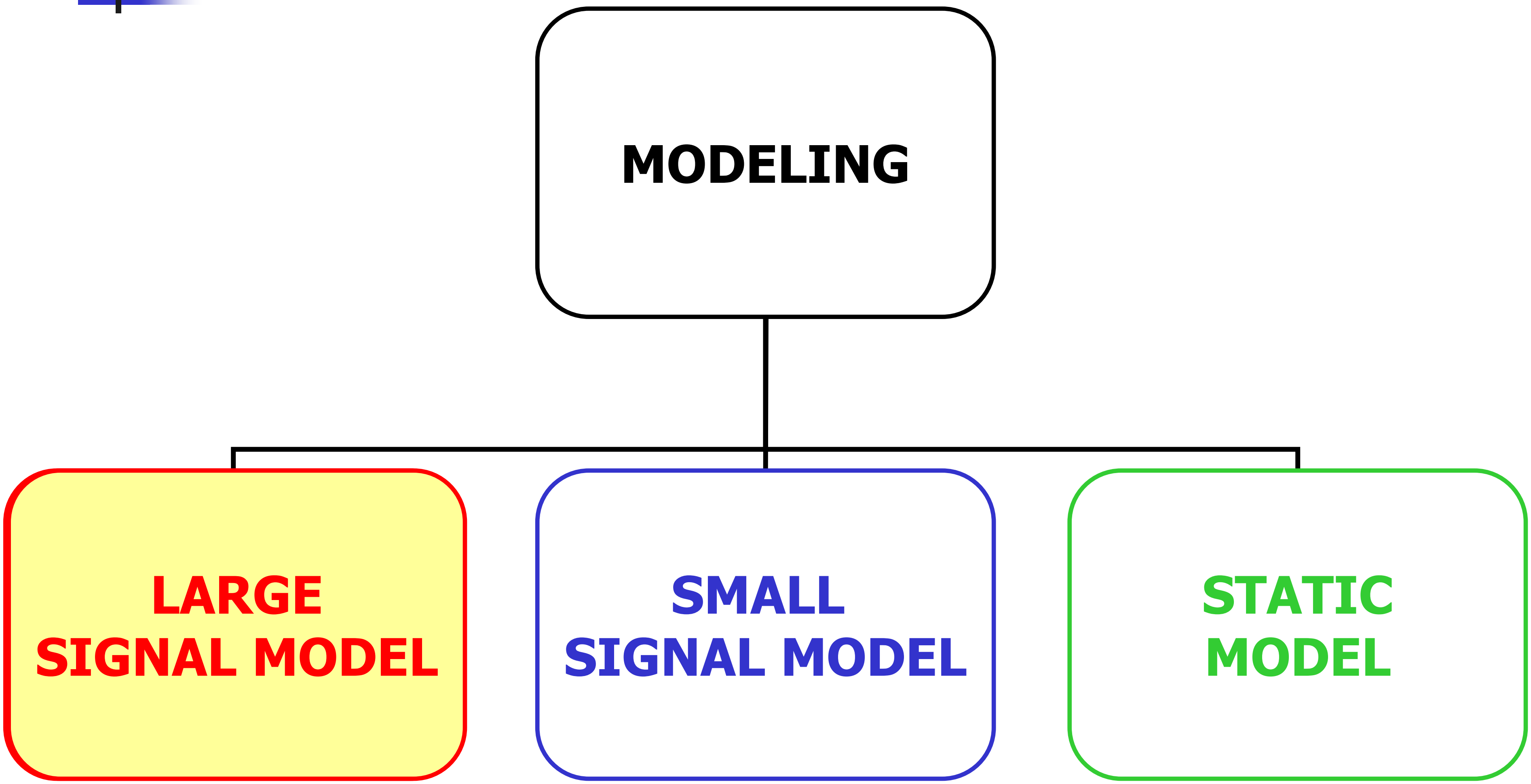

LARGE SIGNAL MODEL

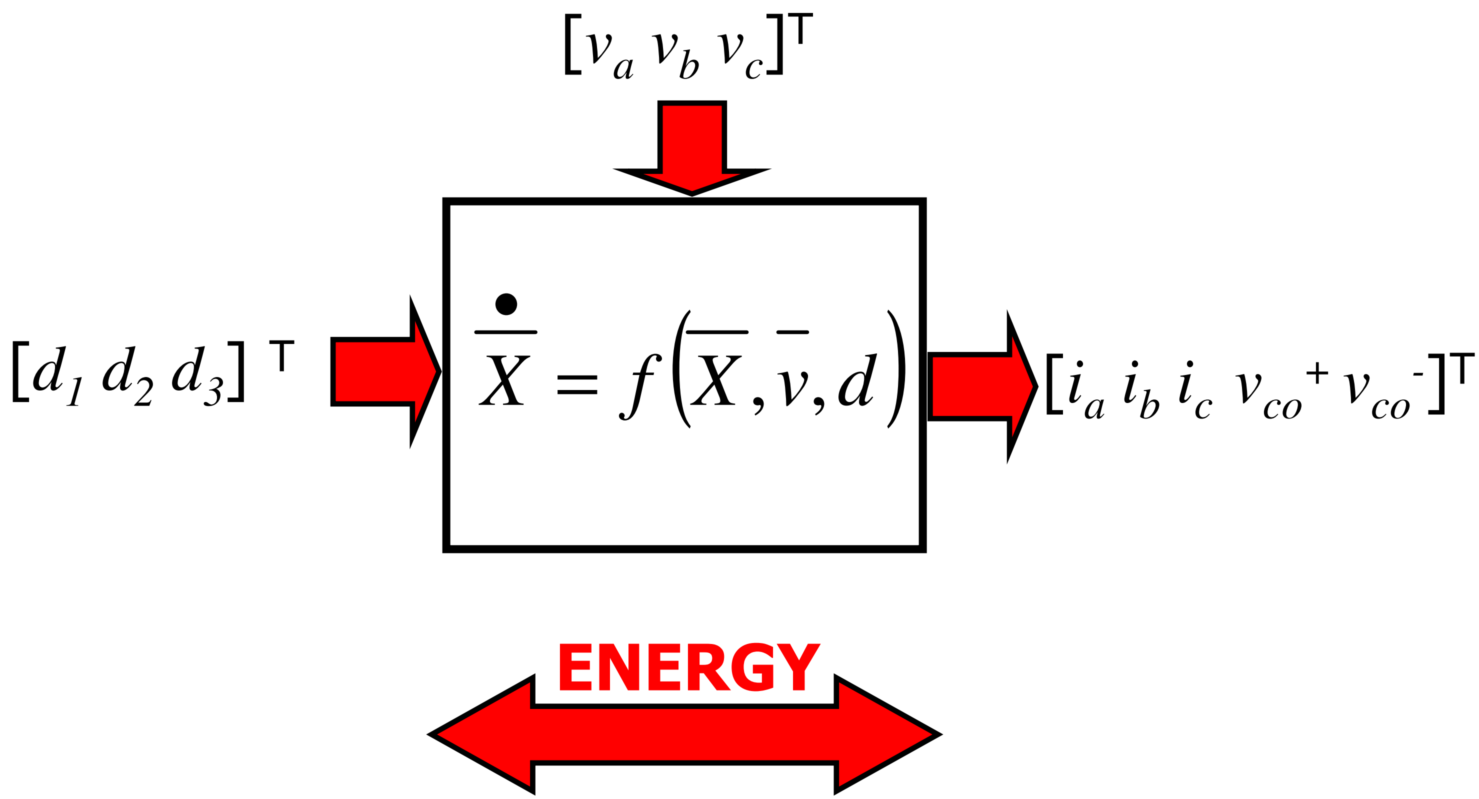

AC SIDE STATE EQUATIONS

Configuration: (0,1,0); (i_a>0, i_b>0, i_c<0)

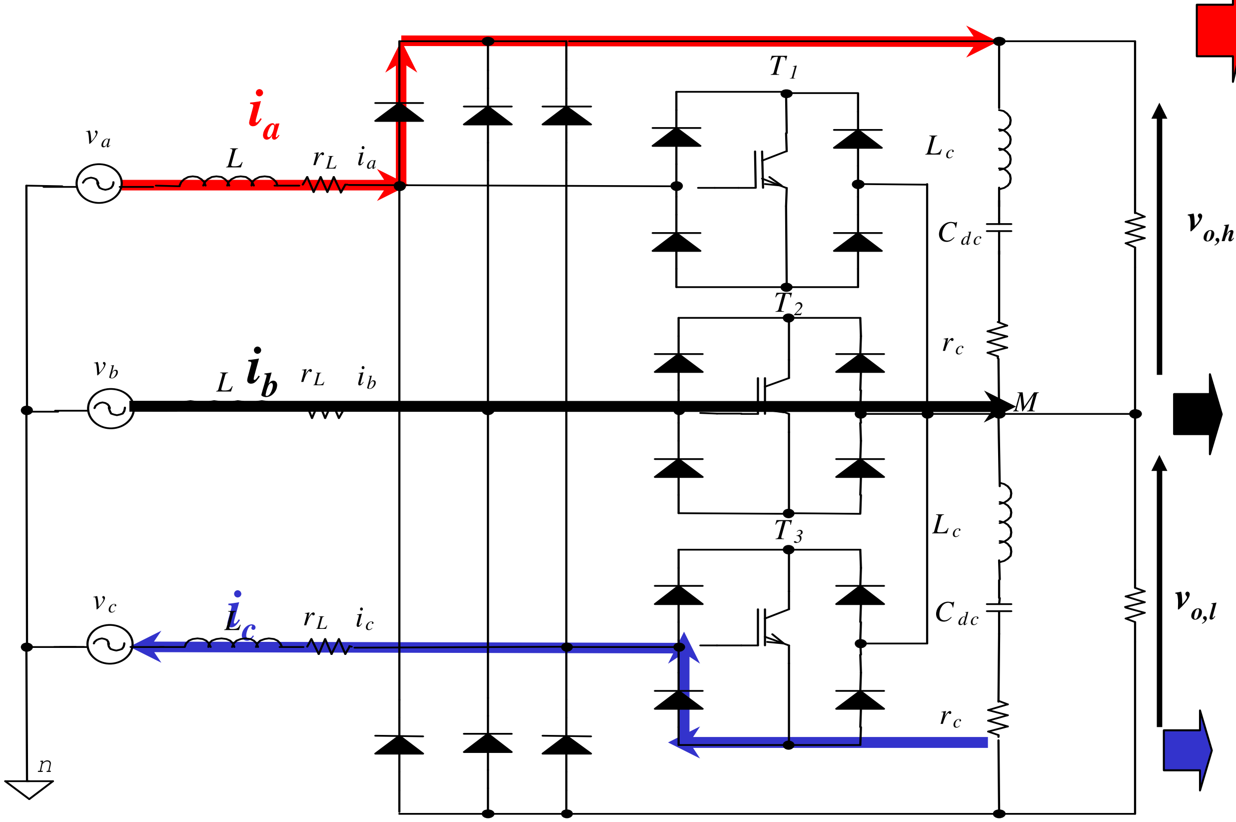

$$v_a = L\frac{di_a}{dt} + v_{o,h} + v_{M,n}$$

$$v_b = L\frac{di_b}{dt} + v_{M,n}$$

$$v_c = L\frac{di_c}{dt} - v_{o,l} + v_{M,n}$$

DUTY CYCLES TRANSFORM

$$v_x = L\frac{\mathrm{d}(i_x)}{\mathrm{dt}} + r_L i_x + \left[v_{dc}^{+}\underline{\theta(i_x)} - v_{dc}^{-}\underline{\overline{\theta(i_x)}}\right](1-d_k) + v_{M,n}, \quad x=\{a,b,c\}, \quad k=\{1,2,3\}$$

$$\boxed{d_k^{'} = 2\ (1-d_k)\left[\frac{v_{dc}^{+}\,\theta(i_x) - v_{dc}^{-}\,\overline{\theta(i_x)}}{v_{dc}^{+} + v_{dc}^{-}}\right], \quad x \in \{a,b,c\}, \quad k=\{1,2,3\}}$$

$$\boxed{v_x = L\frac{\mathrm{d}(i_x)}{\mathrm{dt}} + r_L i_x + \frac{v_{dc}}{6} M d_k^{'}, \qquad M = \begin{pmatrix} 2 & -1 & -1 \\ -1 & 2 & -1 \\ -1 & -1 & 2 \end{pmatrix}}$$

DC SIDE STATE EQUATIONS

$$C_{dc}\frac{\mathrm{d}\left(v_{co}^{+}\right)}{\mathrm{dt}} = i_{co^{+}} = i^{+} - i_{dc}^{+} = \sum_{k=1,x\in\{a,b,c\}}^{3} i_x\,\theta\left(i_x\right)\left(1-d_k\right) - i_{dc}^{+}$$

$$C_{dc}\frac{\mathrm{d}\left(v_{co}^{-}\right)}{\mathrm{dt}} = i_{co}^{-} = i^{-} - i_{dc}^{-} = \sum_{k=1,x\in\{a,b,c\}}^{3} -i_x\,\theta\left(i_x\right)\left(1-d_k\right) - i_{dc}^{-}$$

$$\Downarrow$$

$$C_{dc}\frac{\mathrm{d}\left(v_{co}\right)}{\mathrm{dt}} = \sum_{k=1,x\in\{a,b,c\}}^{3}\left(1-d_k\right)\mathrm{sgn}\left(i_x\right)\, i_x - i_{dc}^{+} - i_{dc}^{-}$$

$$C_{dc}\frac{\mathrm{d}\left(\Delta v_{co}\right)}{\mathrm{dt}} = \sum_{k=1,x\in\{a,b,c\}}^{3} d_k^{'}\left[\mathrm{sgn}\left(i_x\right) - \frac{\Delta v_{dc}}{v_{dc}}\right] i_x - i_{dc}^{+} + i_{dc}^{-}$$

abc/dqo TRANSFORM

$$\begin{bmatrix} \dfrac{\mathrm{d}(Ki_x)}{\mathrm{dt}} \\ C_{dc}\dfrac{\mathrm{d}(v_{co})}{\mathrm{dt}} \\ C_{dc}\dfrac{\mathrm{d}(\Delta v_{co})}{\mathrm{dt}} \end{bmatrix} = \begin{bmatrix} \dot{K}\, i_x + \dfrac{1}{L}\left(Kv_x - r_L K i_x - \dfrac{v_{dc}}{6} MKd_k'\right) \\ \dfrac{3}{2}(Kd_k')^T (Ki_x) - \dfrac{\Delta v_{dc}}{v_{dc}} (Kd_k')^T \left[K\,\mathrm{SGN}^{-1} K^T\right]^{-1} (Ki_x) - i_{dc}^{+} - i_{dc}^{-} \\ (Kd_k')^T \left[K\,\mathrm{SGN}^{-1} K^T\right]^{-1} (Ki_x) - \dfrac{3}{2}\dfrac{\Delta v_{dc}}{v_{dc}} (Kd_k')^T (Ki_x) - i_{dc}^{+} + i_{dc}^{-} \end{bmatrix}$$

$$x = \{a, b, c\}, \quad k = \{1,2,3\}$$

AVERAGE STATE MODEL

$$\frac{\mathrm{d}(i_d)}{\mathrm{dt}} = \frac{1}{L}\left(v_d - r_L i_d + L\omega_o i_q - \frac{v_{dc}}{2} d_d^{'}\right)$$

$$\frac{\mathrm{d}(i_q)}{\mathrm{dt}} = \frac{1}{L}\left(v_q - r_L i_q - L\omega_o i_d - \frac{v_{dc}}{2} d_q^{'}\right)$$

$$\frac{\mathrm{d}(v_{co})}{dt} = \frac{1}{C_{dc}}\left[\frac{3}{2}\left(d_d^{'} i_d + d_q^{'} i_q\right) - \alpha \frac{\Delta v_{dc}}{v_{dc}} d_o^{'} i_d - i_{dc}^{+} - i_{dc}^{-}\right]$$

$$\frac{\mathrm{d}(\Delta v_{co})}{\mathrm{dt}} = \frac{1}{C_{dc}}\left[-\frac{3}{2}\frac{\Delta v_{dc}}{v_{dc}}\left(d_d^{'} i_d + d_q^{'} i_q\right) + \alpha d_o^{'} i_d - i_{dc}^{+} + i_{dc}^{-}\right]$$

EXPERIMENTAL VALIDATION OF THE LARGE SIGNAL MODEL (LSM)

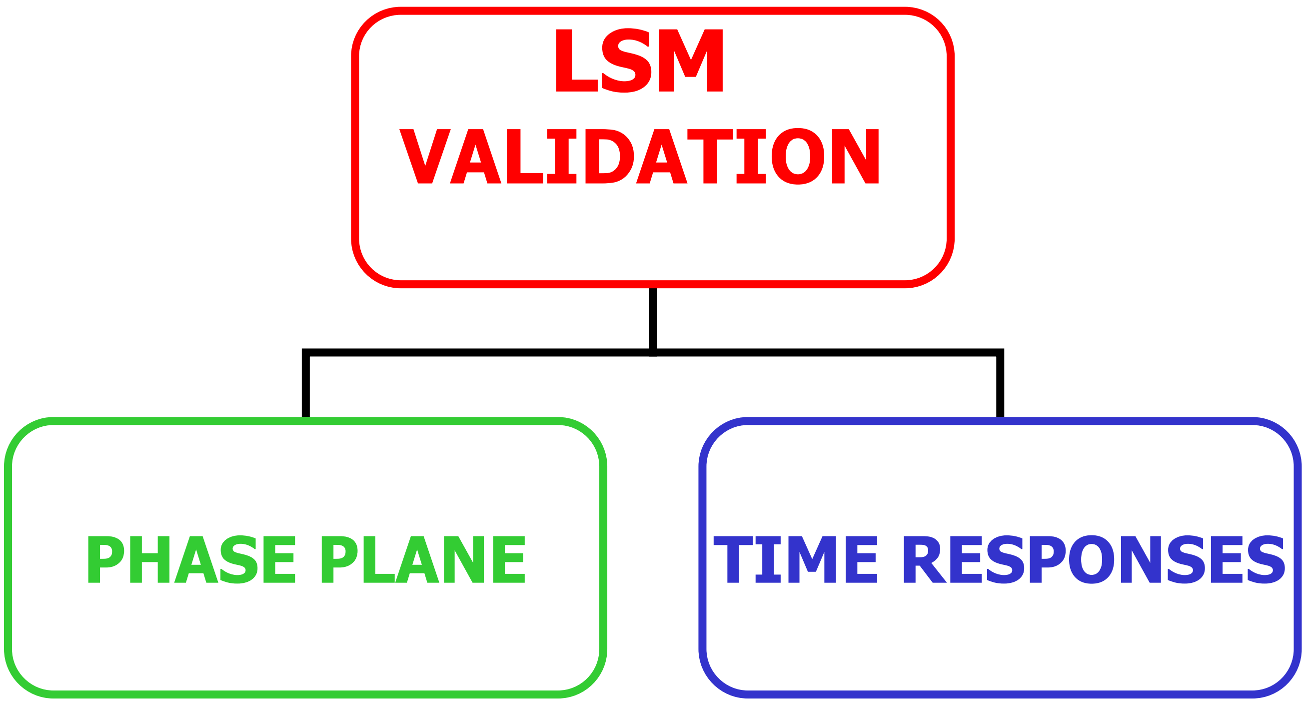

VALIDATION 1: PHASE PLANE METHOD

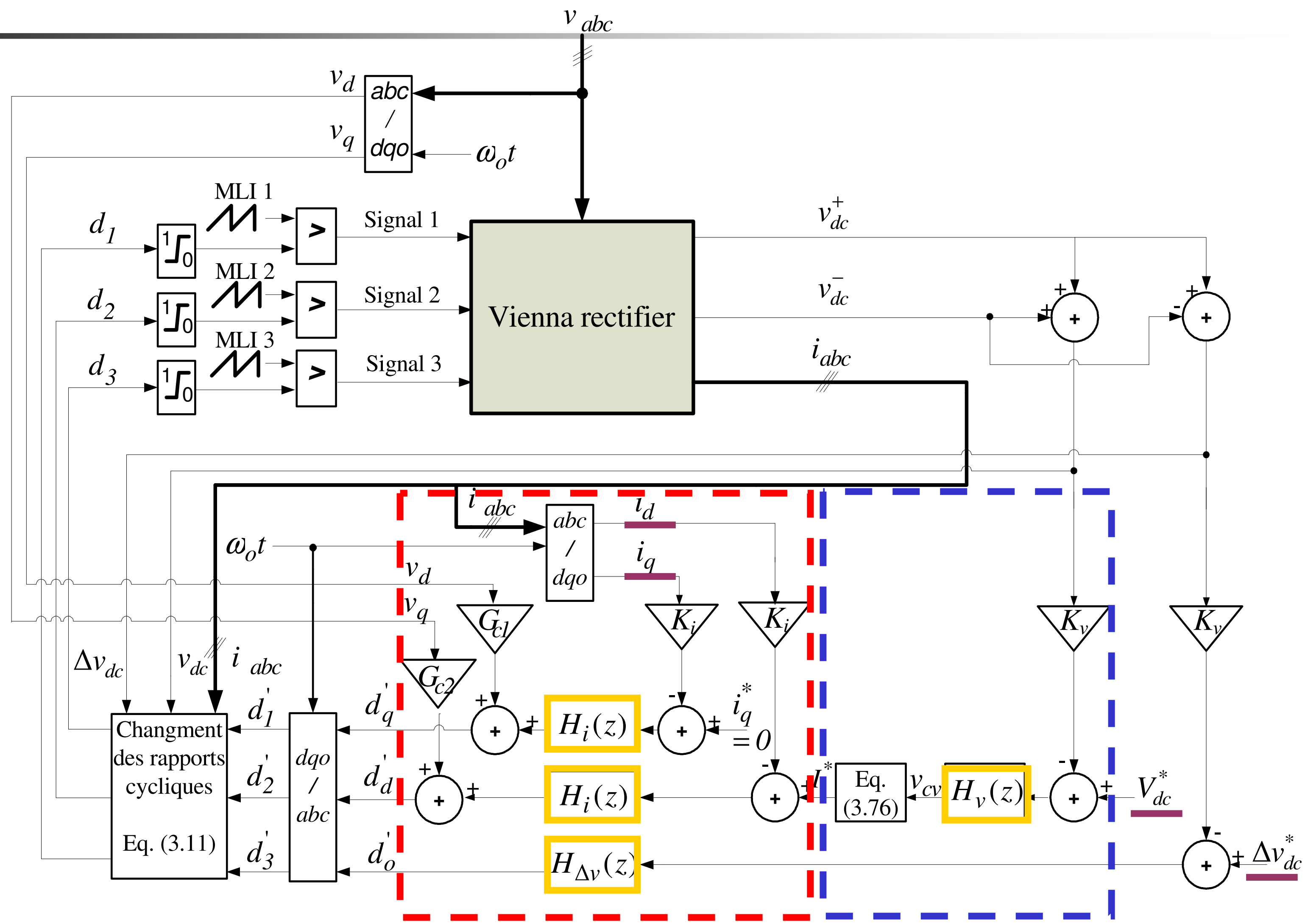

TRAJECTORIES IN THE PHASE PLANE

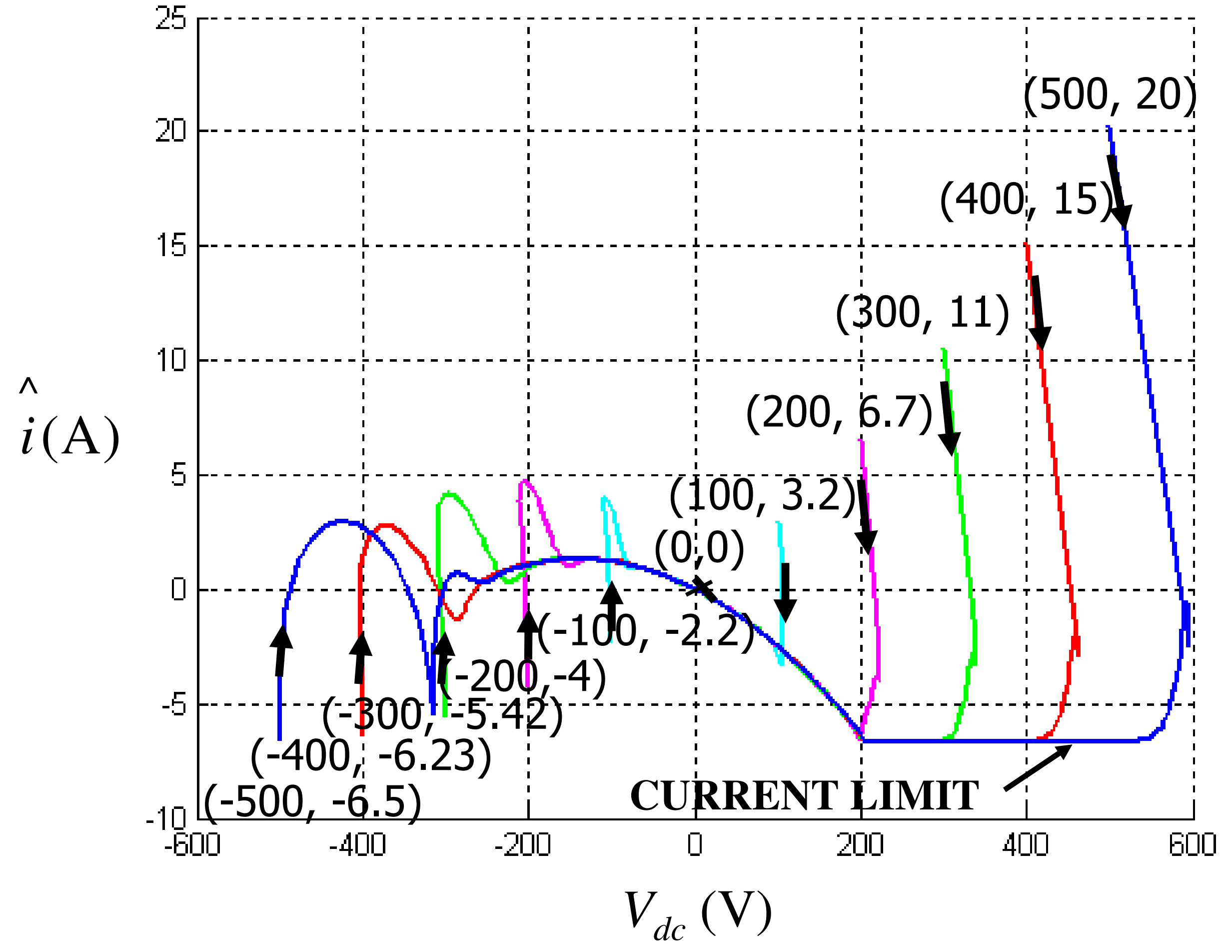

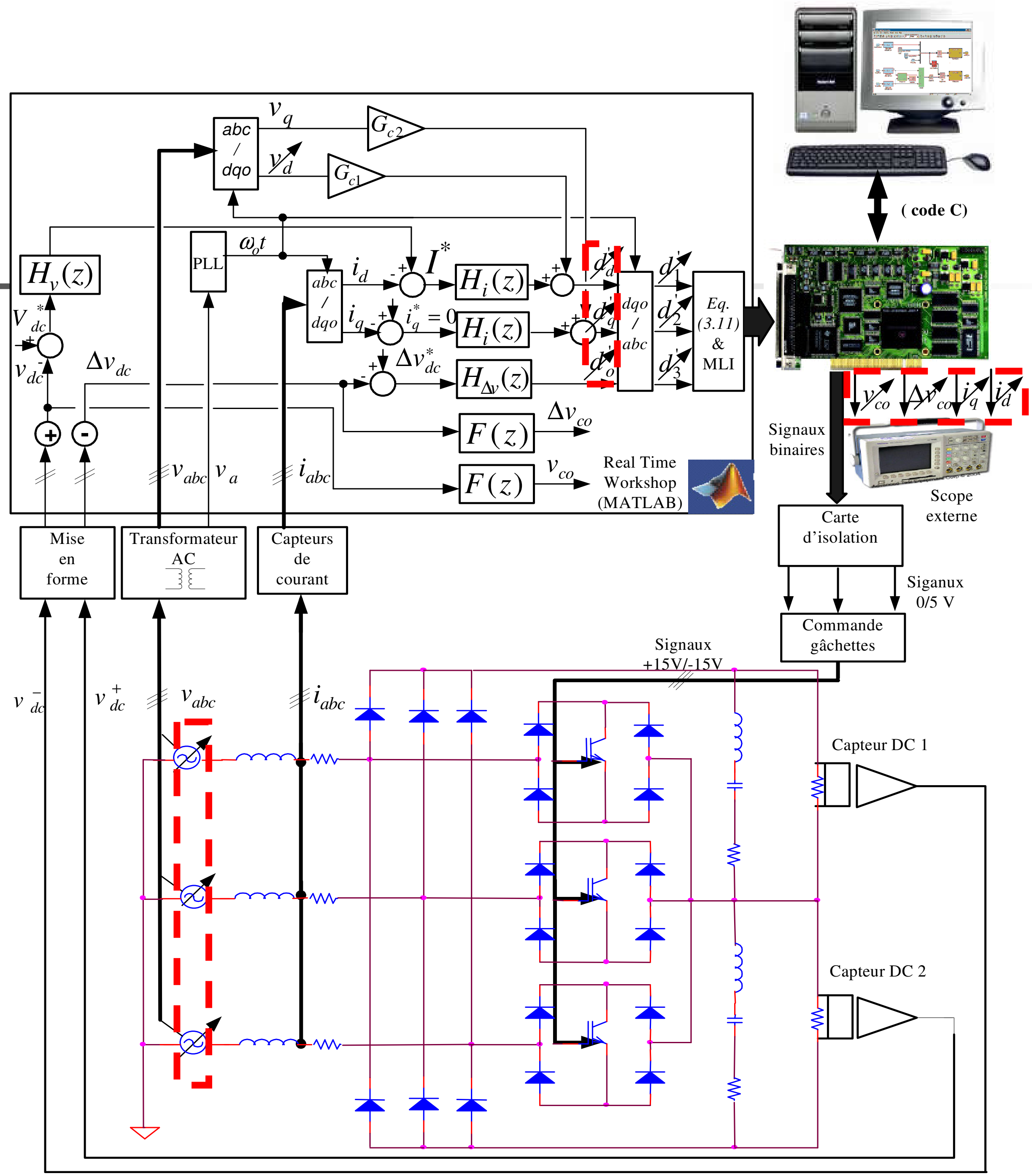

abc / dqo
v_q
v_d
G_{c2}
G_{c1}
$H_v(z)$
PLL
$\omega_o t$
i_d
i_q
I^*
$i_q^* = 0$
$H_i(z)$
$H_{\Delta v}(z)$
Δv_{dc}^*
d_d'
d_q'
d_o'
dqo / abc
d_1'
d_2'
d_3'
Eq. (3.11) & MLI
V_{dc}^*
v_{dc}
Δv_{dc}
$F(z)$
Δv_{co}
v_{co}
v_{abc}
v_a
i_{abc}
Real Time Workshop (MATLAB)
(code C)
Signaux binaires
Scope externe
Carte d'isolation
Siganux 0/5 V
Commande gâchettes
Signaux +15V/-15V
Mise en forme
Transformateur AC
Capteurs de courant
v_{dc}^-
v_{dc}^+
Capteur DC 1
Capteur DC 2

	LSM	Experimental
i_d	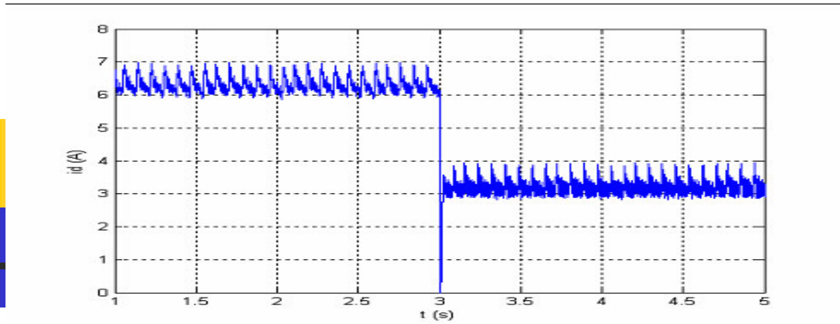	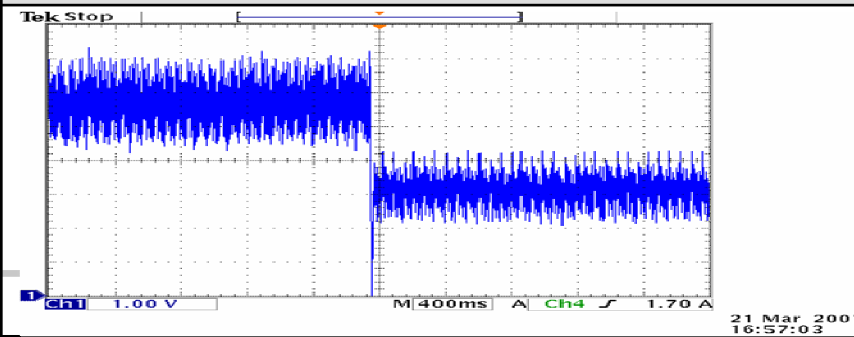
i_q	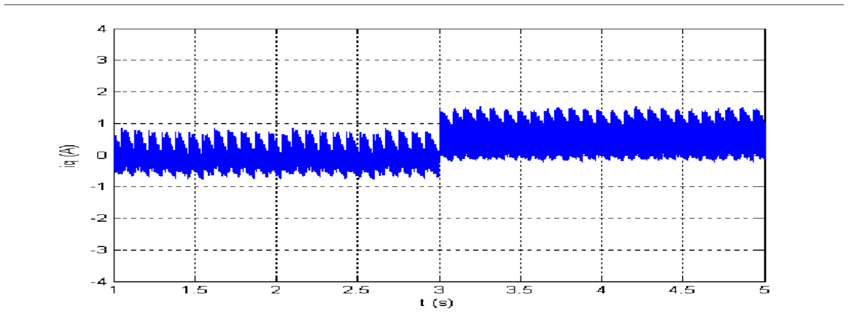	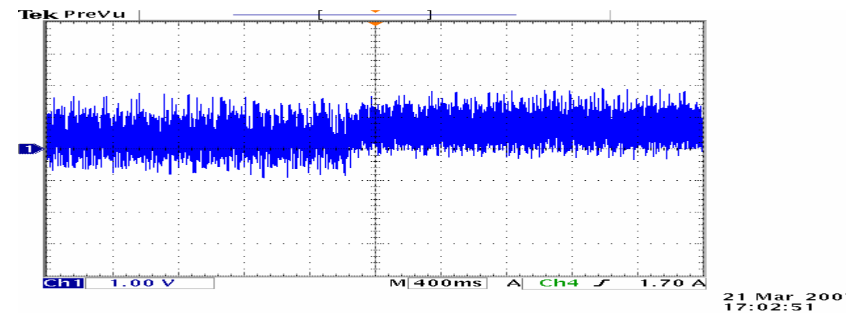
v_{co}	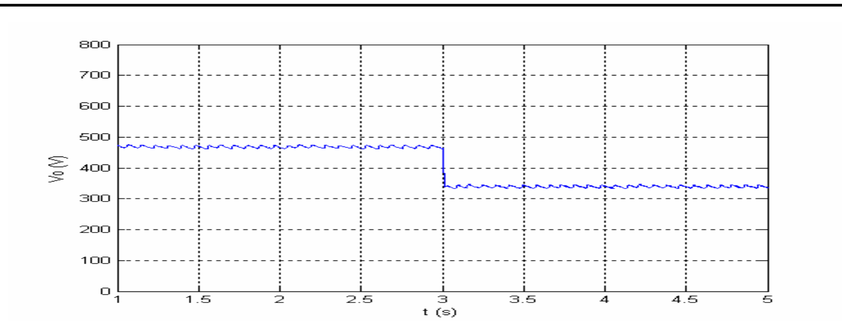	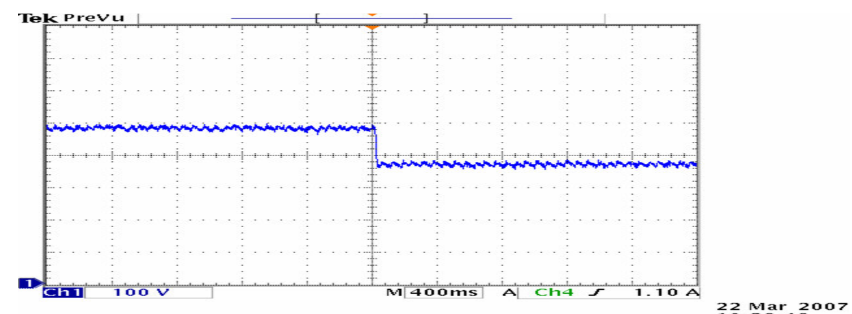
Δv_{co}	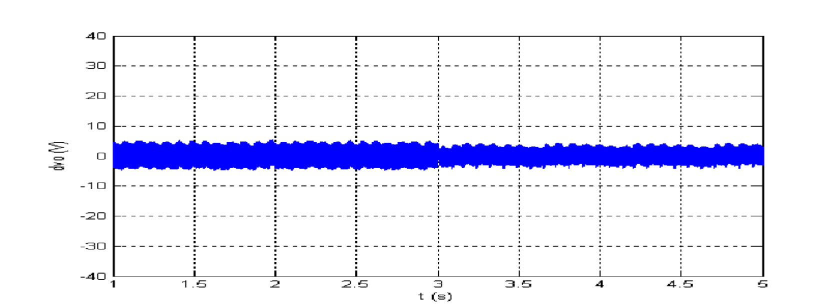	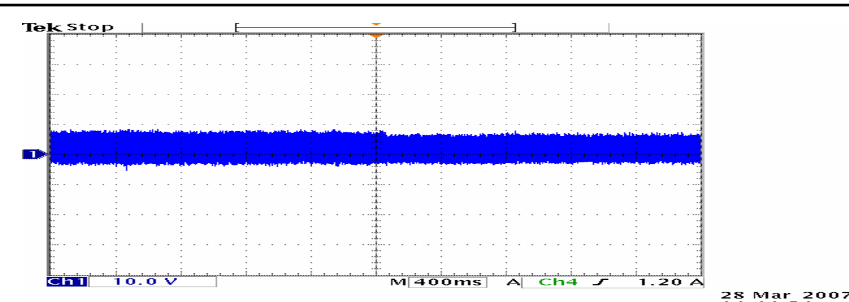

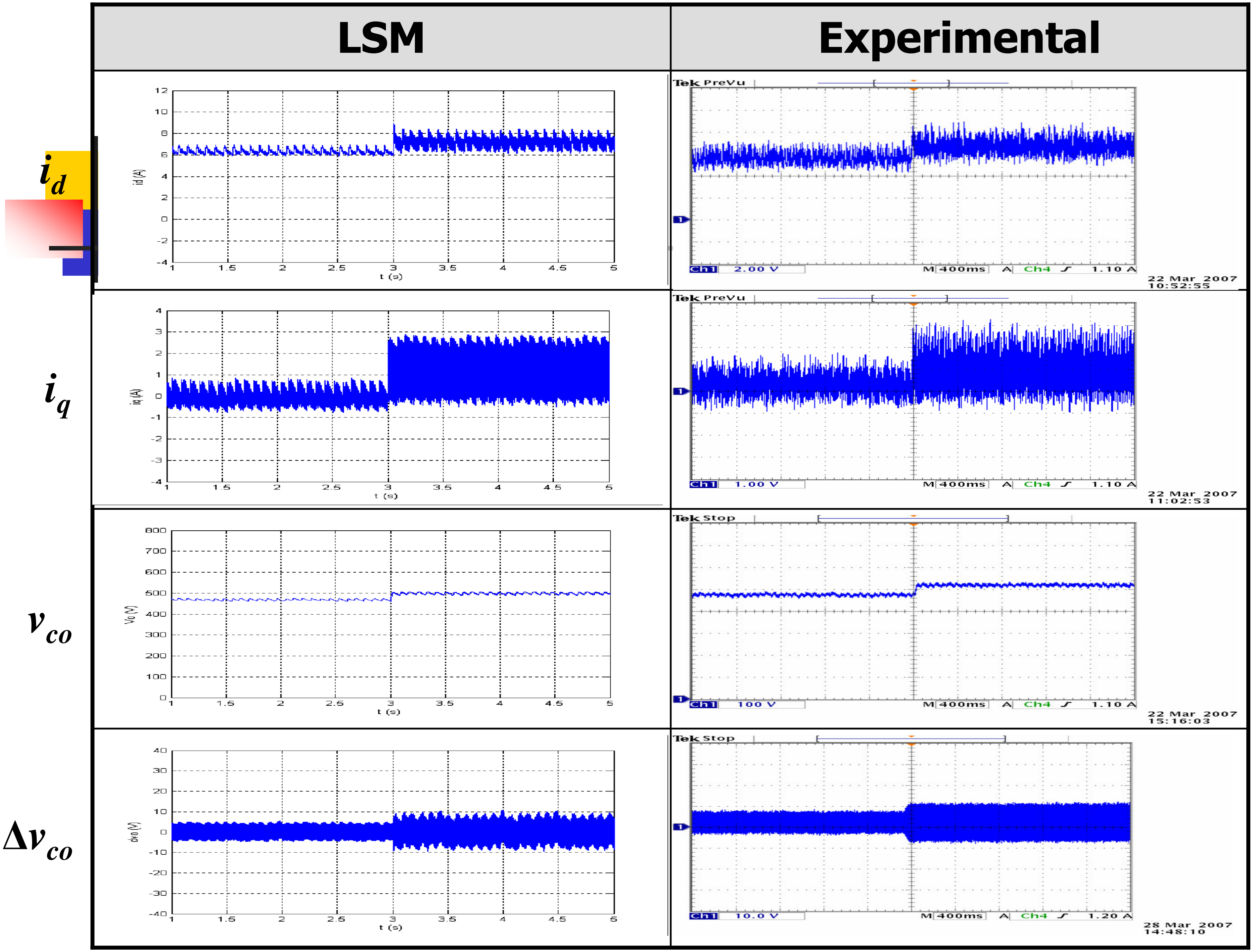
LSM
Experimental
i_d
i_q
v_co
Δv_co
id (A)
iq (A)
Vo (V)
dvo (V)
t (s)
Tek PreVu
Ch1 2.00 V
M 400ms A Ch4 1.10 A
22 Mar 2007
10:52:55
Tek PreVu
Ch1 1.00 V
M 400ms A Ch4 1.10 A
22 Mar 2007
11:02:53
Tek Stop
Ch1 100 V
M 400ms A Ch4 1.10 A
22 Mar 2007
15:16:03
Tek Stop
Ch1 10.0 V
M 400ms A Ch4 1.20 A
28 Mar 2007
14:48:10

LSM | **Experimental**

i_d

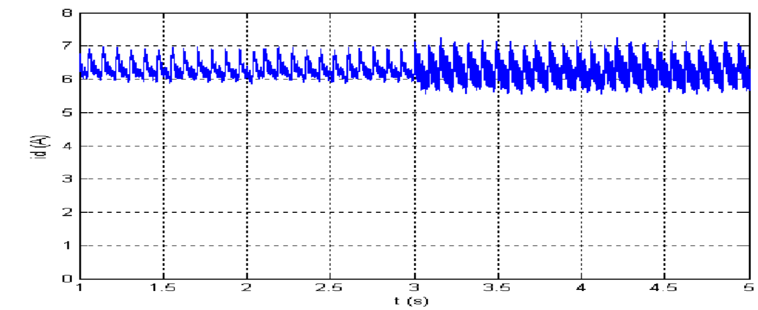

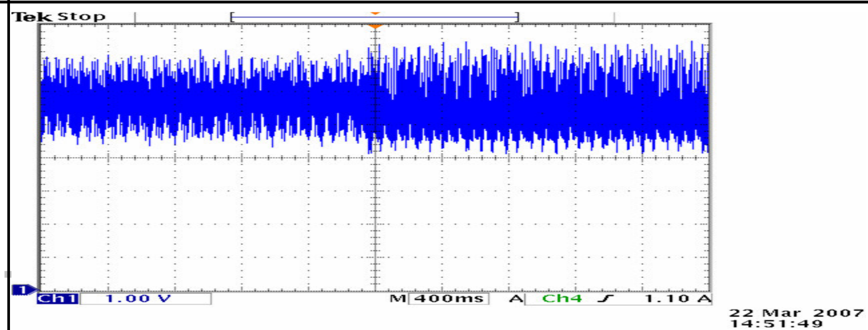

i_q

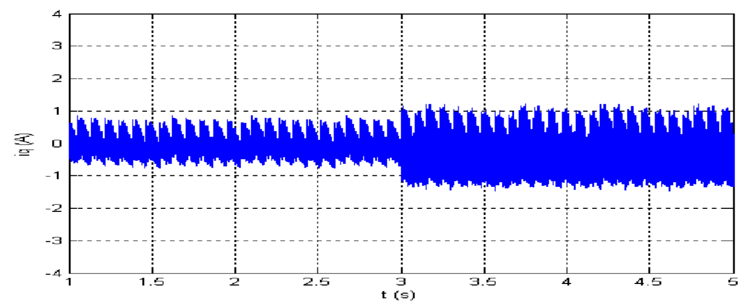

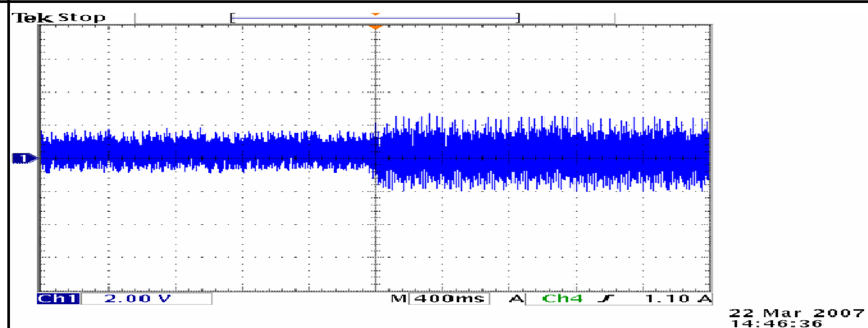

v_{co}

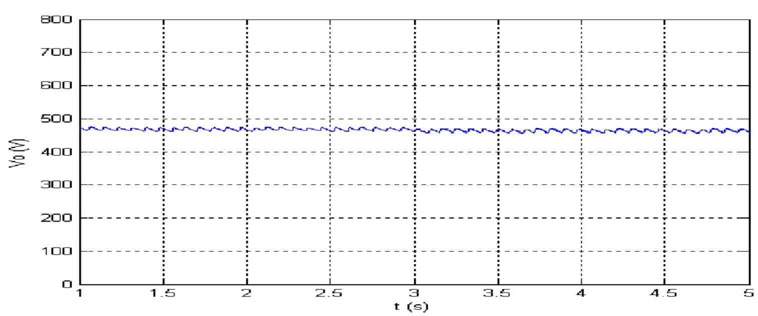

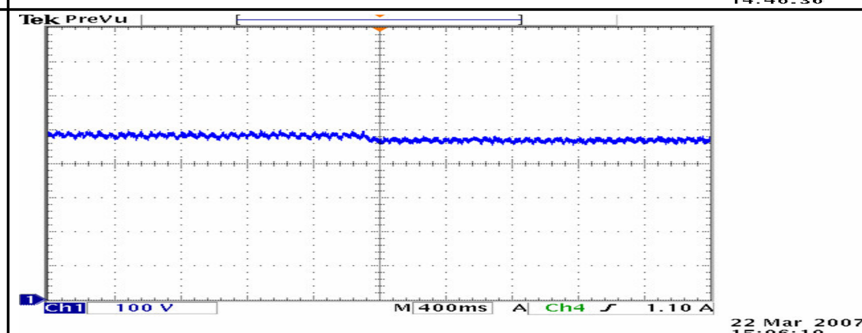

Δv_{co}

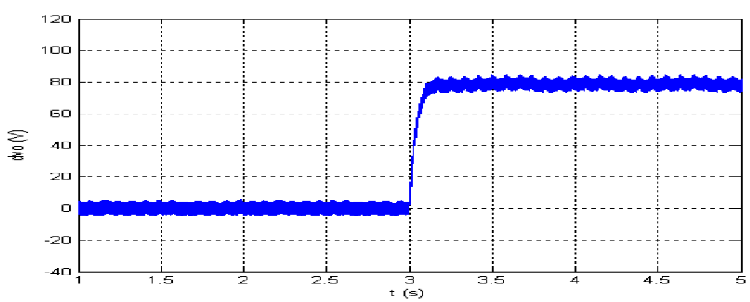

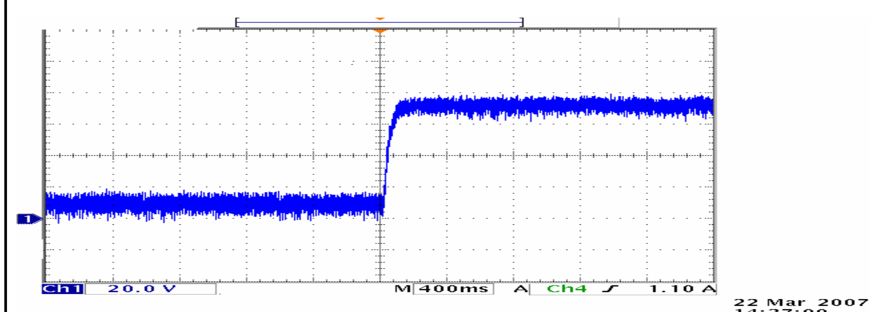

	LSM	Experimental
i_d	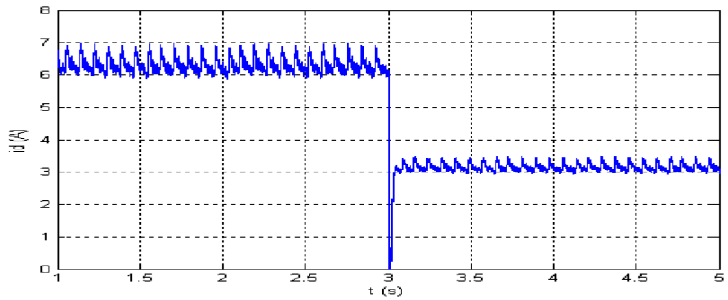	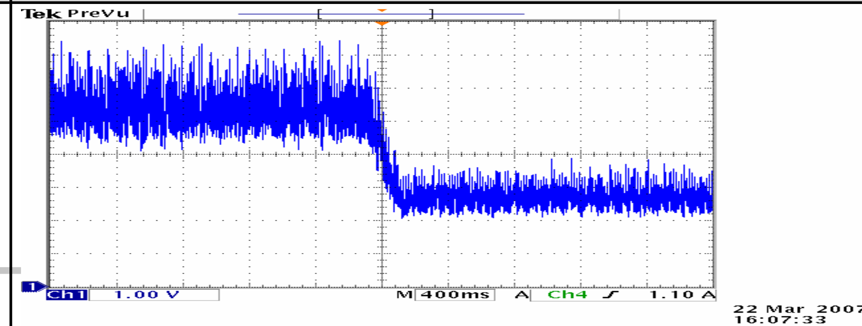
i_q	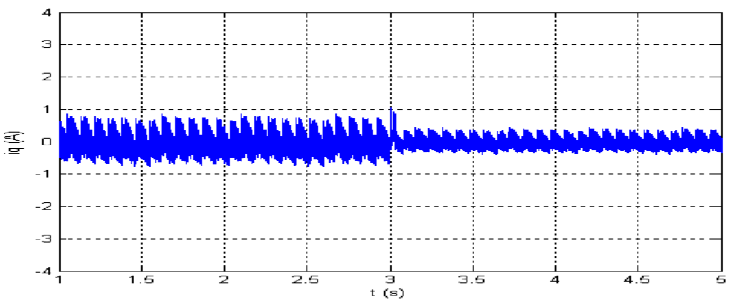	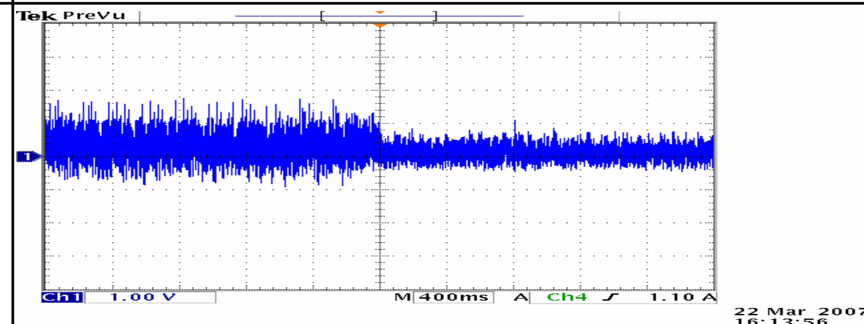
v_{co}	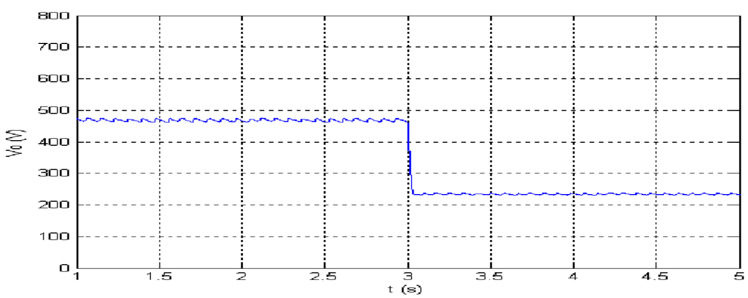	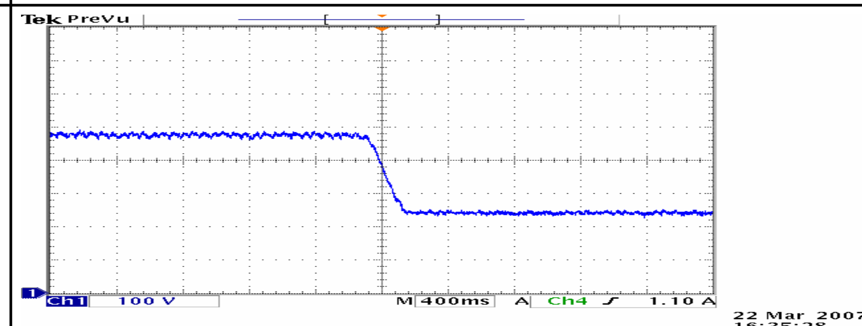
Δv_{co}	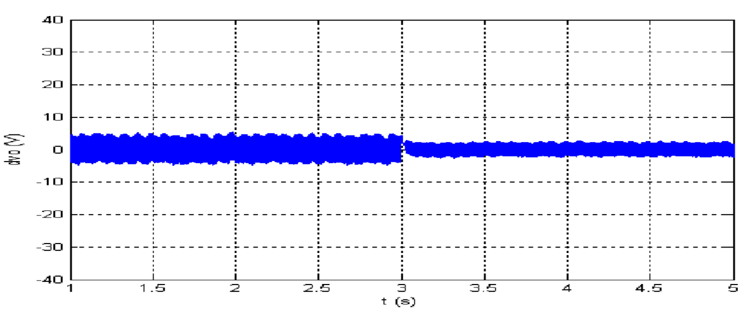	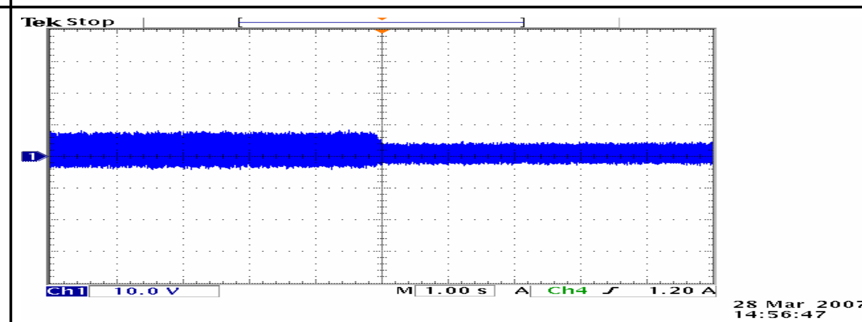

MODELS TYPES

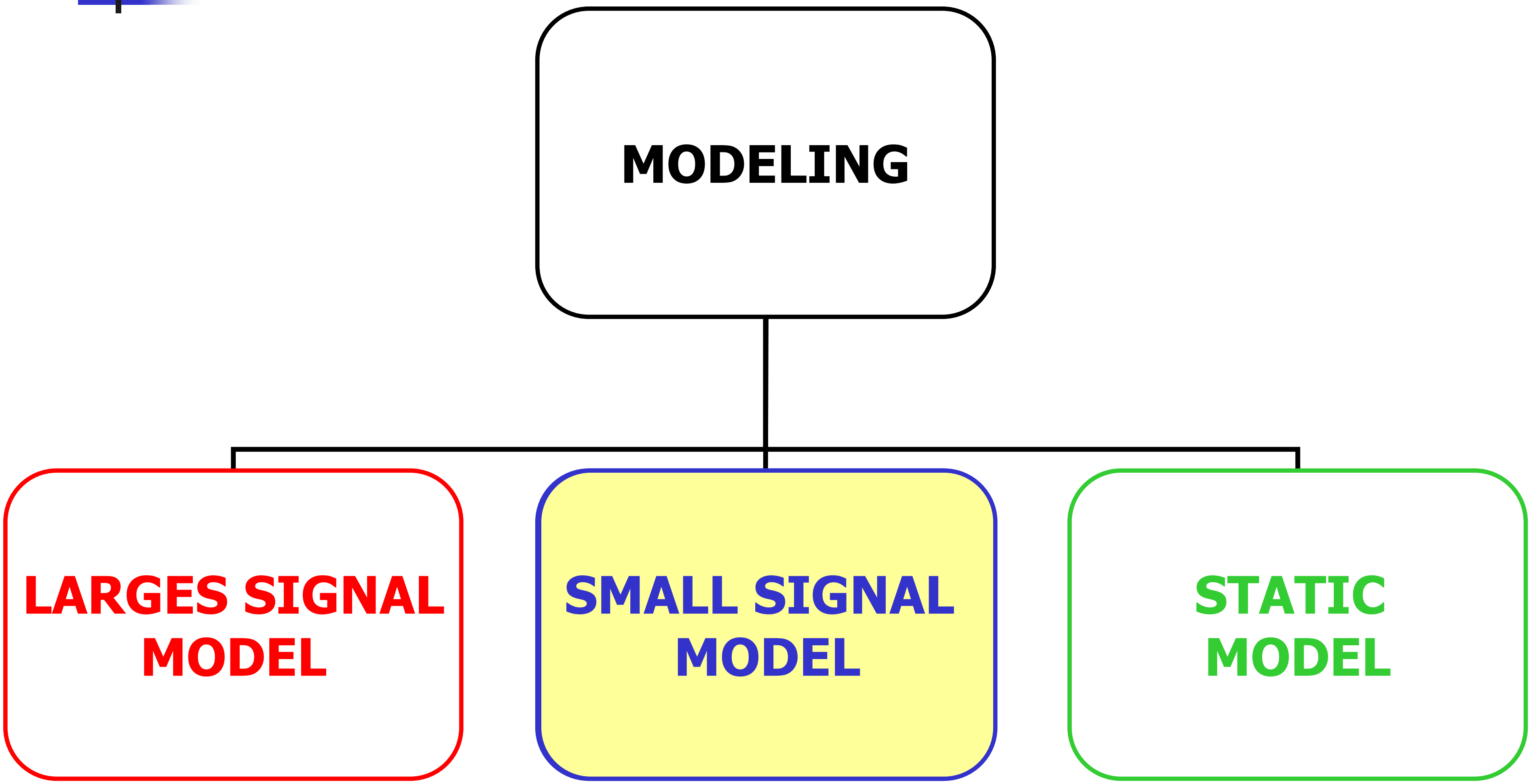

SMALL SIGNAL MODEL

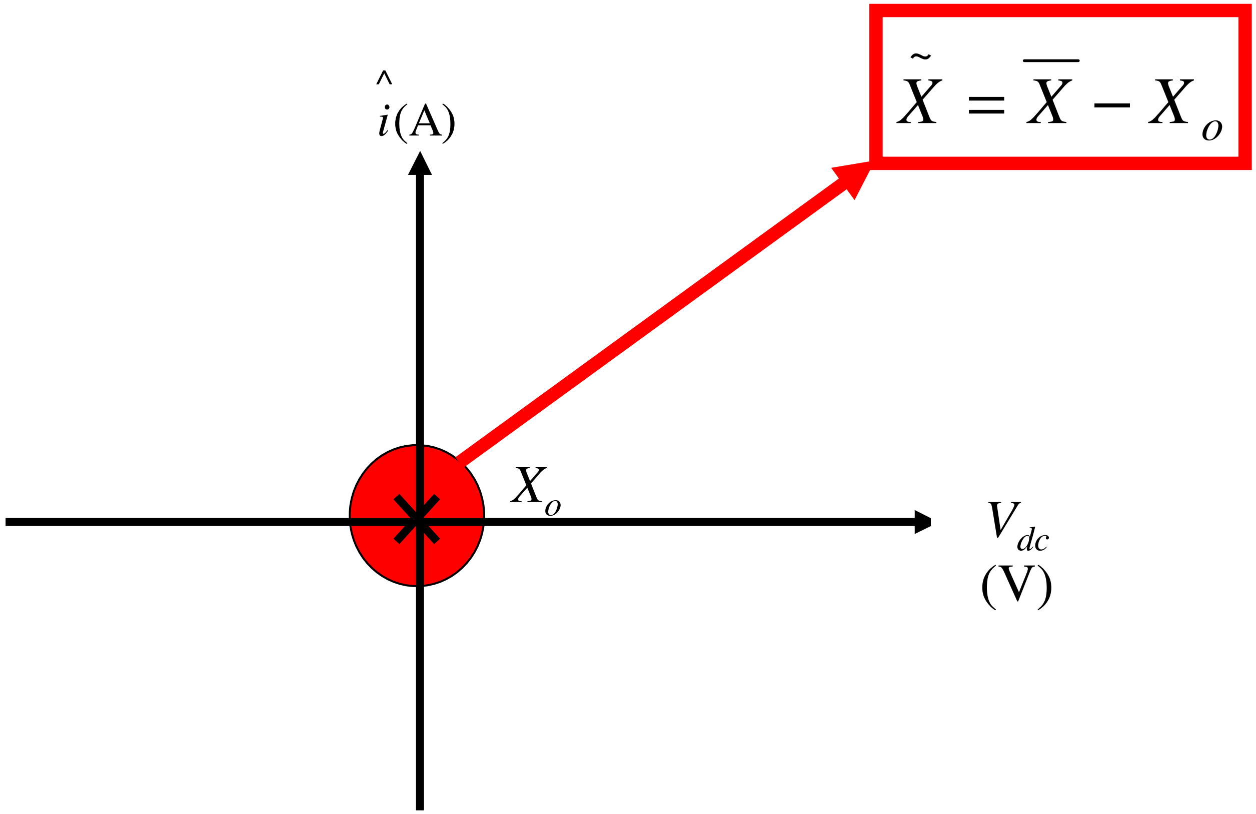

TRANSFERT FUNCTIONS DERIVATION

$$\tilde{X}(s) = \left(sI - A\right)^{-1} B\,\tilde{d}(s) + \left(sI - A\right)^{-1} E\,\tilde{v}(s)$$

$$A = \left.\frac{\partial f}{\partial \overline{X}}\right|_{X=X_o} , \quad B = \left.\frac{\partial f}{\partial d}\right|_{X=X_o} , \quad E = \left.\frac{\partial f}{\partial \overline{v}}\right|_{X=X_o}$$

EXPERIMENTAL VALIDATION OF THE SMALL SIGNAL MODEL

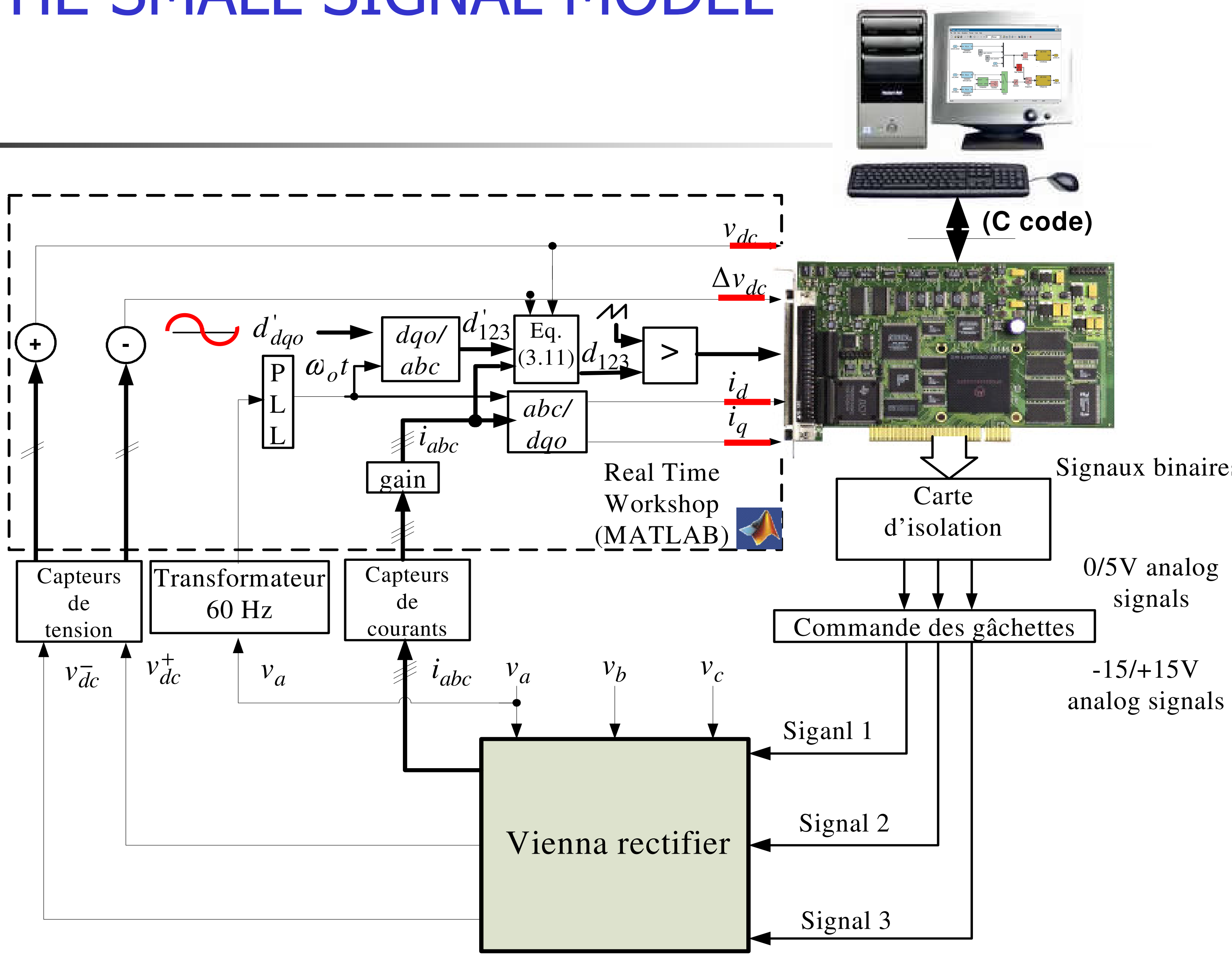

EQUIVALENT MODEL OF THE RECTIFIER IN THE FREQUENCY DOMAIN

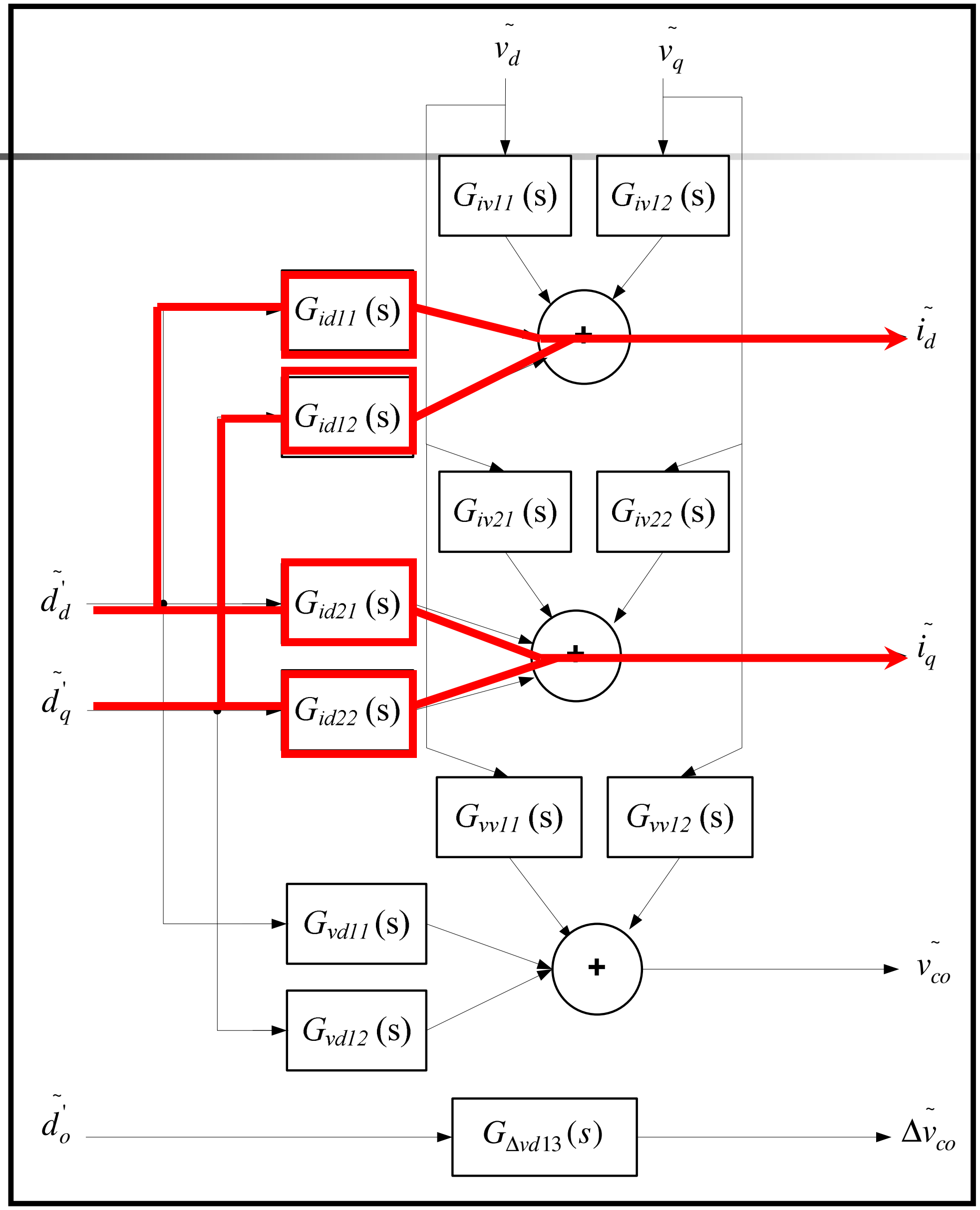

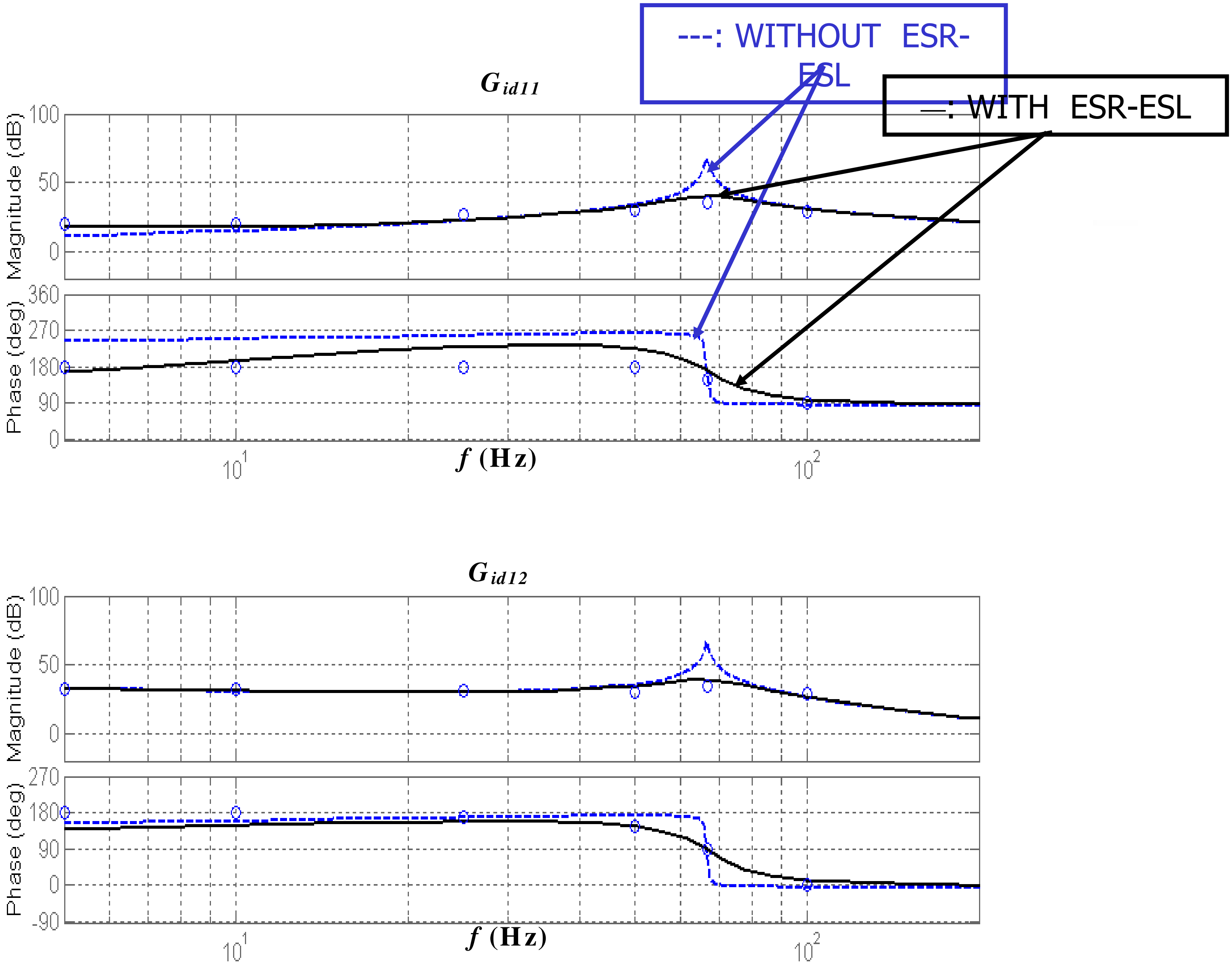
---: WITHOUT ESR-ESL
—: WITH ESR-ESL
G_{id11}
Magnitude (dB)
100
50
0
Phase (deg)
360
270
180
90
0
f (Hz)
10^1
10^2
G_{id12}
Magnitude (dB)
100
50
0
Phase (deg)
270
180
90
0
-90
f (Hz)
10^1
10^2

G_{id21}

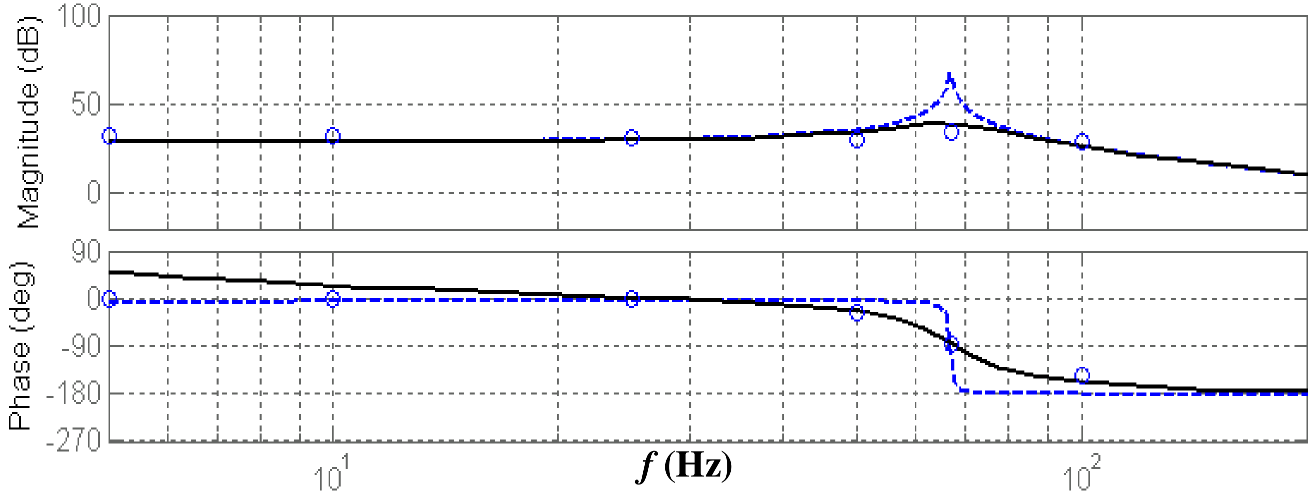

100
50
0
Magnitude (dB)
90
0
-90
-180
-270
Phase (deg)
10^1
10^2
f (Hz)

G_{id22}

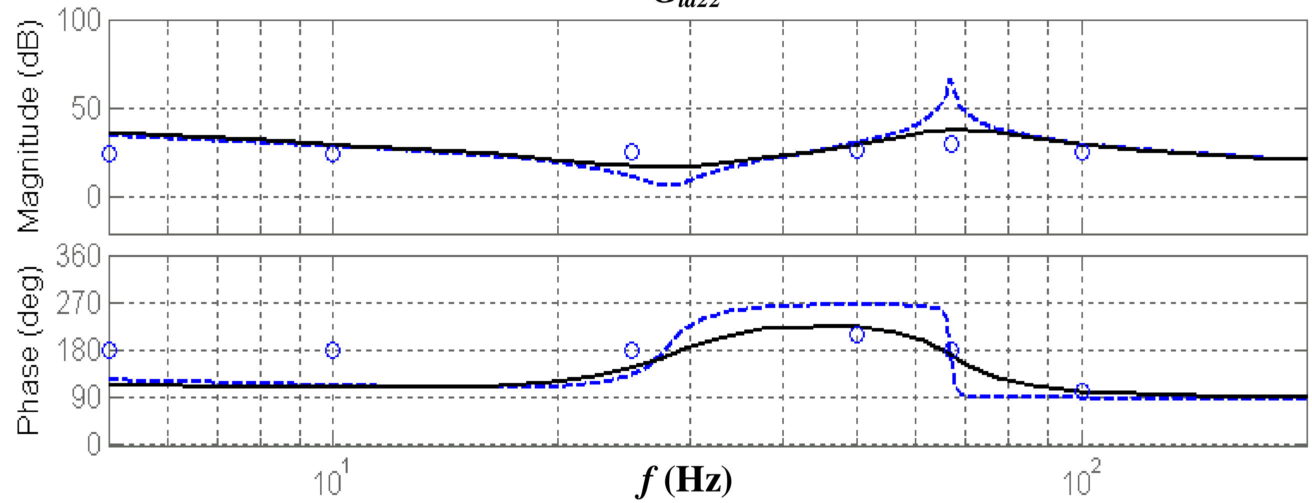

100
50
0
Magnitude (dB)
360
270
180
90
0
Phase (deg)
10^1
10^2
f (Hz)

G_{vd11}

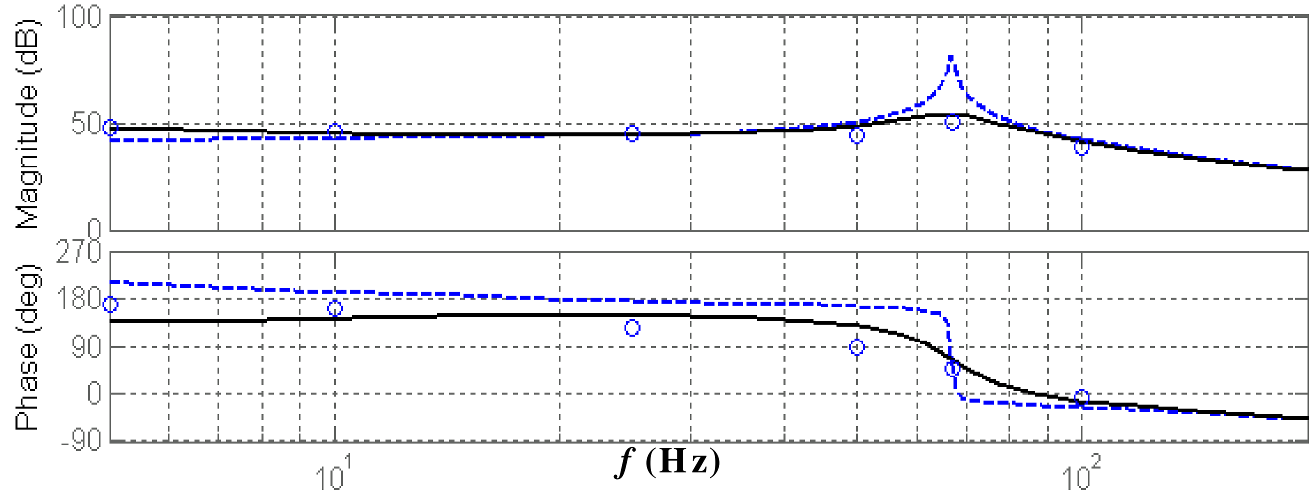
100
50
0
Magnitude (dB)
270
180
90
0
-90
Phase (deg)
10^1
10^2
f (Hz)

G_{vd12}

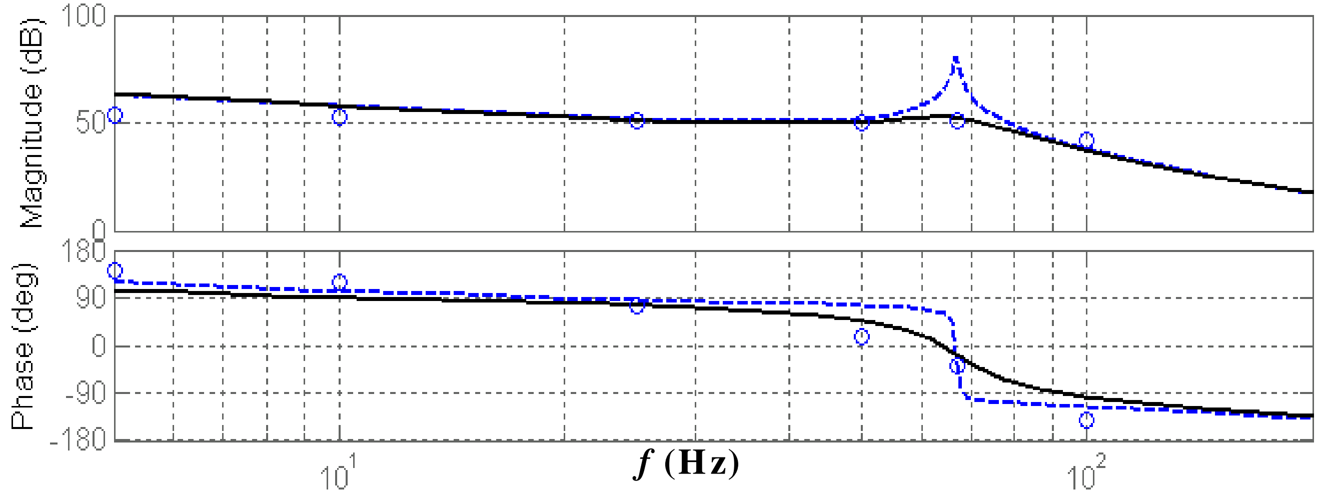
100
50
0
Magnitude (dB)
180
90
0
-90
-180
Phase (deg)
10^1
10^2
f (Hz)

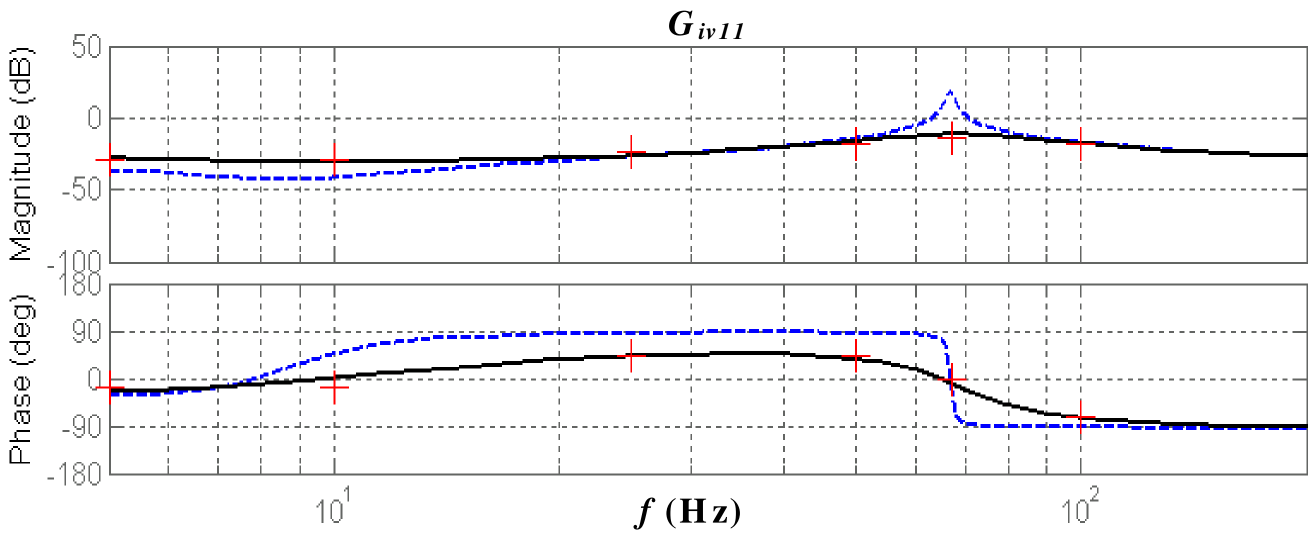

G_{iv11}
Magnitude (dB)
50
0
-50
-100
Phase (deg)
180
90
0
-90
-180
10^1
10^2
f (Hz)

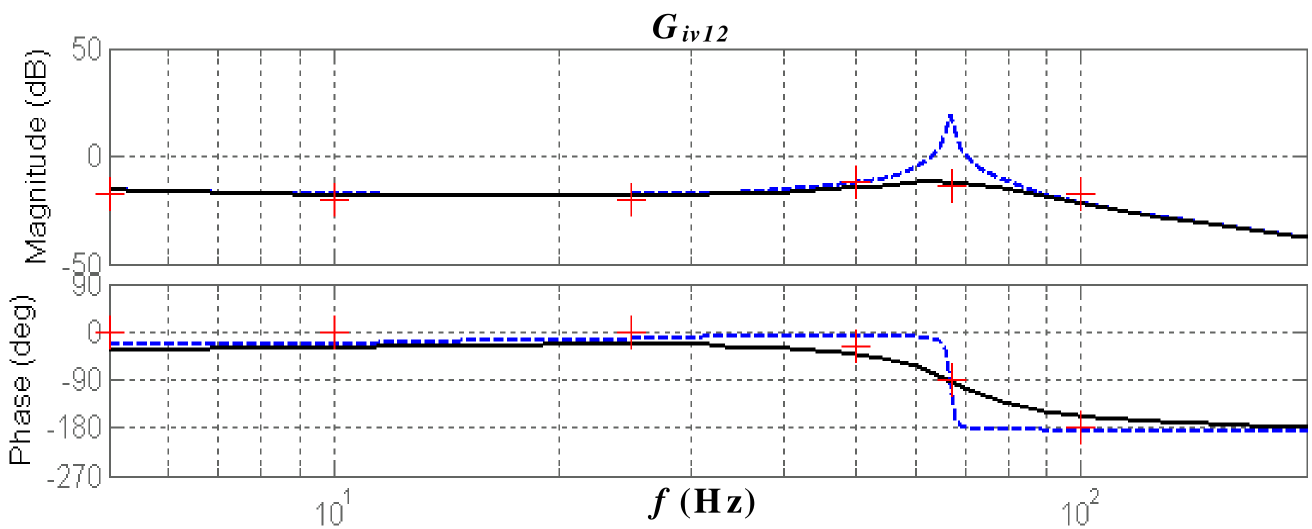

G_{iv12}
Magnitude (dB)
50
0
-50
Phase (deg)
90
0
-90
-180
-270
10^1
10^2
f (Hz)

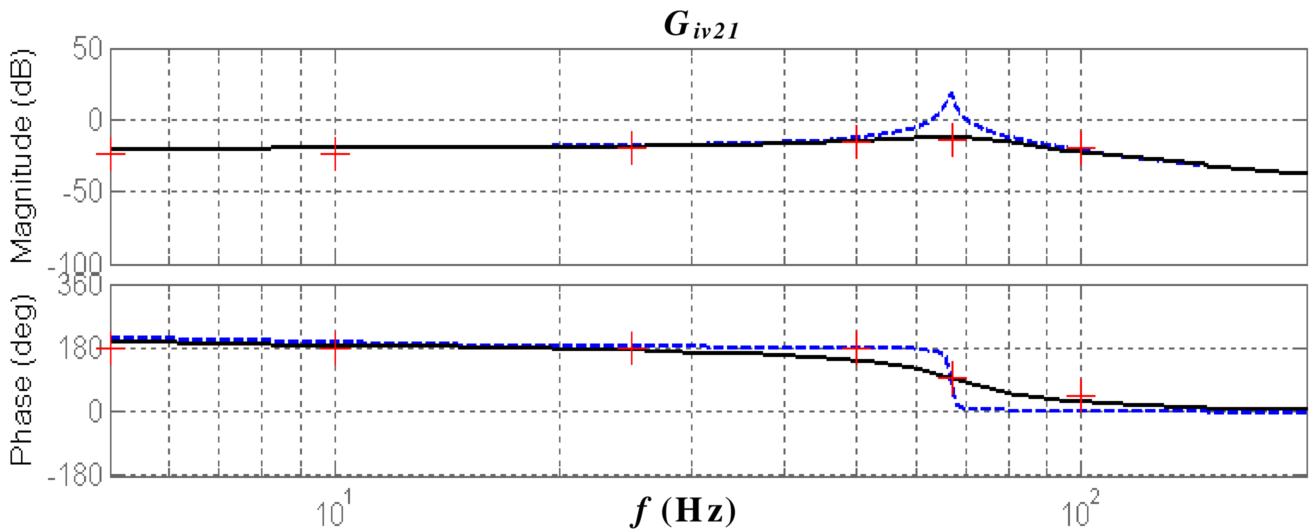

G_{iv21}
50
0
-50
-100
Magnitude (dB)
360
180
0
-180
Phase (deg)
10^1
10^2
f (Hz)

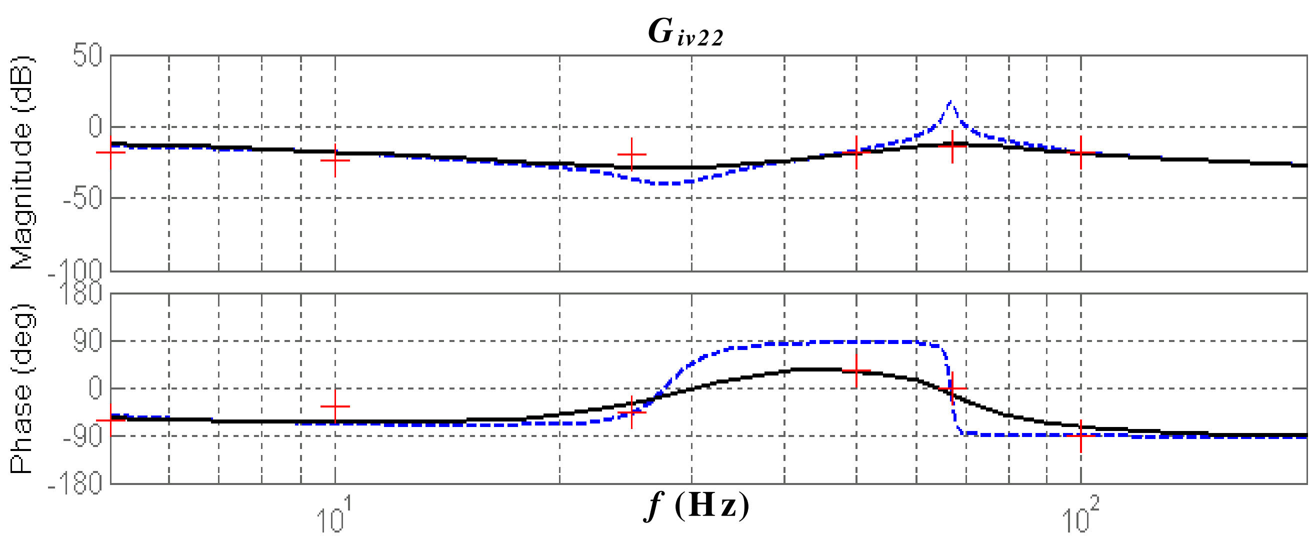

G_{iv22}
50
0
-50
-100
Magnitude (dB)
180
90
0
-90
-180
Phase (deg)
10^1
10^2
f (Hz)

G_{vv11}

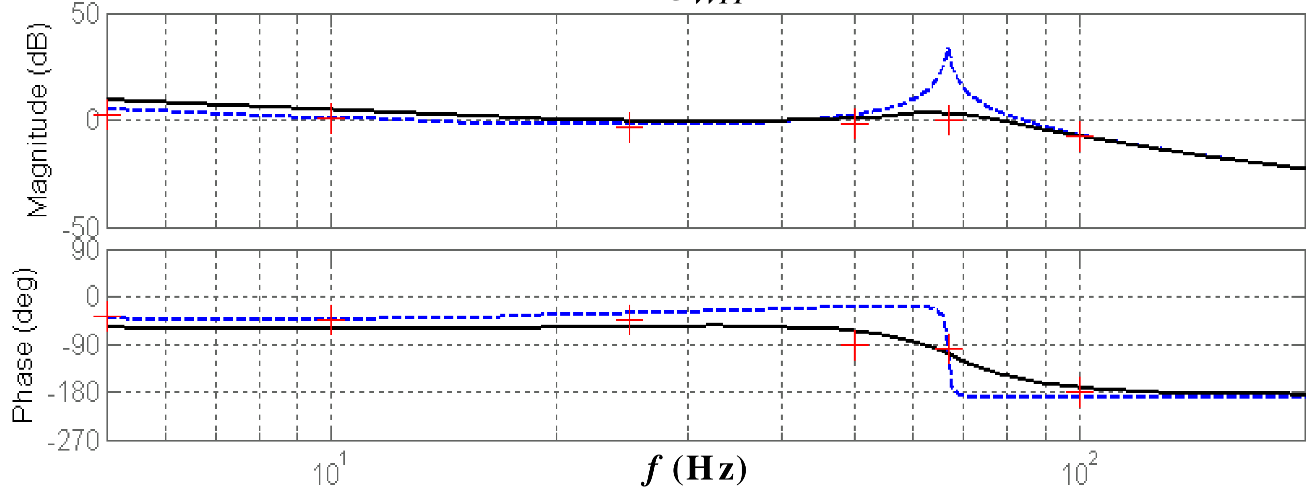
Magnitude (dB)
50
0
-50
Phase (deg)
90
0
-90
-180
-270
10^1
10^2
f (Hz)

G_{vv12}

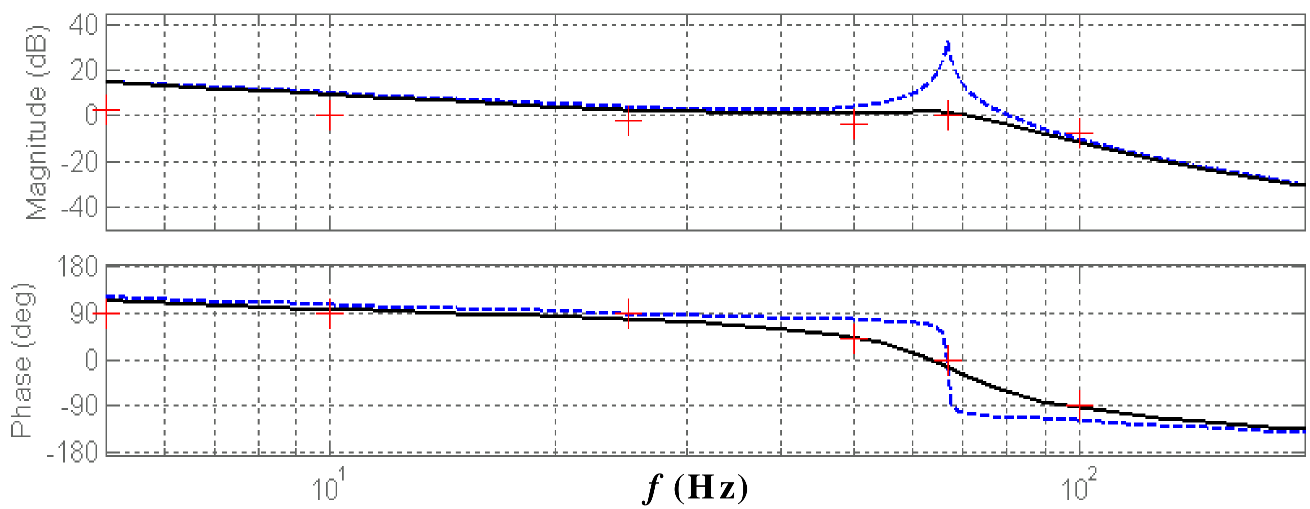
Magnitude (dB)
40
20
0
-20
-40
Phase (deg)
180
90
0
-90
-180
10^1
10^2
f (Hz)

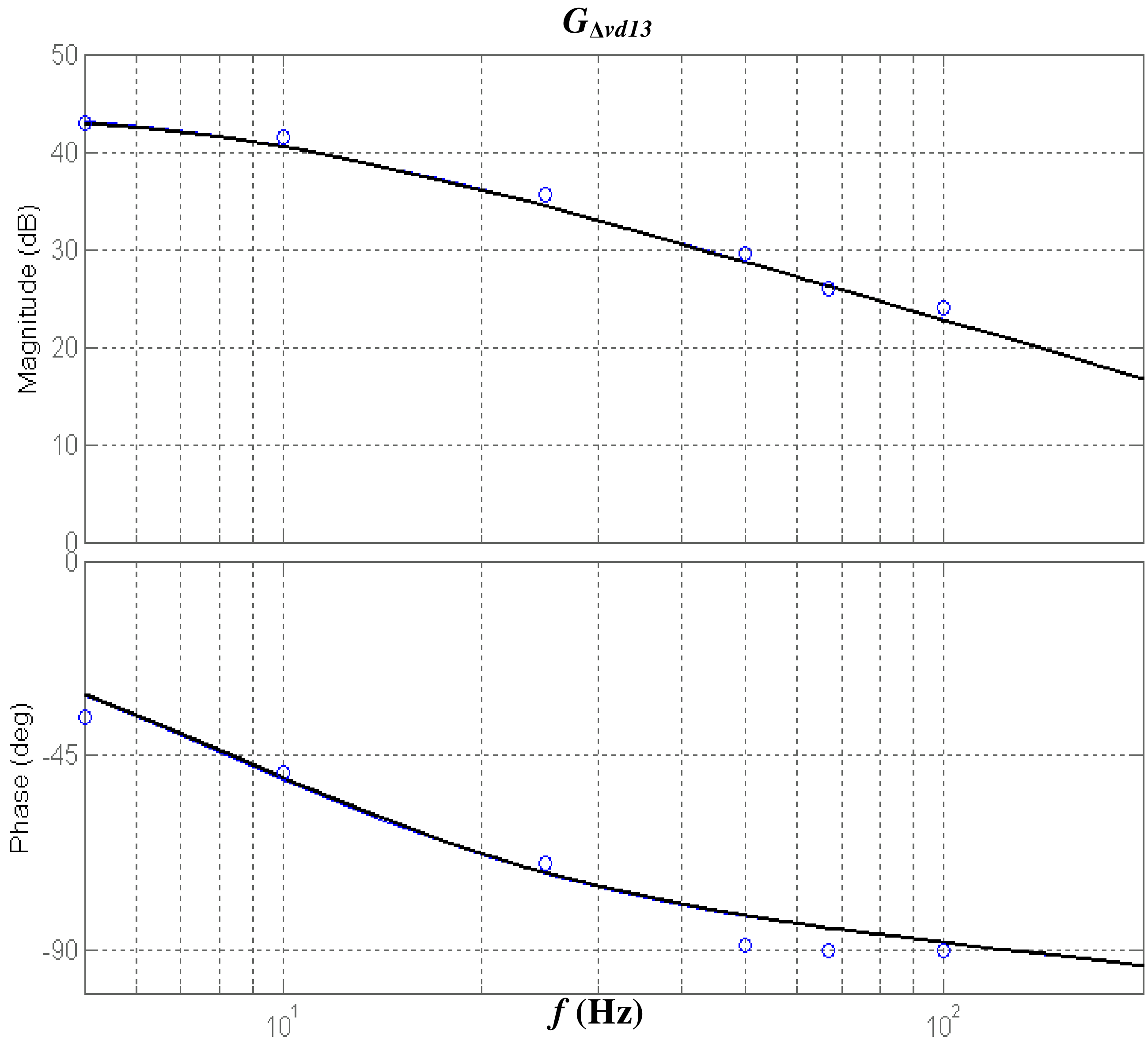

$G_{\Delta vd13}$
Magnitude (dB)
50
40
30
20
10
0
Phase (deg)
0
-45
-90
10^1
10^2
f (Hz)

MODELS TYPES

- **MODELING**
  - **LARGE SIGNAL MODEL**
  - **SMALL SIGNAL MODEL**
  - **STATIC MODEL**

STATIC MODEL

$$\begin{bmatrix} V_d \\ V_q \\ V_{so} \end{bmatrix} = \begin{bmatrix} \hat{V} \\ 0 \\ 0 \end{bmatrix}; \quad \begin{bmatrix} I_d \\ I_q \\ I_o \end{bmatrix} = \begin{bmatrix} \hat{I}^* \\ 0 \\ 0 \end{bmatrix}; \quad V_{dc} = V_{dc}^*; \quad V_{dc}^+ = V_{dc}^- = \frac{V_{dc}^*}{2}; \quad \Delta V_{dc}^* = 0$$

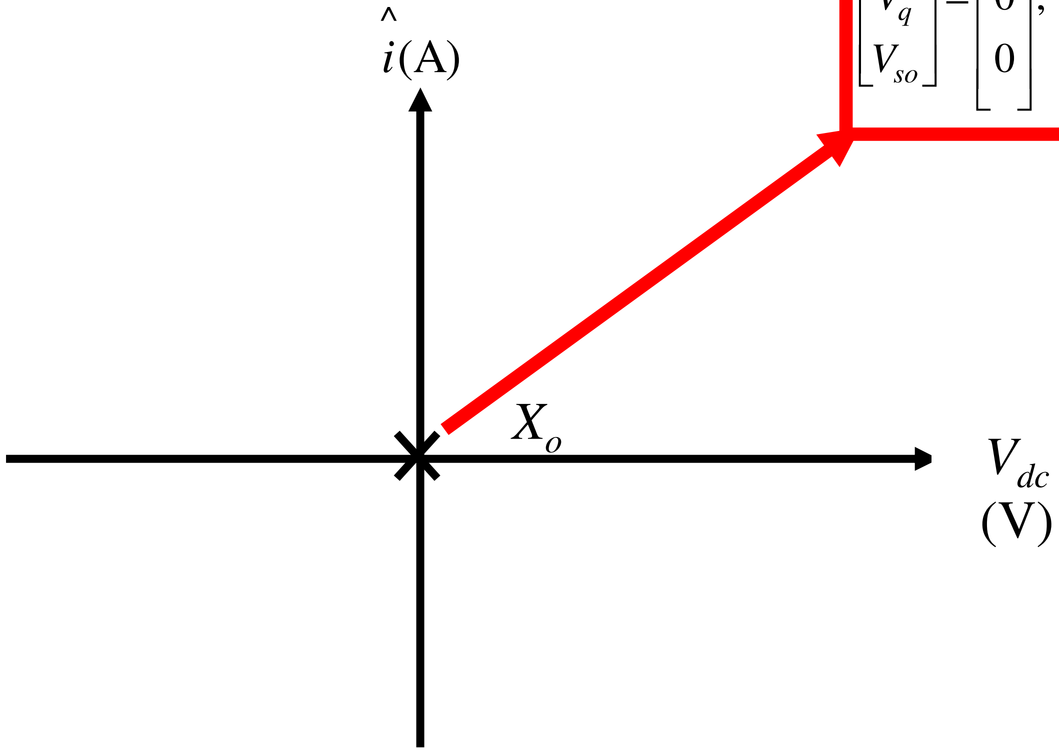

ELABORATION OF THE STATIC MODEL

$$\boxed{D_d^{'} = \frac{2(V_d - r_L I_d)}{V_{dc}^{*}}}$$

$$\boxed{D_q^{'} = -\frac{2L\omega_o I_d}{V_{dc}^{*}}}$$

$$\boxed{D_o^{'} = \frac{\left(I_{dc}^{+} - I_{dc}^{-}\right)}{\alpha I_d}}$$

FUNCTION DUTY CYCLE- DC VOLTAGE

$$D_d^{'} = \frac{2(V_d - r_L I_d)}{V_{dc}^{*}}$$

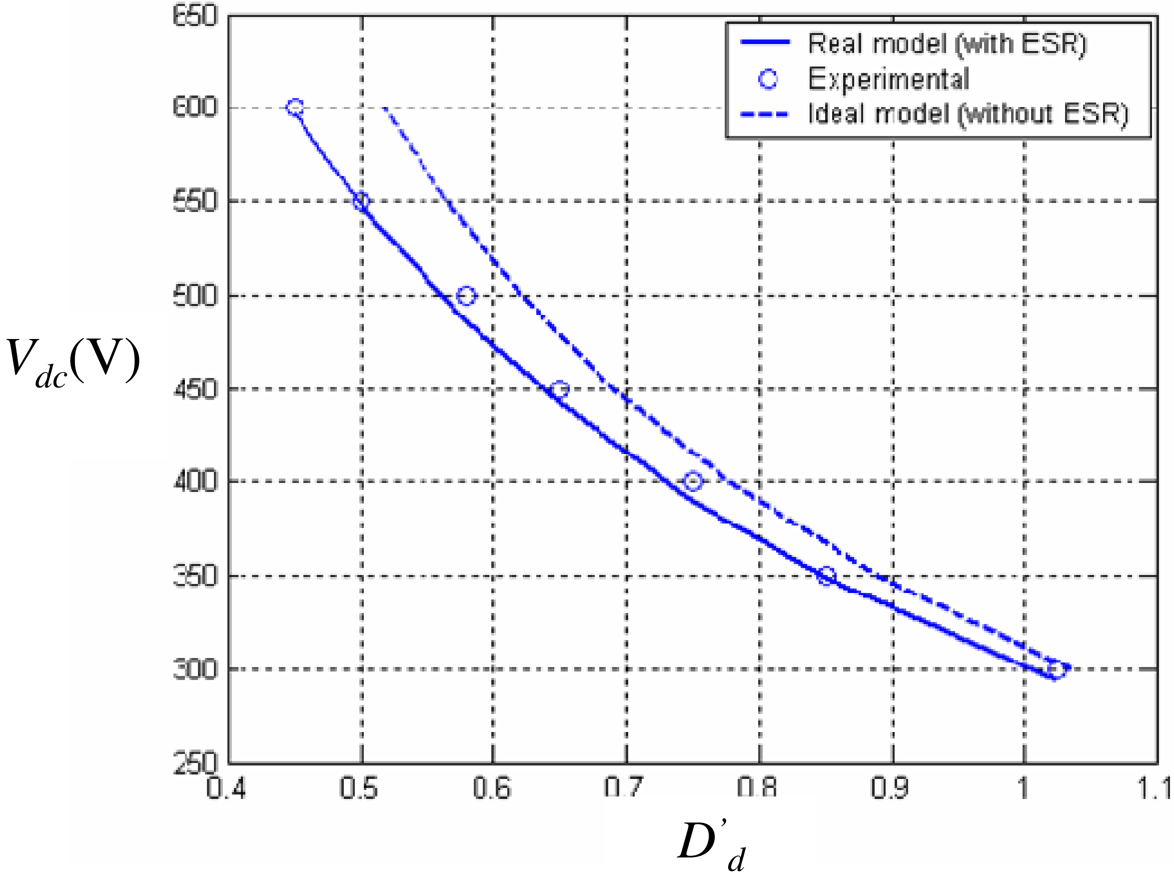

FUNCTION DUTY CYCLE-DIRECT CURRENT

$$D_d^{'} = \frac{2(V_d - r_L I_d)}{V_{dc}^{*}}$$

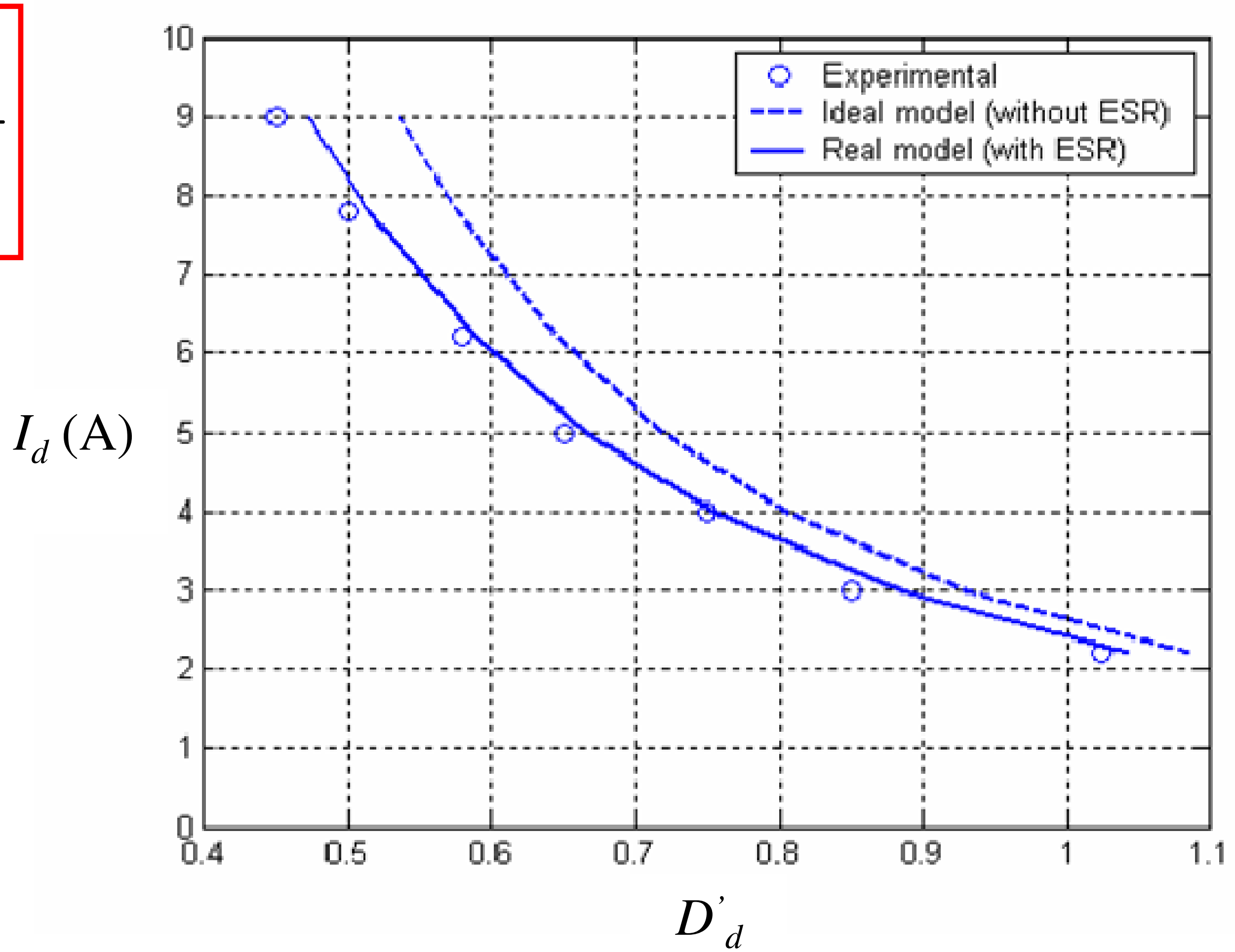

FUNCTION DUTY CYCLE-DC VOLTAGES UNBALANCE

$$D_o' = \frac{\Delta v_{dc}}{\alpha R_{dc,n} I_d}$$

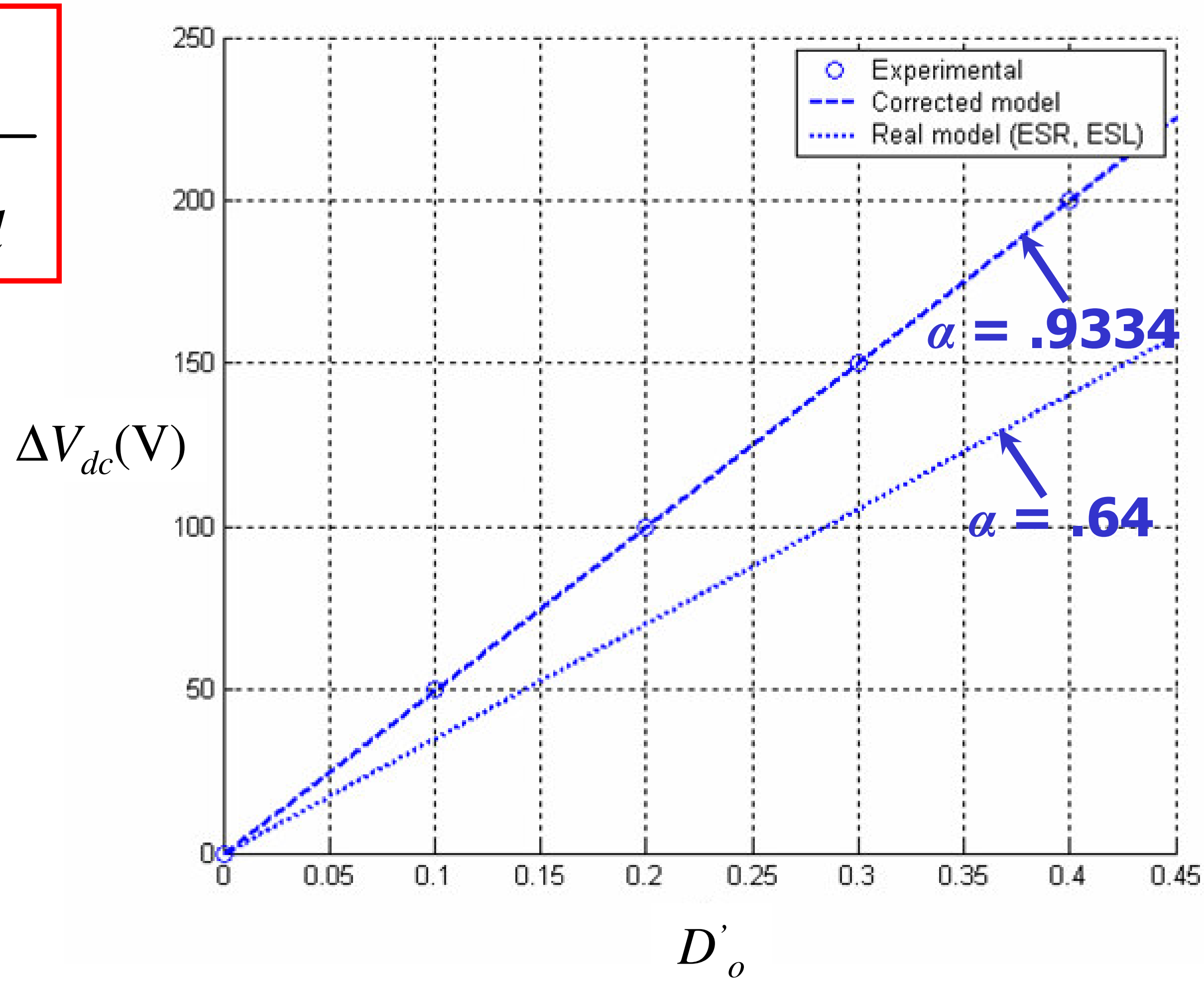

MAIN RESEARCH OBJECTIVES

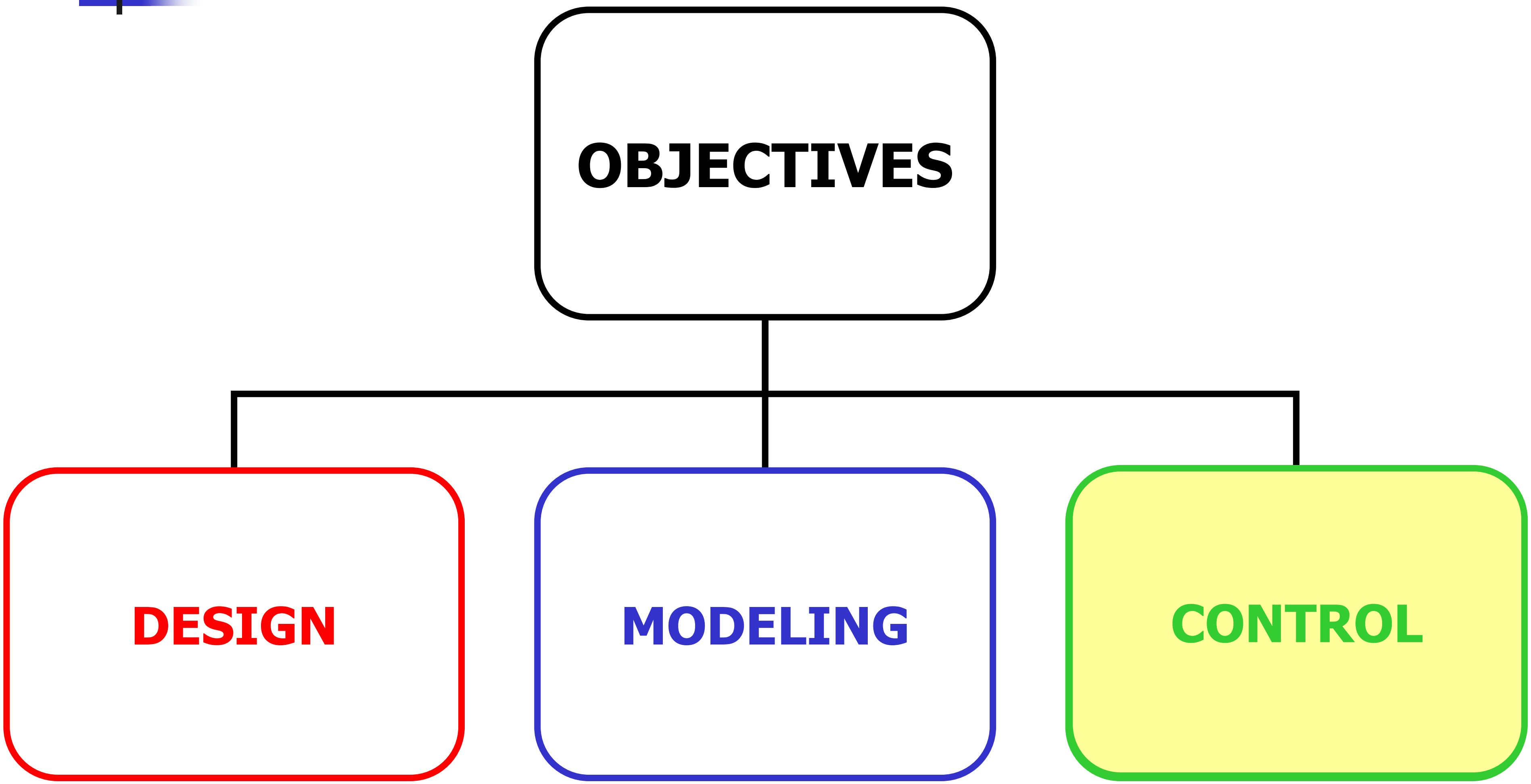

CONTROL TECHNIQUES APPLIED TO THE RECTIFIER

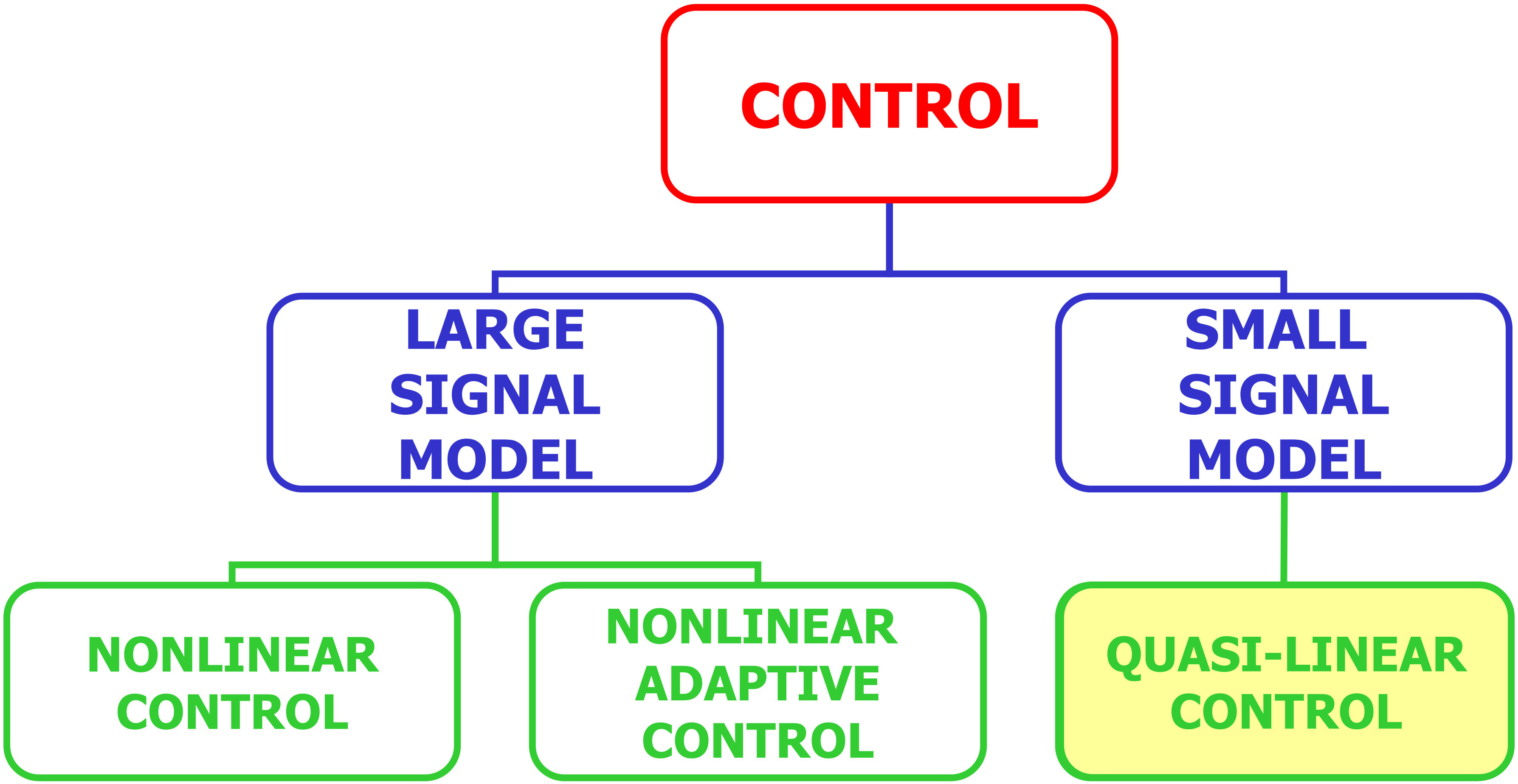

QUASI-LINEAR CONTROL

- This concept has been recently introduced by Kelemen/Bensoussan in 2002, for SISO continuous systems.
- A quasi-linear controller is a lead/lag compensator, which gain may be indefinely increased and its poles are accordingly adjusted:

$$\boxed{G_c(\mathrm{s}) = \frac{k\prod_{i=1}^{r-1}(\mathrm{s}+z_i)}{\prod_{i=1}^{r-1}\left(\mathrm{s}+\underline{a_i k^f}\right)}}$$

Arbitrarily fast and robust tracking by feedback

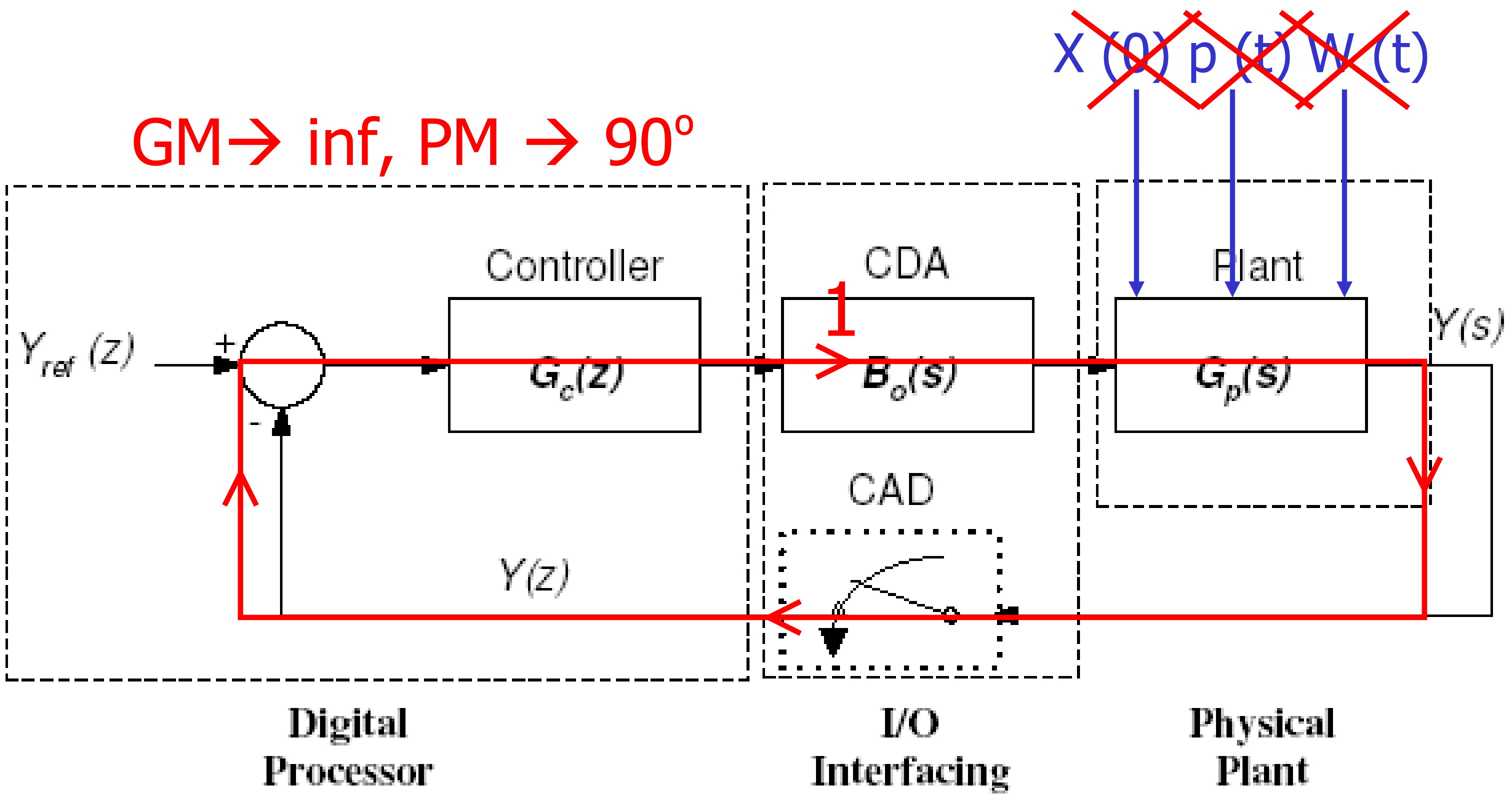

EXAMPLE

$$\boxed{G_p(s)=\frac{\theta^2}{s(s+\theta)^2}, \quad 0.1\le\theta\le3, \quad \theta=1 \ \text{nominal}}$$

$$\boxed{G_c(s)=\frac{k(s+1)}{(s+2)}}$$

Step responses of a conventional lead/lag controller for different gain values

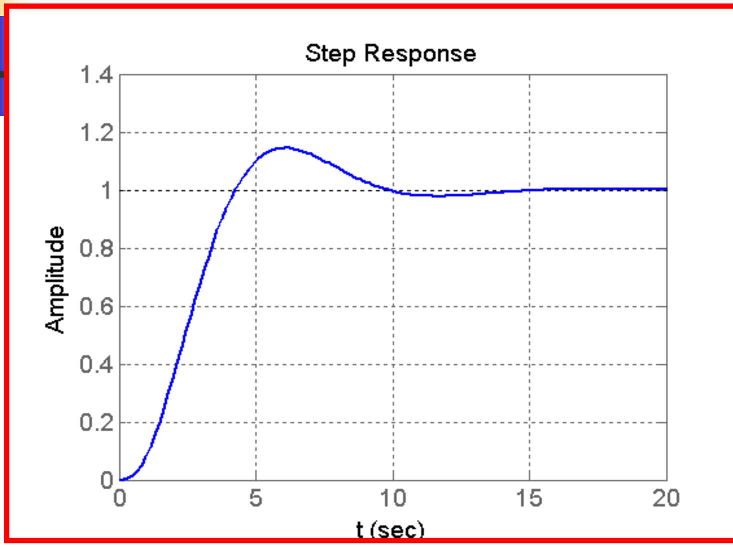

$k = 1$

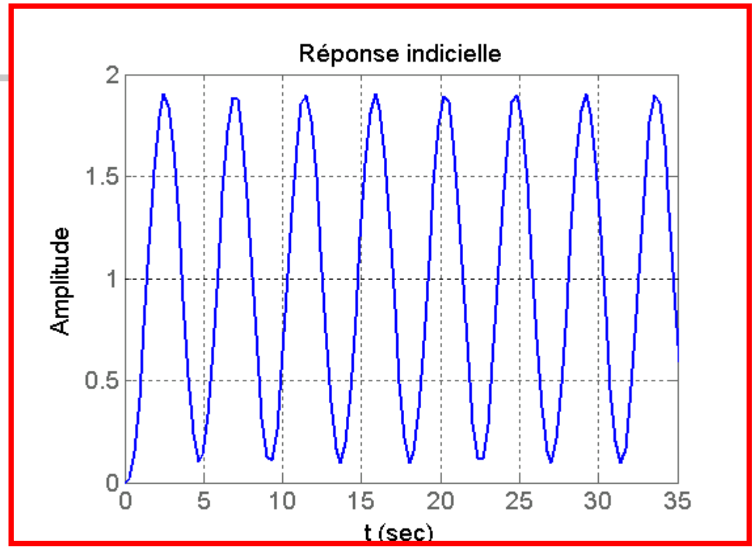

$k = 6$

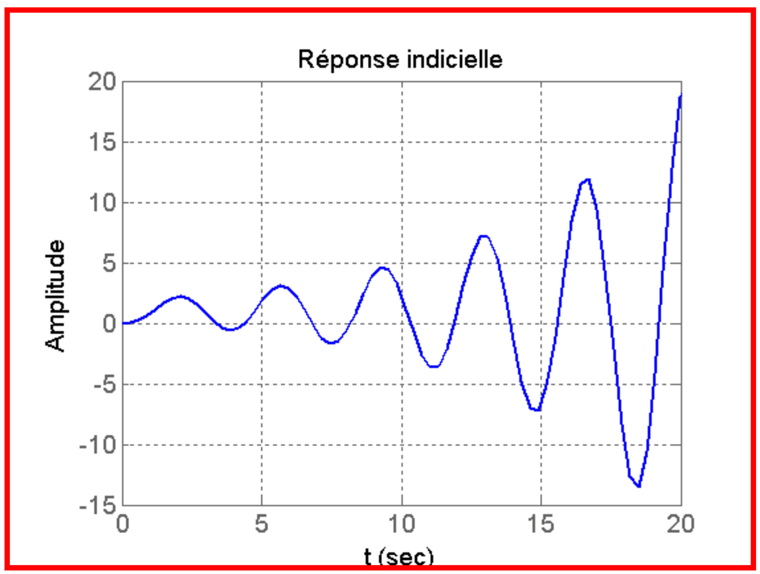

$k = 10$

Linear controller: paranmetric variations and system stability

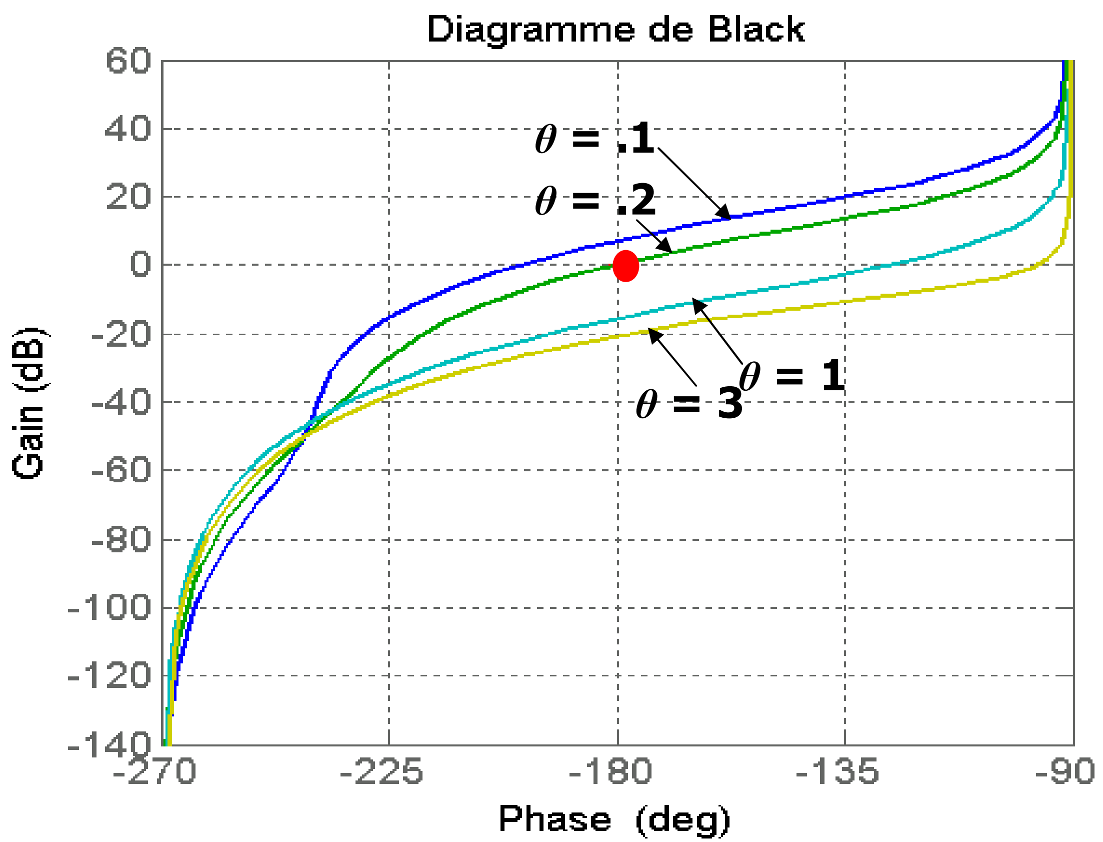

Step responses of a quasi-linear controller for different gain values

$$G_c(s) = \frac{k(s+z_1)(s+z_2)}{\left(s+a_1k^f\right)\left(s+a_2k^f\right)}, \qquad f = 5/12$$

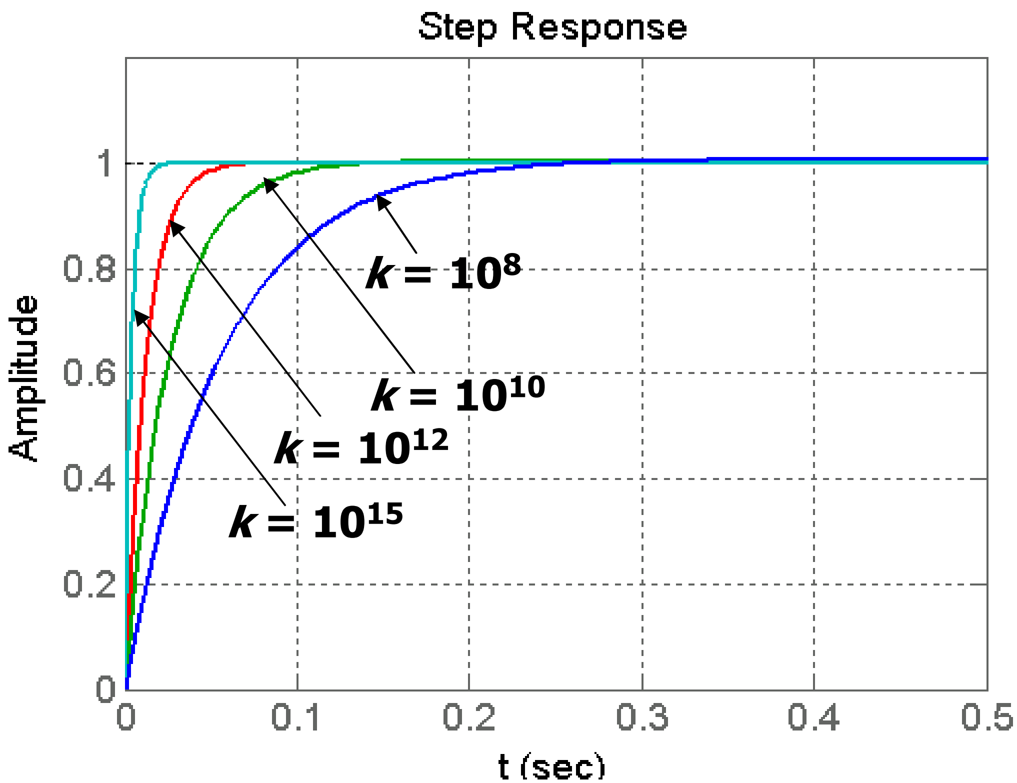

Quasi-linear controller: parametric variations and system stability

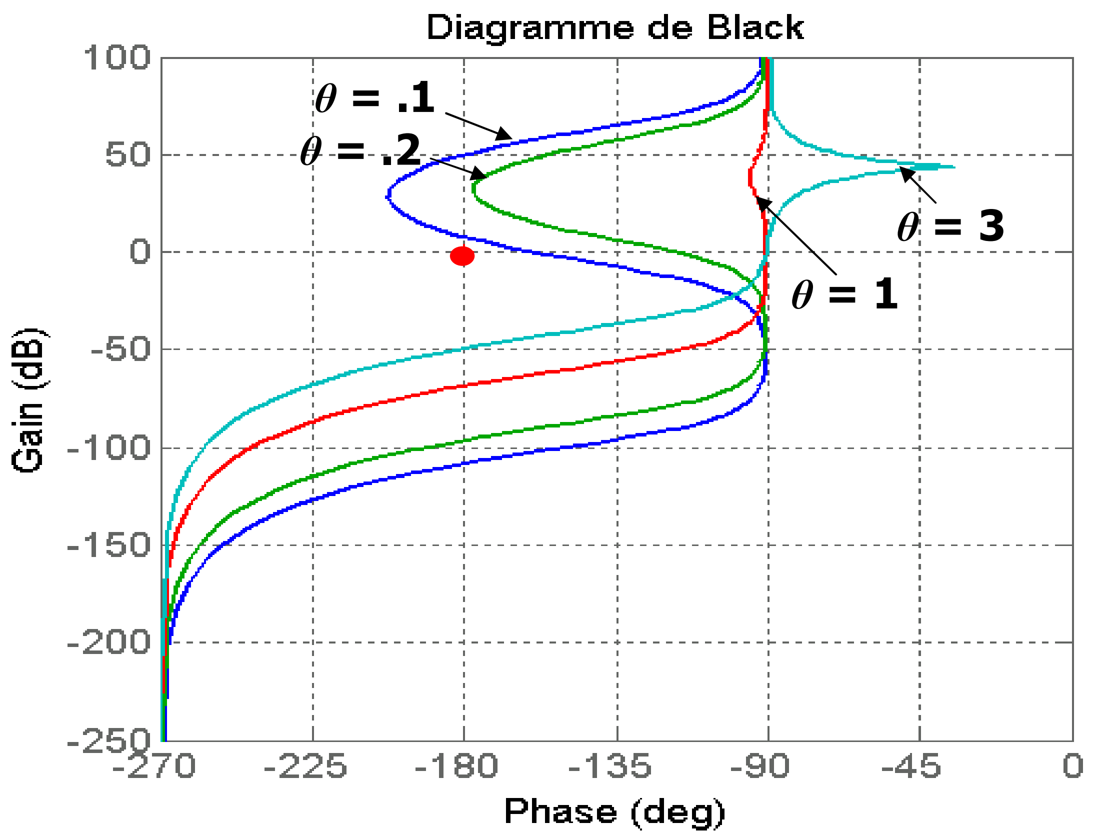

Design of quasi-linear controllers for Vienna converter

Inner loops

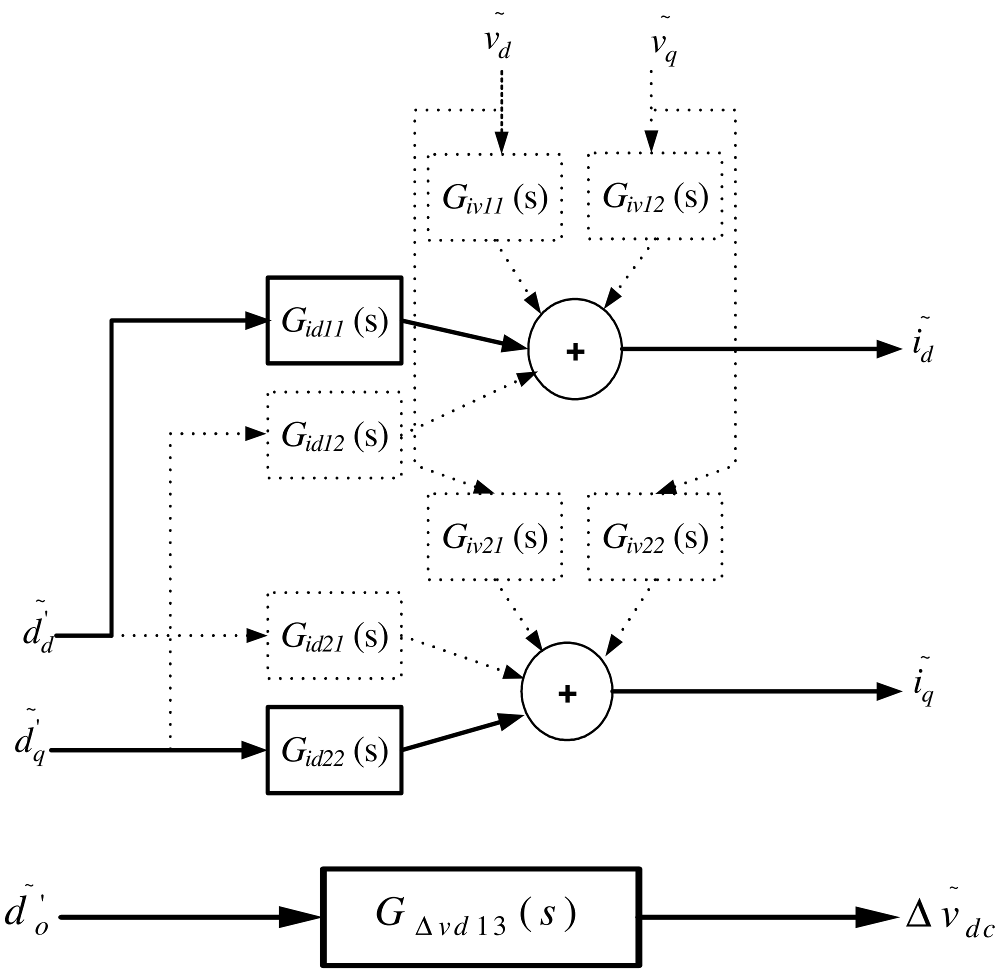

Outer loop

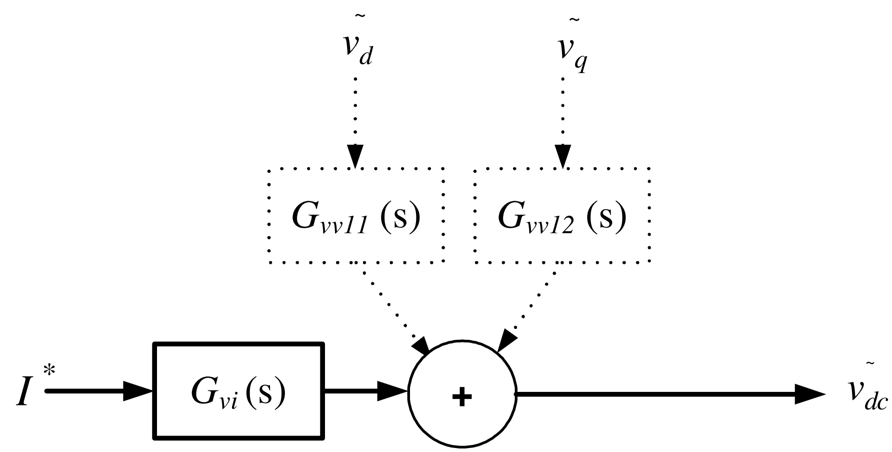

QUASI-LINEAR CONTROLLERS EXPRESSIONS

$$G_{id11}(s) = -\frac{V_o^*}{2L}\frac{\cancel{s}(s+\alpha_{11})}{den(s)} \Rightarrow H_{id}(s)=\frac{K_{id}(s+z_{id})}{\cancel{s}(s+a_{id}(-K_{id})^{f_{id}})}, \quad K_{id}<0$$

$$G_{id22}(s) = -\frac{V_o^*}{2L}\frac{\left(s^2+\tau_o s+\alpha_{13}\right)}{den(s)} \Rightarrow H_{iq}(s)=\frac{K_{iq}}{\left(s+a_{iq}(-K_{iq})^{f_{iq}}\right)}, \quad K_{iq}<0$$

$$G_{\Delta vd13}(s) = \frac{\alpha\sqrt{2}I_s^*}{C_o\left(s+\alpha_{15}\right)} \Rightarrow H_{\Delta v}(s)=\frac{K_{\Delta v}(s+z_{\Delta v})}{s(s+a_{\Delta v}K_{\Delta v}^{f_{\Delta v}})}, \quad K_{\Delta v}>0$$

$$G_{vi}(s) = \frac{6V_s}{C_oV_o^*\left(s+\alpha_{11}\right)} \Rightarrow H_v(s)=\frac{K_v(s+z_v)}{s(s+a_vK_v^{f_v})}, \quad K_v>0$$

$$den(s) = s^3+\tau_o s^2+(\omega_o^2\alpha_{12}+\alpha_{13})s+\tau_o\omega_o^2$$

QUASI-LINEAR CONTROLLERS PERFORMANCES IN CLOSED-LOOP

Variable contrôlée	Paramètres dans le continu	Paramètres dans le discret	Pôles dans le continu	t_s (ms)
i_d	$z_{id} = 1$ $a_{id} = 0.05$ $f_{id} = 0.75$ $k_{id} = -(10^{12})$	$z_{idd} = 1$ $a_{idd} = -0.9524$ $k_{idd} = -10.0265$	-6.315×10^{7} -9.69×10^{4} -2045 -52.07	0.31
i_q	$a_{iq} = \sqrt{2}$ $f_{iq} = 0.5$ $k_{iq} = -(10^{10})$	$a_{iqd} = -0.8880$ $k_{iqd} = -9.3471$	-1.4137×10^{5} -10 + 420 i -10 – 420 i -20	0.46
Δv_{dc}	$a_{\Delta v} = 0.25$ $z_{\Delta v} = 2$ $f_{\Delta v} = 0.75$ $k_{\Delta v} = (10^{8})$	$z_{\Delta vd} = 0.9997$ $a_{\Delta vd} = -0.0586$ $k_{\Delta vd} = 4.4104$	-8910 -542.2 -2	50.6
v_{dc}	$a_v = 0.25$ $z_v = 2$ $f_v = 0.75$ $k_v = (10^{6})$	$z_{vd} = 1$ $a_{vd} = 0.2873$ $k_{vd} = 0.0133$	-1160 -265.2 -6.39	712

REAL-TIME IMPLEMENTATION OF THE QUASI-LINEAR CONTROL SCHEME

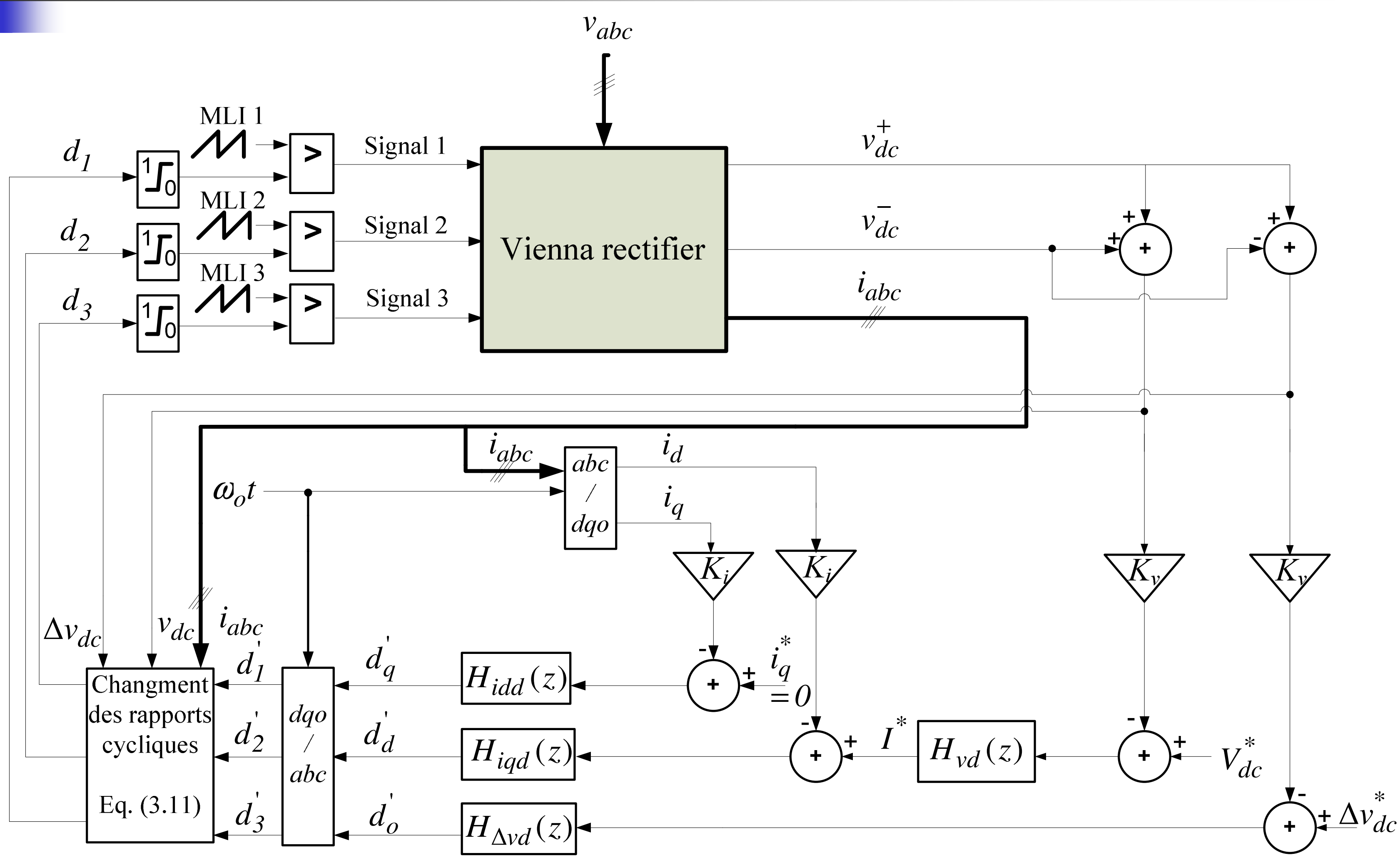

STEADY STATE RESULTS

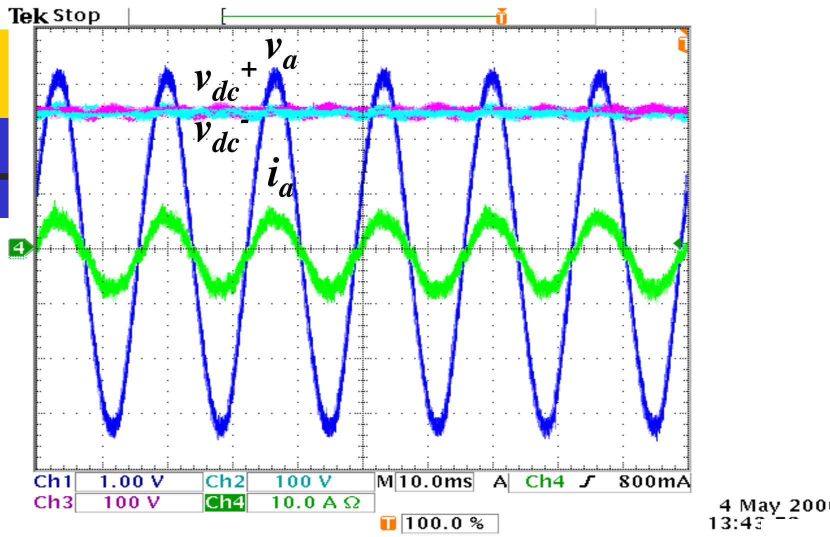

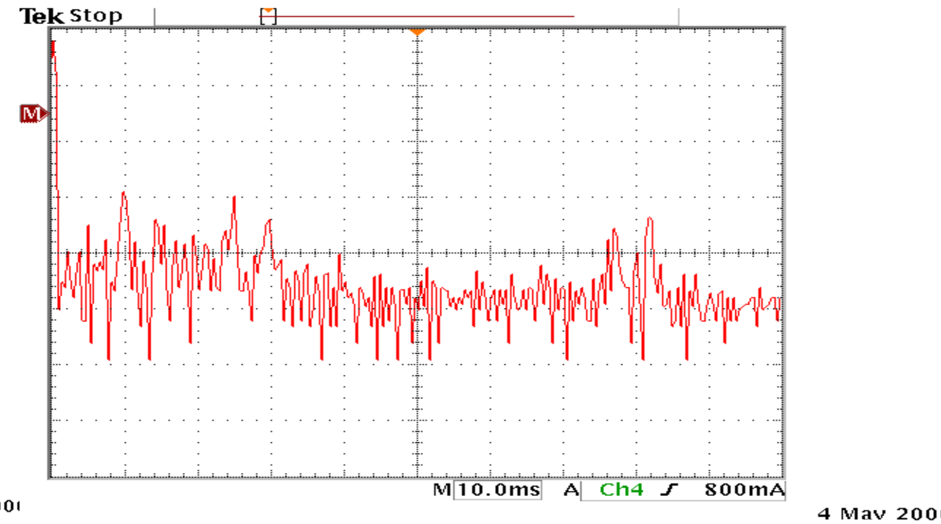

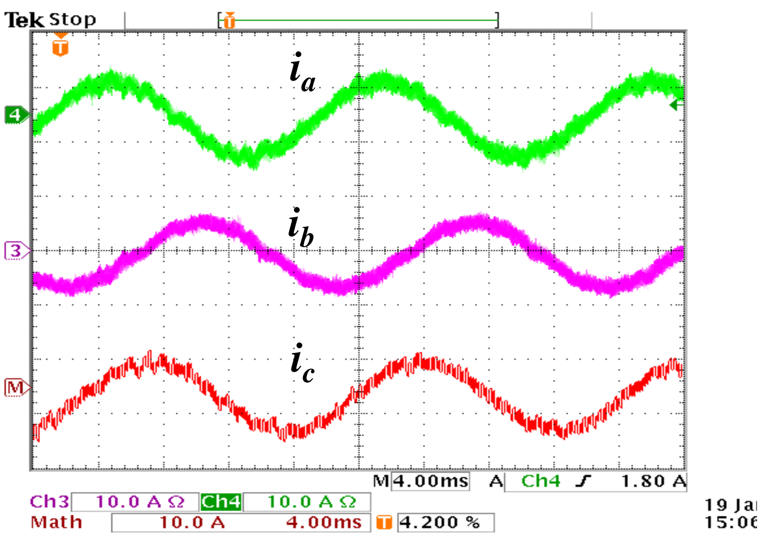

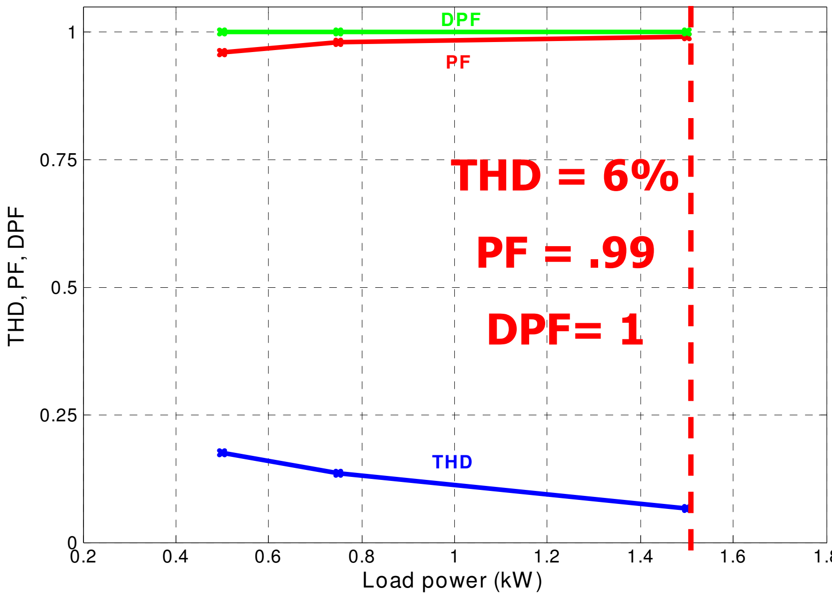

CONTROL TECHNIQUES APPLIED TO THE VIENNA RECTIFIER

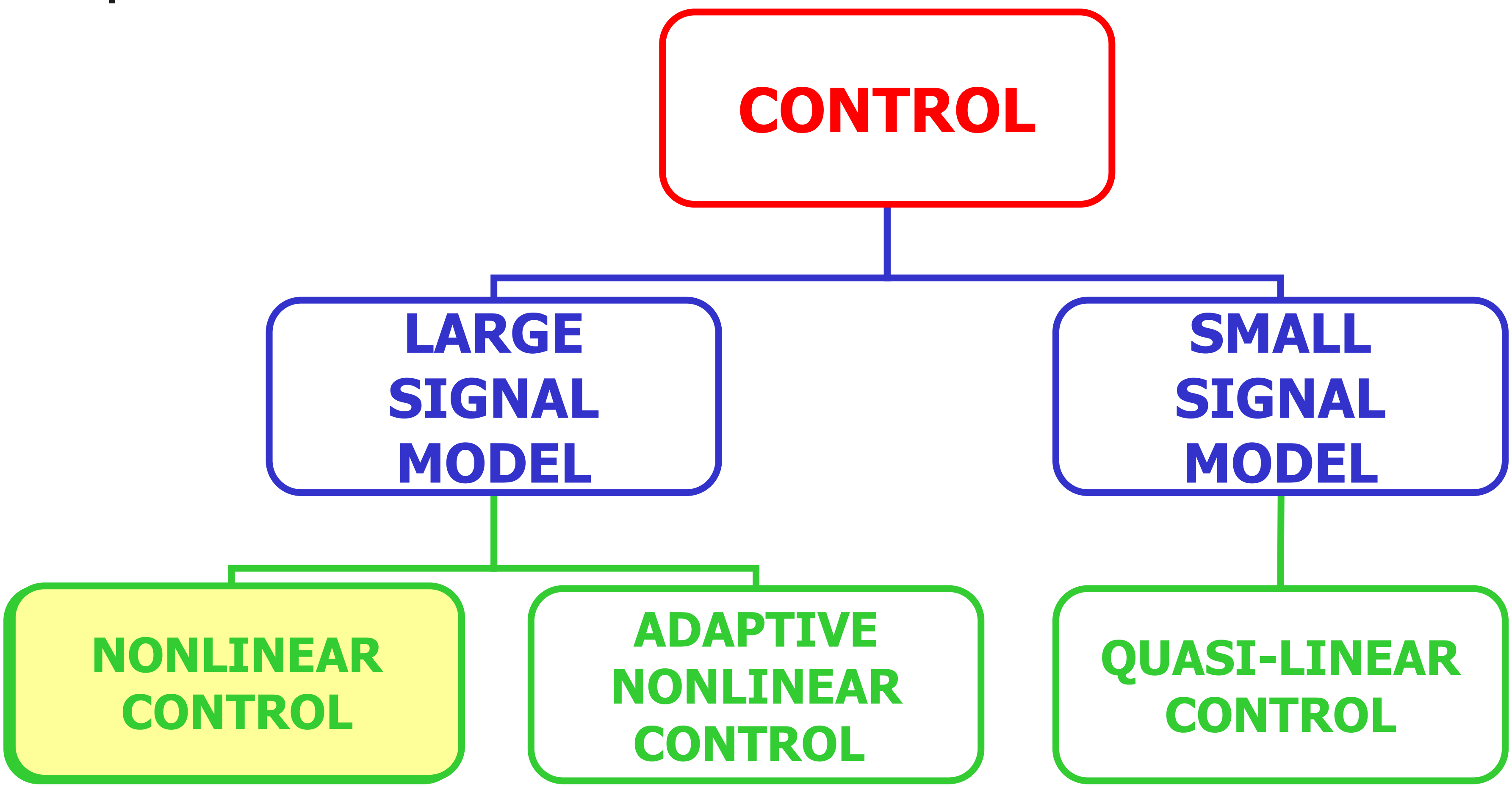

NONLINEARITY-COMPENSATING CONTROL SCHEME

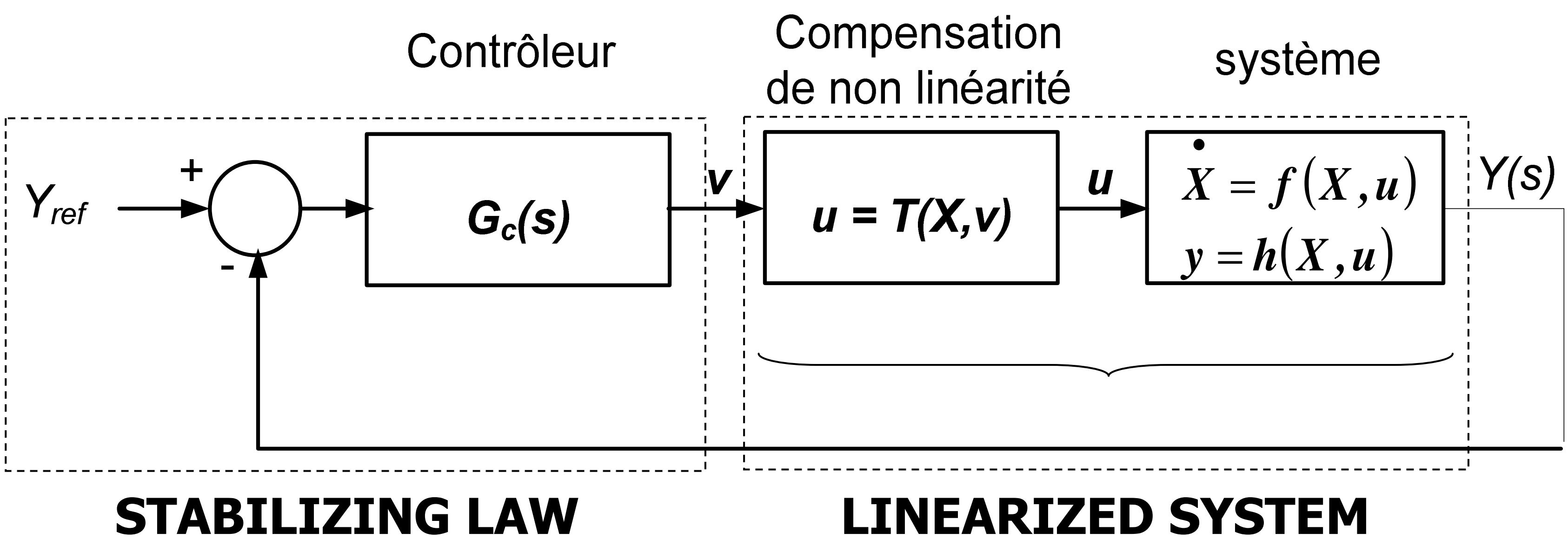

APPLICATION TO THE VIENNA CONVERTER

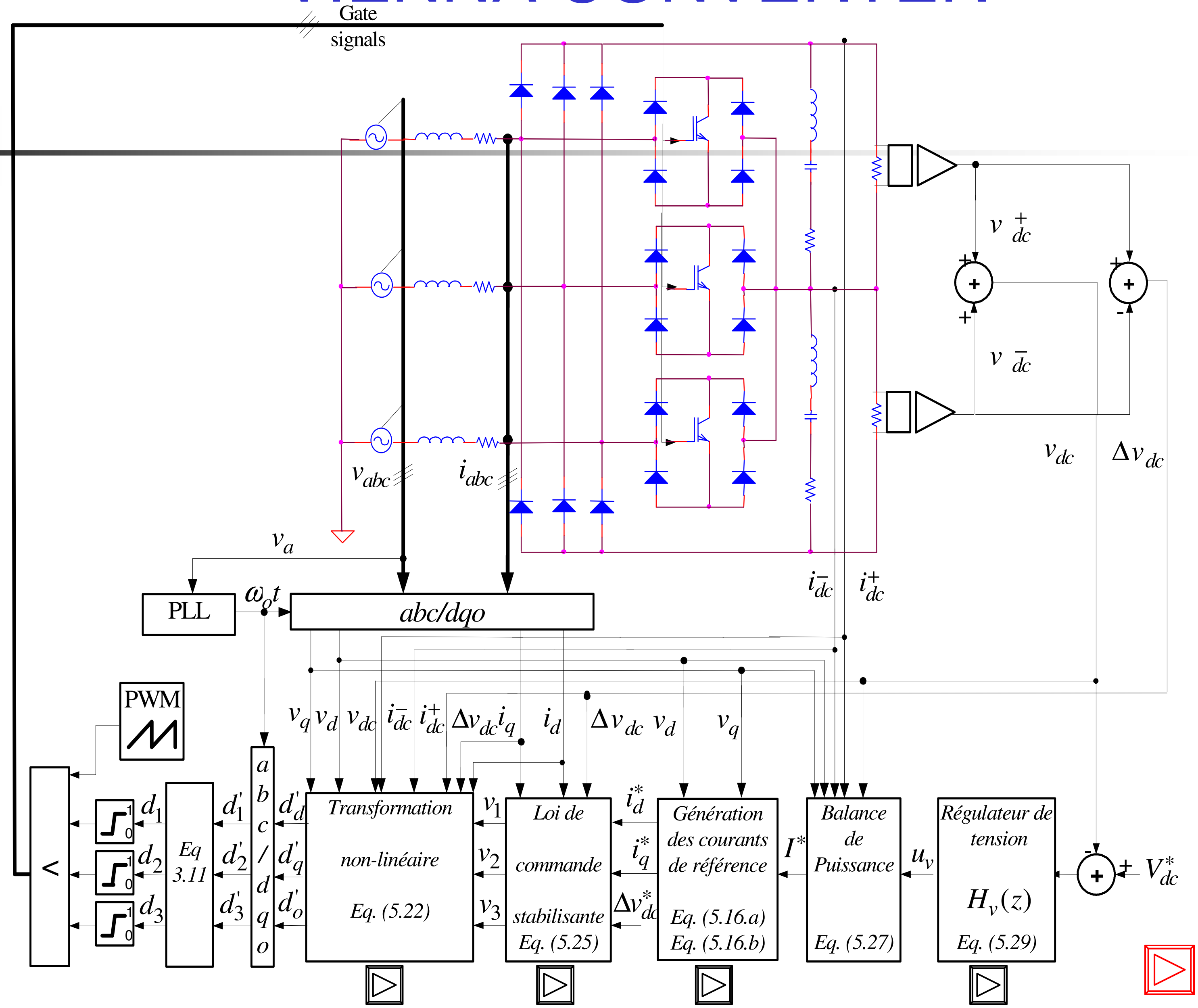

NONLINEARITY COMPENSATION

$$\begin{bmatrix} i_d(k+1) \\ i_q(k+1) \\ \Delta v_{dc}(k+1) \end{bmatrix} = F_d(X,\theta_d) + G_d(X,\theta_d)d(k)$$

$$\Downarrow$$

$$d(k) = T_d^{-1}(X,\theta_d,v) = G_d^{-1}(X,\theta_d)[-F_d(X,\theta_d)+v(k)]$$

STABILIZING CONTROL LAWS

$$i_d(k+1) = a_i i_d(k-1) + b_i i_d(k) + c_i i_d^*(k)$$

$$i_q(k+1) = a_i i_q(k-1) + b_i i_q(k) + c_i i_q^*(k)$$

$$\Delta v_{dc}(k+1) = a_{\Delta v}\Delta v_{dc}(k-2) + b_{\Delta v}\Delta v_{dc}(k-1) + c_{\Delta v}\Delta v_{dc}(k) + d_{\Delta v}\Delta v_{dc}^*(k-1) + e_{\Delta v}\Delta v_{dc}^*(k)$$

$$\Updownarrow$$

$$v_1(k) = a_i i_d(k-1) + b_i i_d(k) + c_i i_d^*(k)$$

$$v_2(k) = a_i i_q(k-1) + b_i i_q(k) + c_i i_q^*(k)$$

$$v_3(k) = a_{\Delta v}\Delta v_{dc}(k-2) + b_{\Delta v}\Delta v_{dc}(k-1) + c_{\Delta v}\Delta v_{dc}(k) + d_{\Delta v}\Delta v_{dc}^*(k-1) + e_{\Delta v}\Delta v_{dc}^*(k)$$

REFERENCE CURRENTS GENERATION

$$v_{dc}(k+1) = v_{dc}(k) + \frac{T_s}{C_{dc}}\left[\frac{3}{v_{dc}(k)}\hat{V}\,\hat{I}^*(k) - i_{dc}^+(k) - i_{dc}^-(k)\right]$$

$$\hat{V} = \sqrt{v_d^2 + v_q^2}$$

$$\hat{I}^*(k) = \frac{C_{dc}v_{dc}(k)v_4(k) + v_{dc}(k)\left(i_{dc}^+(k) + i_{dc}^-(k)\right)}{3\sqrt{v_d^2(k) + v_q^2(k)}}$$

$$i_d^* = \frac{\hat{I}^*}{\sqrt{v_d^2 + v_q^2}}v_d$$

$$i_q^* = \frac{\hat{I}^*}{\sqrt{v_d^2 + v_q^2}}v_q$$

DC VOLTAGE REGULATION

$$\boxed{v_{dc}(k+1) = v_{dc}(k) + T_s v_4(k) \Leftrightarrow \frac{v_{dc}(k)}{v_4(k)} = \frac{T_s}{(z-1)}}$$

$$\Downarrow$$

$$\boxed{H_v(z) = \frac{K_v(z+a_v)}{(z-1)(z+z_v)}}$$

STEADY STATE RESULTS

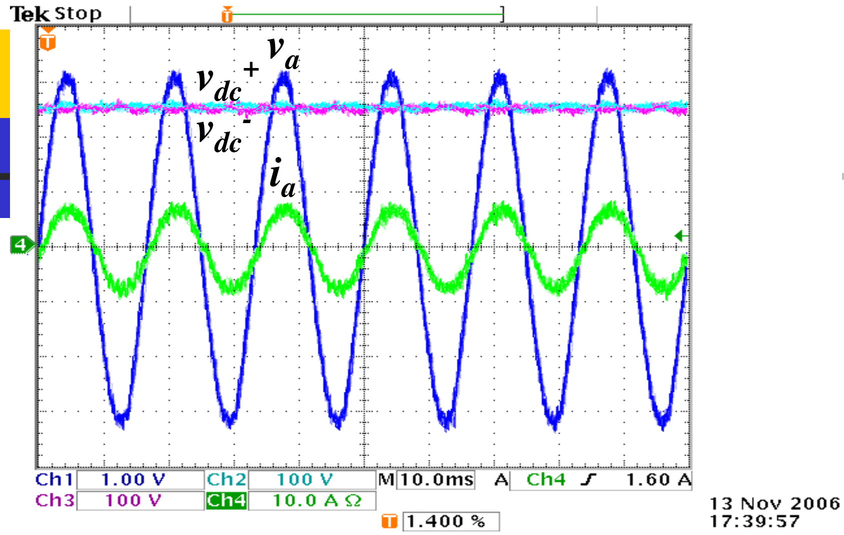

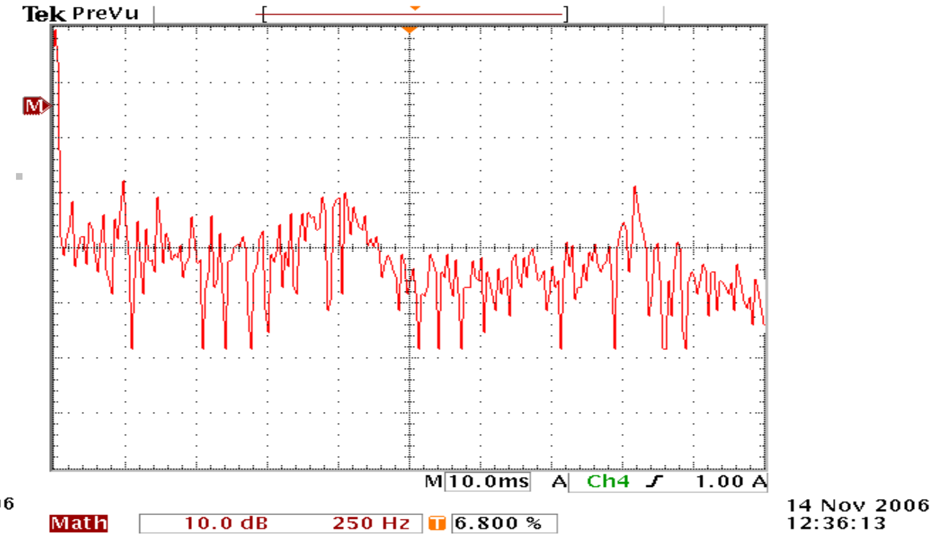

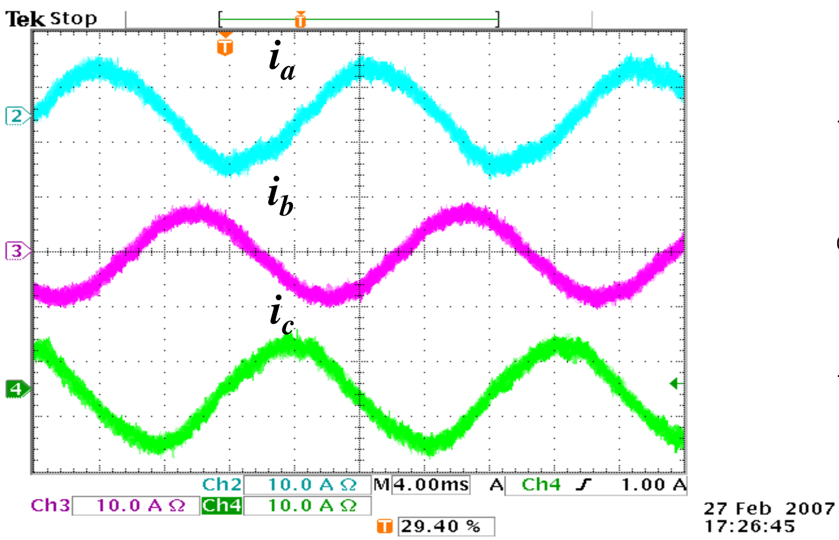

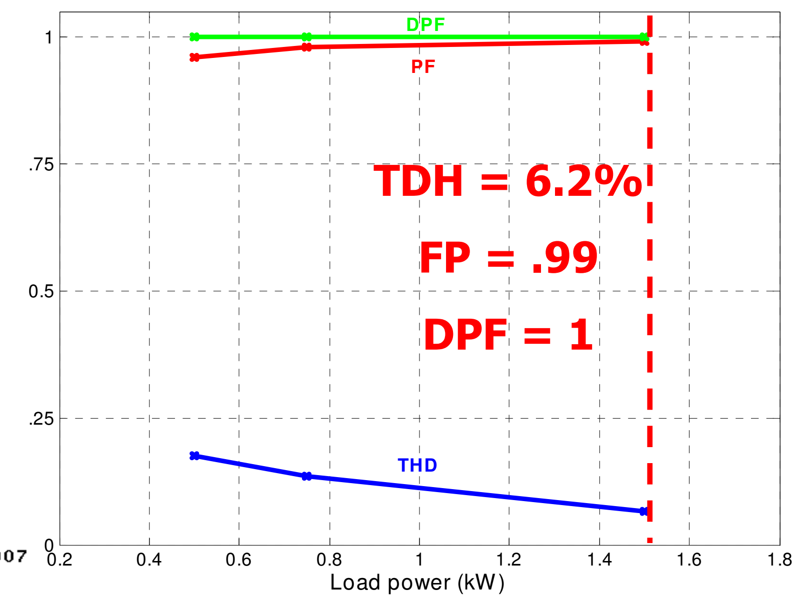

CONTROL TECHNIQUES APLLIED TO THE VIENNA CONVERTER

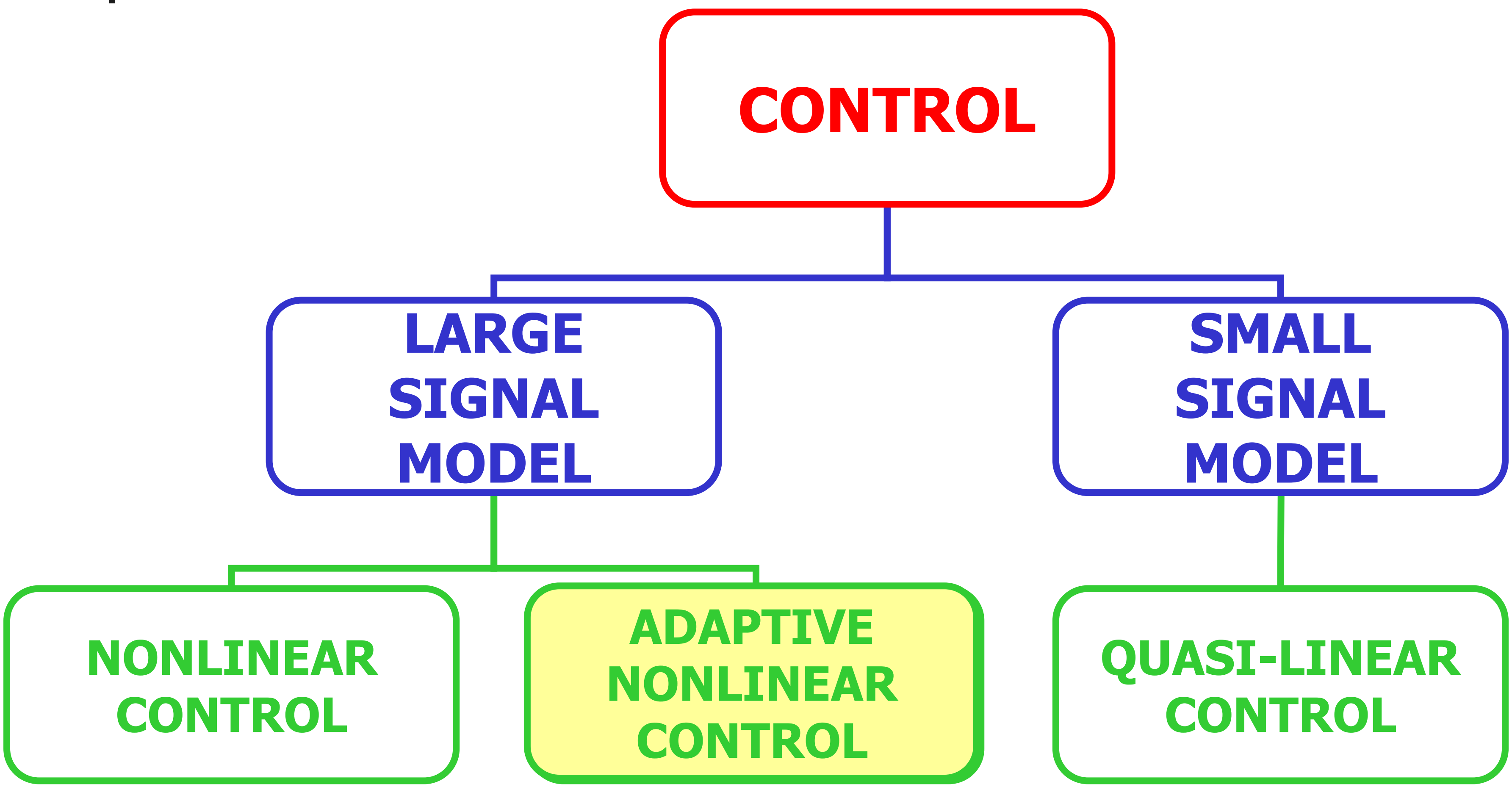

MODEL REFERENCE ADAPTIVE CONTROL

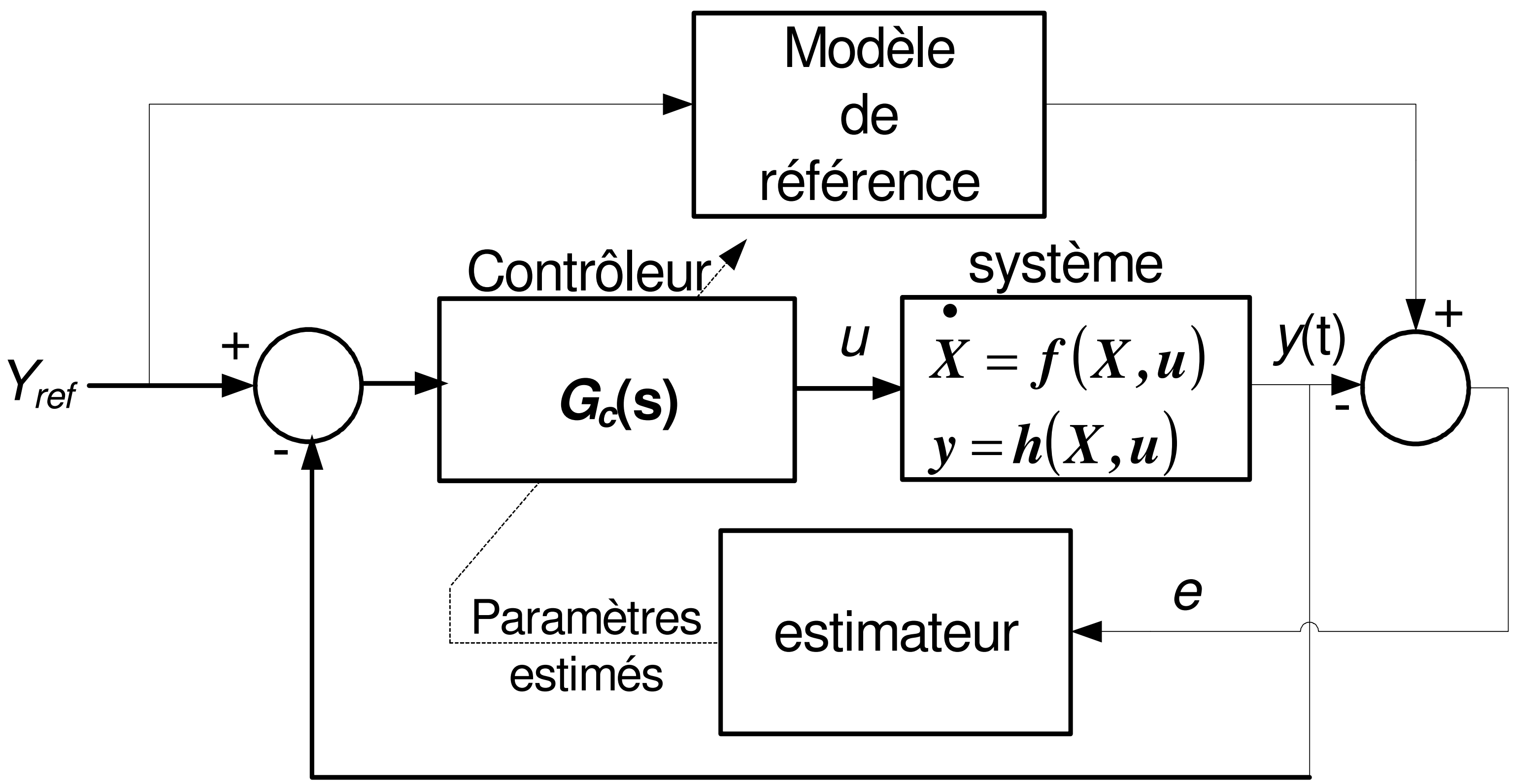

PRINCIPLE OF THE INPUT/OUTPUT LINEARIZATION

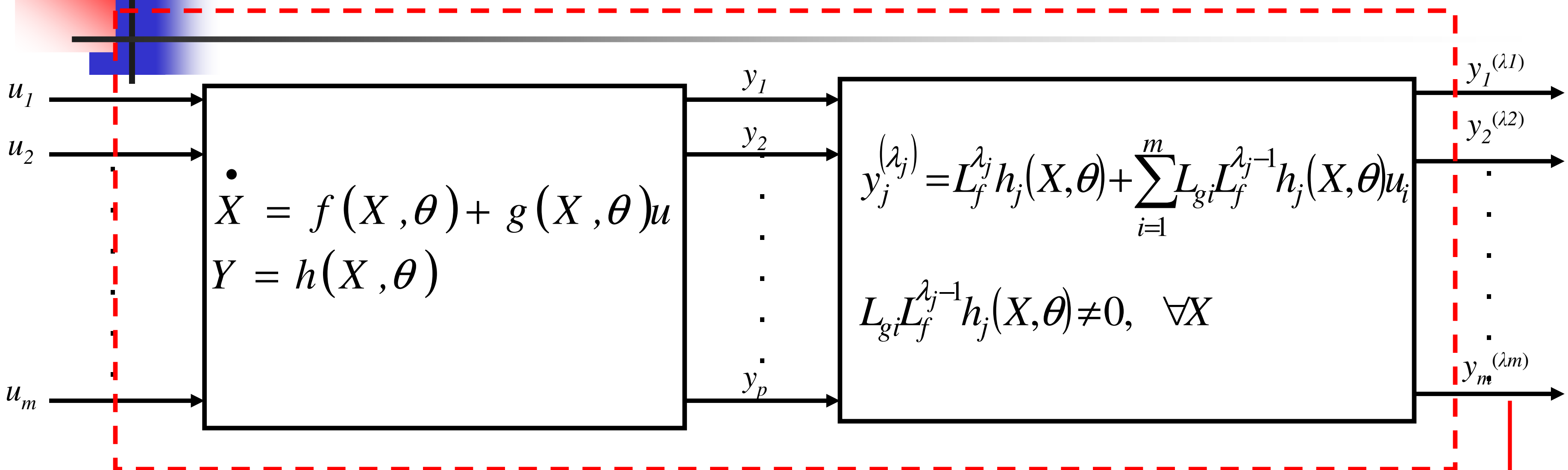

$$\begin{bmatrix} y_1^{(\lambda_1)} \\ \cdot \\ \cdot \\ \cdot \\ y_m^{(\lambda_m)} \end{bmatrix} = \begin{bmatrix} L_f^{(\lambda_1)} h_1 \\ \cdot \\ \cdot \\ \cdot \\ L_f^{(\lambda_m)} h_m \end{bmatrix} + A(X,\theta) \begin{bmatrix} u_1 \\ \cdot \\ \cdot \\ \cdot \\ u_m \end{bmatrix}$$

ADAPTIVE LINEARIZING CONTROL LAWS

$$\boxed{\hat{\theta} = \theta - \Delta\theta}$$

$$\boxed{\hat{u} = u\left(X, \hat{\theta}\right) = A^{-1}\left(X, \hat{\theta}\right)\begin{bmatrix} L_f^{(\lambda_1)}\hat{h}_1 \\ \cdot \\ \cdot \\ \cdot \\ L_f^{(\lambda_m)}\hat{h}_m \end{bmatrix} + A\left(X, \hat{\theta}\right)\begin{bmatrix} \underline{\hat{v}_1} \\ \cdot \\ \cdot \\ \cdot \\ \underline{\hat{v}_m} \end{bmatrix}}$$

STABILIZING ADAPTIVE CONTROL LAWS

$$\boxed{\hat{v}_i = -\sum_{j=1}^{r_i} k_j^i \, \hat{y}_j^i + R_i}$$

LYAPUNOV FUNCTION (ENERGY)

$$\hat{\eta} = \hat{E} - \hat{\varepsilon}, \qquad \dot{\hat{\varepsilon}} = A_{ref}\,\hat{\varepsilon} + W^2\left(X, \hat{\theta}\right)\dot{\hat{\theta}}$$

$$V = \eta^T P \eta + \Delta\theta^T \Gamma^{-1} \Delta\theta$$

$$\dot{V} = -\eta^T \eta + 2\eta^T P W^1 \Delta\theta + 2\Delta\dot{\theta}\,\Gamma^{-1}\Delta\theta \leq 0$$

=

0

PARAMETERS ADAPTATION SCHEME

$$\boxed{\dot{\hat{\theta}} = -\Delta\dot{\theta} = \Gamma \sum_{i=1}^{m} W_i^{1T}\left(X, \hat{\theta}, \hat{u} \right) P_i \, \hat{\eta}_i}$$

APPLICATION TO THE VIENNA RECTIFIER

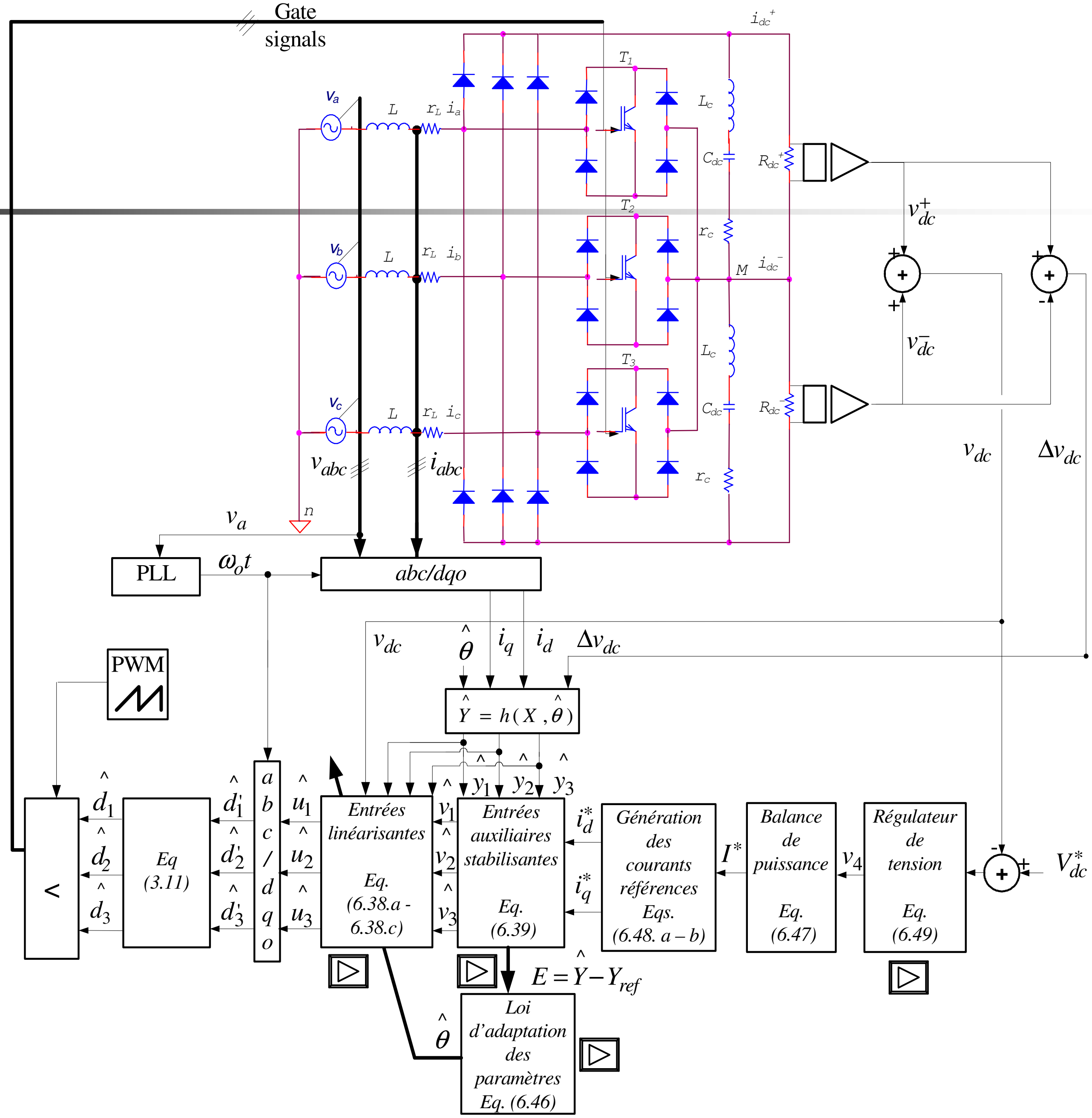

DERIVATION OF THE LINEARIZING INPUTS

$$\hat{y}_1 = i_d\,, \qquad \hat{y}_2 = i_q\,, \qquad \hat{y}_3 = \Delta v_{dc}$$

$$\hat{y}_1^{(1)} = \left(\hat{y}_1(k) + \hat{\theta}_{1d} + \hat{\theta}_{2d}\,\hat{y}_2(k) - \hat{\theta}_{3d}\,X_4(k)\underline{\hat{u}_1(k)}\right) + \left(\Delta\theta_{1d} + \Delta\theta_{2d}\,\hat{y}_2(k) - \Delta\theta_{3d}X_4(k)\underline{\hat{u}_1(k)}\right);$$

$$\hat{y}_2^{(1)} = \left(\hat{y}_2(k) + \hat{\theta}_{4d} - \hat{\theta}_{2d}\,\hat{y}_1(k) - \hat{\theta}_{3d}\,X_4(k)\underline{\hat{u}_2(k)}\right) + \left(\Delta\theta_{4d} - \Delta\theta_{2d}\,\hat{y}_2(k) - \Delta\theta_{3d}X_4(k)\underline{\hat{u}_2(k)}\right);$$

$$\hat{y}_3^{(1)} = \left[\hat{y}_3(k) + \hat{\theta}_{6d}\,\hat{y}_1(k)\underline{\hat{u}_1(k)} + \hat{\theta}_{7d}\,\hat{y}_3(k) + \hat{\theta}_{8d}\,X_4(k) - \hat{\theta}_{5d}\,\frac{\hat{y}_3(k)}{X_4(k)}\left(\hat{y}_1(k)\underline{\hat{u}_1(k)} + \hat{y}_2(k)\underline{\hat{u}_2(k)}\right)\right]$$

$$+ \left[\Delta\theta_{6d}\,\hat{y}_1(k)\underline{\hat{u}_1(k)} + \Delta\theta_{7d}\,\hat{y}_3(k) + \Delta\theta_{8d}X_4(k) - \Delta\theta_{5d}\,\frac{\hat{y}_3(k)}{X_4(k)}\left(\hat{y}_1(k)\underline{\hat{u}_1(k)} + \hat{y}_2(k)\underline{\hat{u}_2(k)}\right)\right]$$

DERIVATION OF THE STABILIZING CONTROL LAWS

$$\boxed{\hat{v}_i(k) = -k_1^i\,\hat{y}_i(k) + b_i\, y_{ref}^i(k); \quad i = \{1,2,3\}}$$

$$\boxed{\begin{bmatrix} k_1^1 \\ k_1^2 \\ k_1^3 \end{bmatrix} = \begin{bmatrix} .001 \\ .001 \\ .1 \end{bmatrix}, \qquad \begin{bmatrix} b_1 \\ b_2 \\ b_3 \end{bmatrix} = \begin{bmatrix} .999 \\ .999 \\ .9 \end{bmatrix}}$$

PARAMETERS ADAPTATION SCHEME

$$\hat{\theta}_d(k+1) = \hat{\theta}_d(k) + \Gamma W^{1T} PE$$

$$E(k) = \hat{Y}(k) - Y_{ref}(k)$$

$$W^1(\cdot) = \begin{pmatrix} T_s & X_2T_s & -X_3T_s\hat{u}_1 & 0 & 0 & 0 & 0 & 0 \\ 0 & -X_1T_s & -X_3T_s\hat{u}_2 & T_s & 0 & 0 & 0 & 0 \\ 0 & 0 & 0 & 0 & -\frac{X_4}{X_3}T_s\left(X_1\hat{u}_1 + X_2\hat{u}_2\right) & X_1T_s\hat{u}_3 & X_4T_s & X_3T_s \end{pmatrix}$$

ZERO DYNAMICS STABILITY

➢Internal dynamics describing the DC voltage (v_{dc}) ont été ignorées lors de la phase de linérisation.

➢The zero dynamics describe the internal behaviour of the system when the inputs and initial conditions are chosen in a way to zero the outputs:

$$\boxed{v_{dc}(k+1) = v_{dc}(k)\left[1 - \frac{T_s}{2C_{dc}}\left(\frac{1}{R_{dc}^{+}} + \frac{1}{R_{dc}^{-}}\right)\right]}$$

is asymptotically stable for: $\left[1 - \frac{T_s}{2C_{dc}}\left(\frac{1}{R_{dc}^{+}} + \frac{1}{R_{dc}^{-}}\right)\right] \neq 0$

STEADY STATE RESULTS

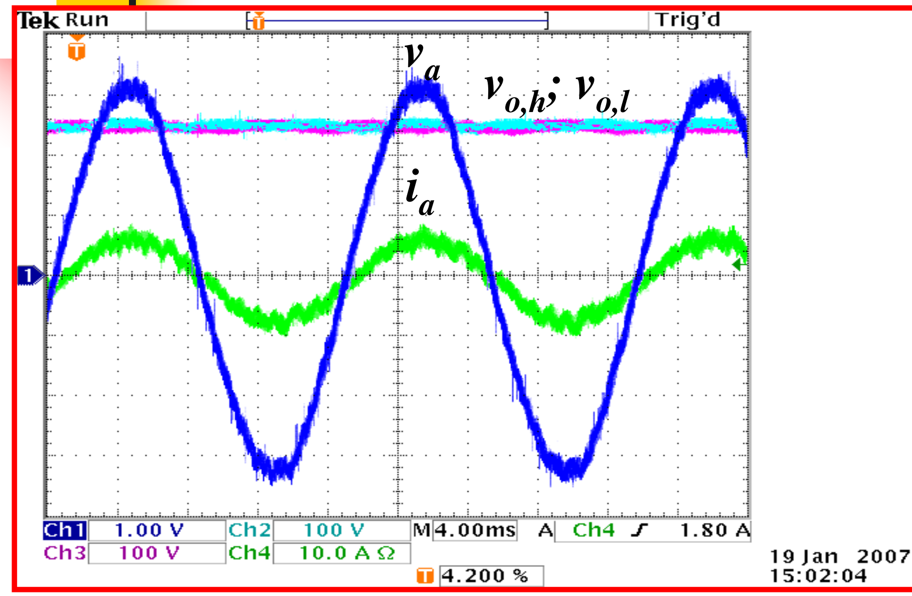

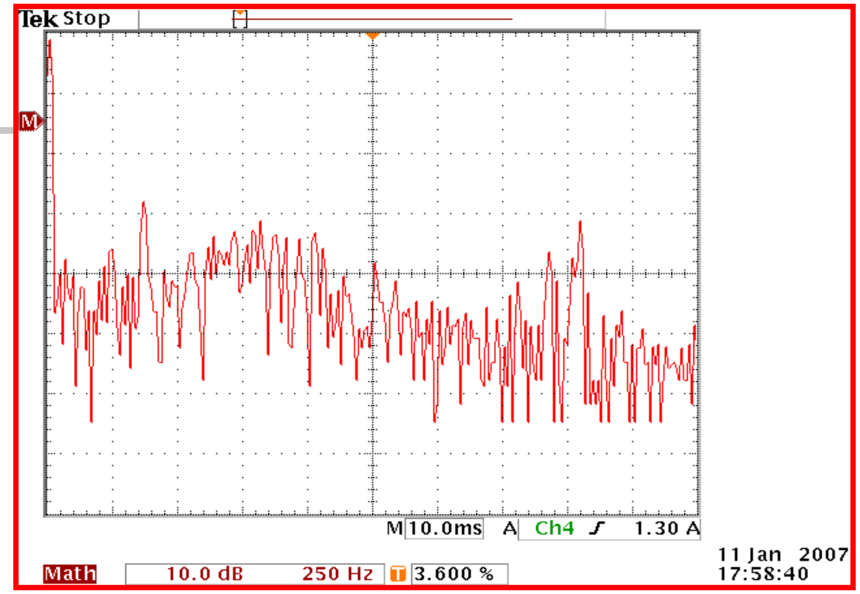

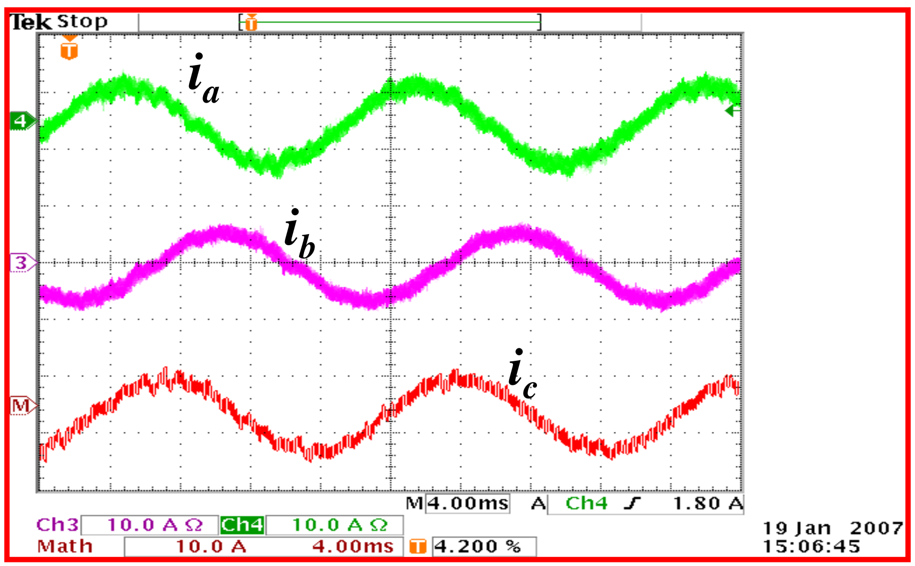

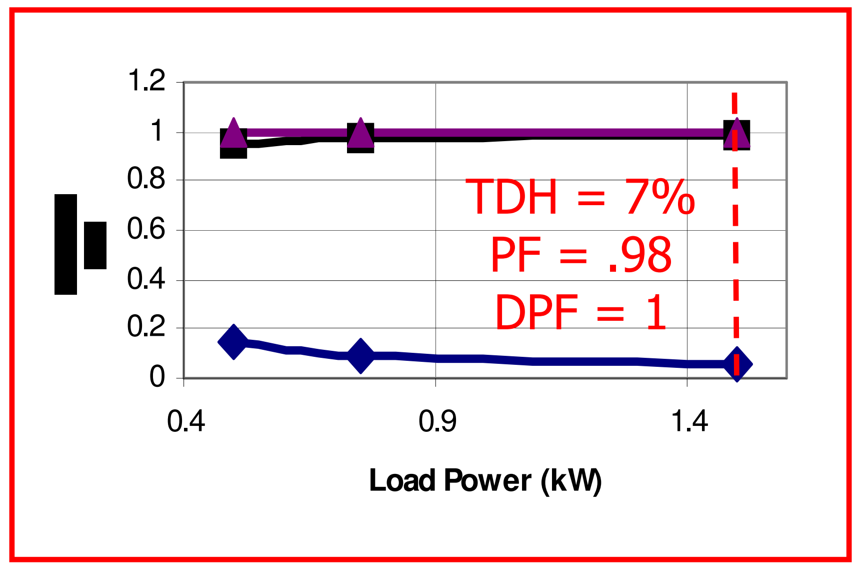

Critère	Conditions	Entités comparées	QL	NL	NLA
Efforts d'implantation	**Toutes**	**Pas de calcul (µs)**	38	39	39
		Nombre de variables mesurées	5	10	10
		Nombre de paramètres à régler	11	11	22
Performances en régime permanent	**Puissance nominale**	**THD (%)**	6	6	7
		FP	0.99	0.99	0.98
		FDP	1	1	1
	50% de la puissance nominale	**THD (%)**	7	9	13
		FP	0.98	0.97	0.96
		FDP	1	1	1
	30% de la puissance nominale	**THD (%)**	10	15	19
		FP	0.97	0.95	0.94
		FDP	1	1	1
Transitoires durant un déséquilibre de charges	**Puissance nominale $R_{dc}^- = 60\% R_{dc}^+$**	**THD (%)**	6.5	8	10
		Dépassement en tension (%)	9	0	2.3
		temps de stabilisation à ±5% (s)	1.3	0.24	0.04
	50% de la puissance nominale $R_{dc}^- = 50\% R_{dc}^+$	**THD (%)**	7	9	11
		Dépassement en tension (%)	16	0	2.5
		temps de stabilisation à ±5% (s)	4.32	140	0.05
	30% de la puissance nominale $R_{dc}^- = 30\% R_{dc}^+$	**THD (%)**	13	15	16
		Dépassement en tension (%)	40	0	4.8
		temps de stabilisation à ±5% (s)	6.24	0.2	0.08
Transitoires durant la perte d'une phase	**Puissance nominale**	**Dépassement en courant (%)**	45	33	33
		Dépassement en tension (%)	32	8	5
		temps de stabilisation à ±5% (s)	5	0.02	0.032
		Ondulation de la tension DC (%)	10.5	9.3	11

STEADY STATE PERFORMANCES

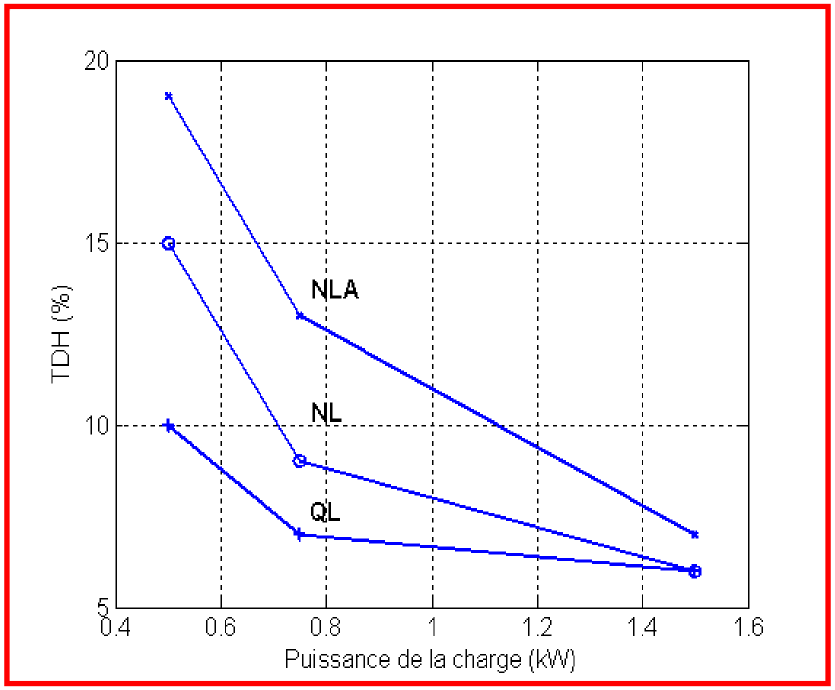

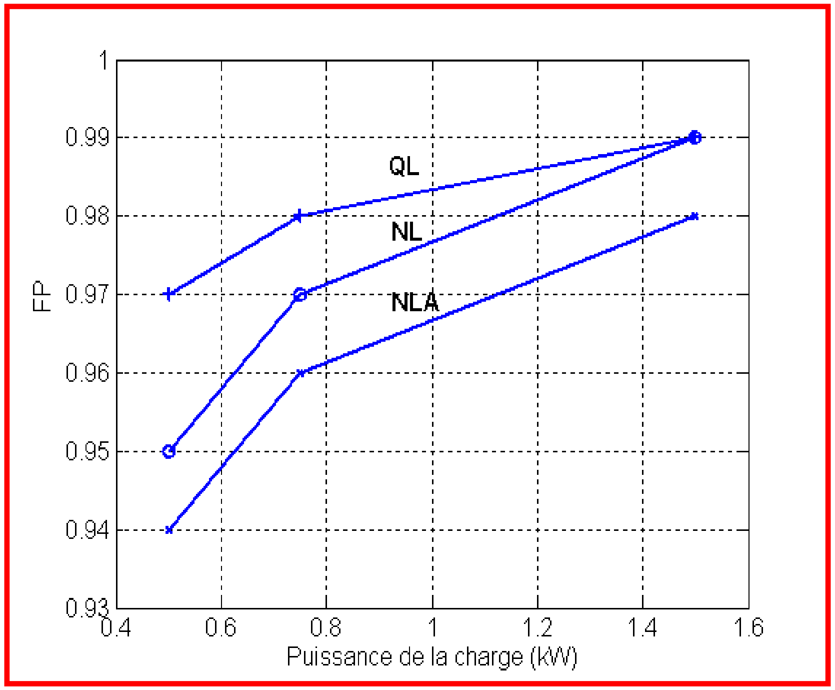

PHASE PLANE TRAJECTORIES

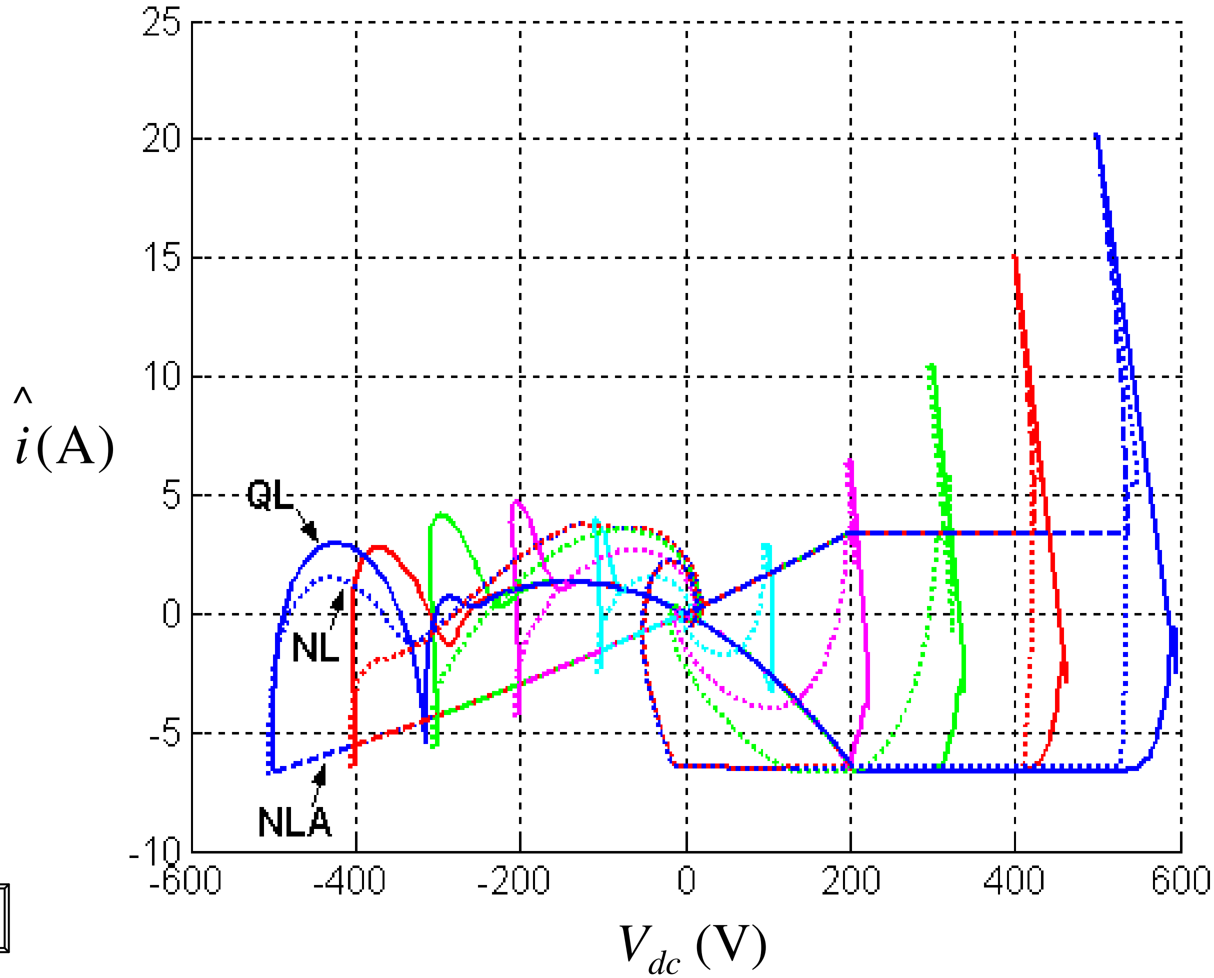

TRANSIENTS DURING DC LOADS UNBALANCE (2)

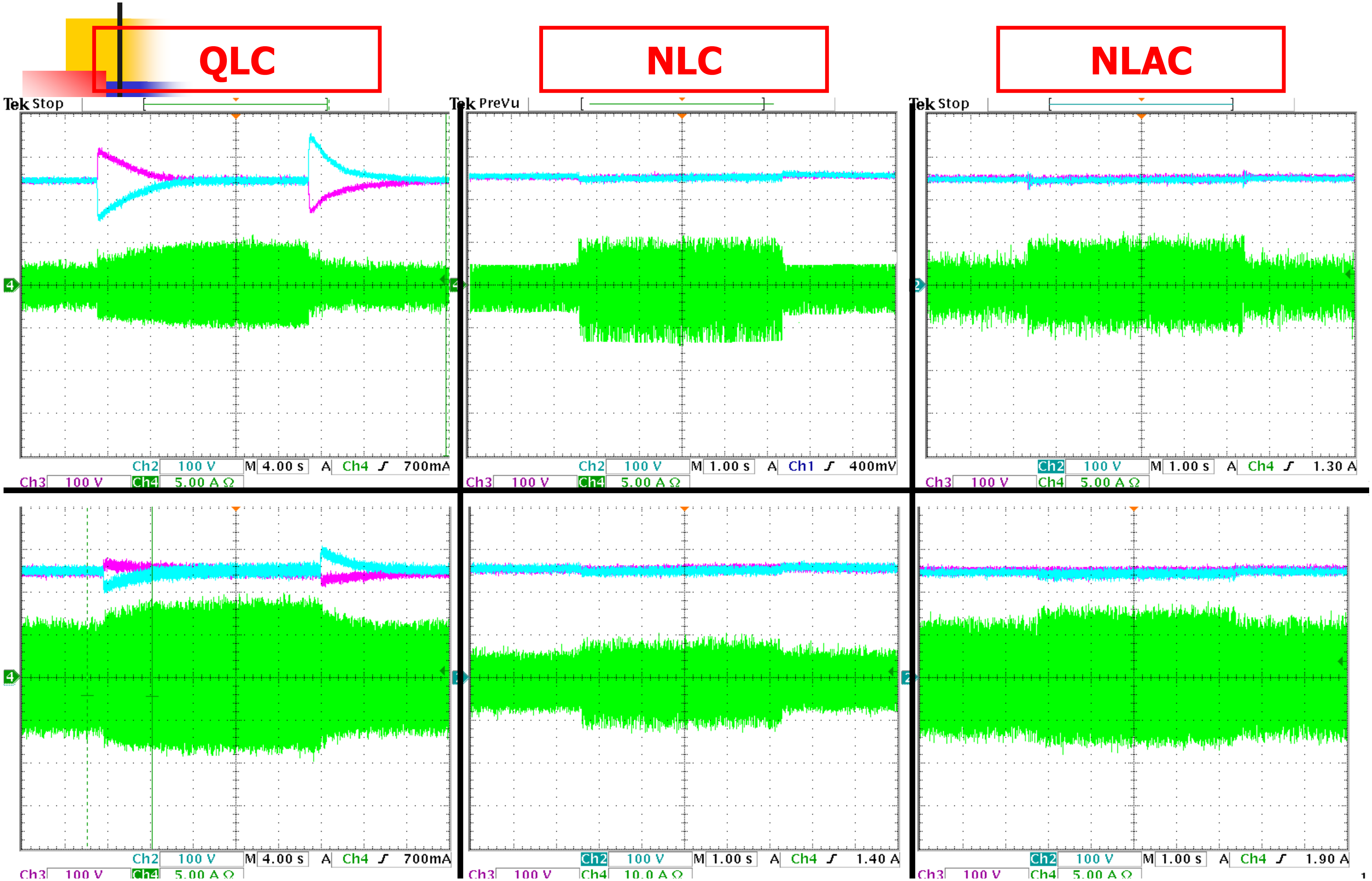

UNBALANCE OF PARTIAL DC LOADS: QLC VS NLAC

QLC

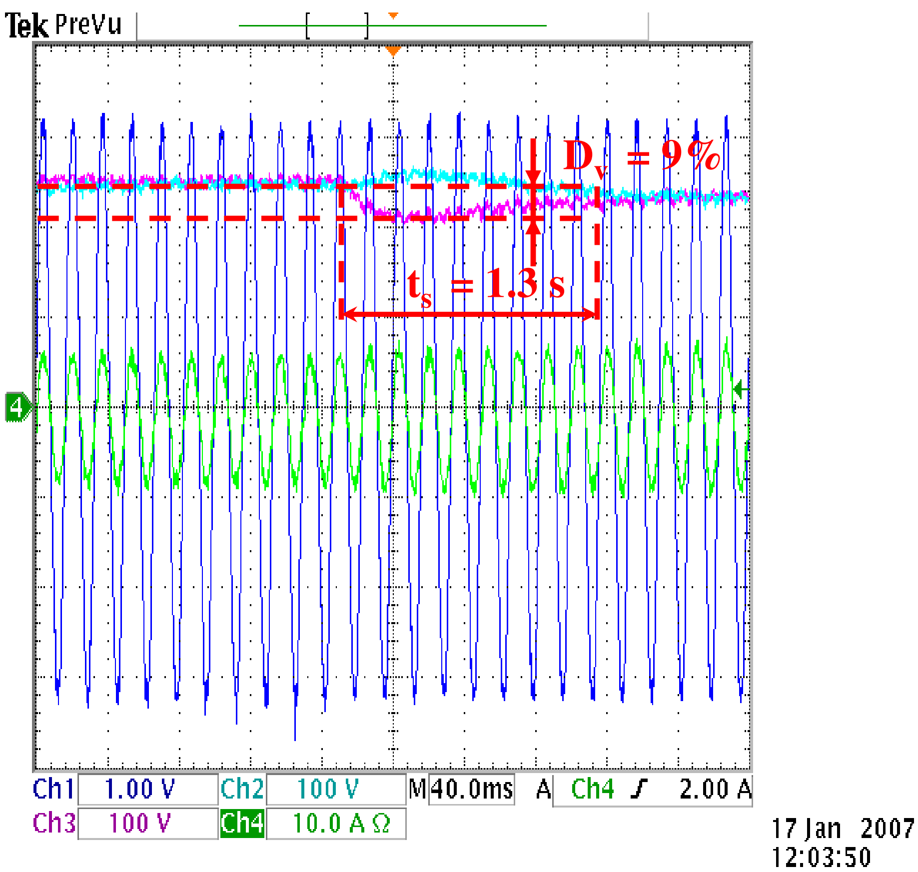

NLAC

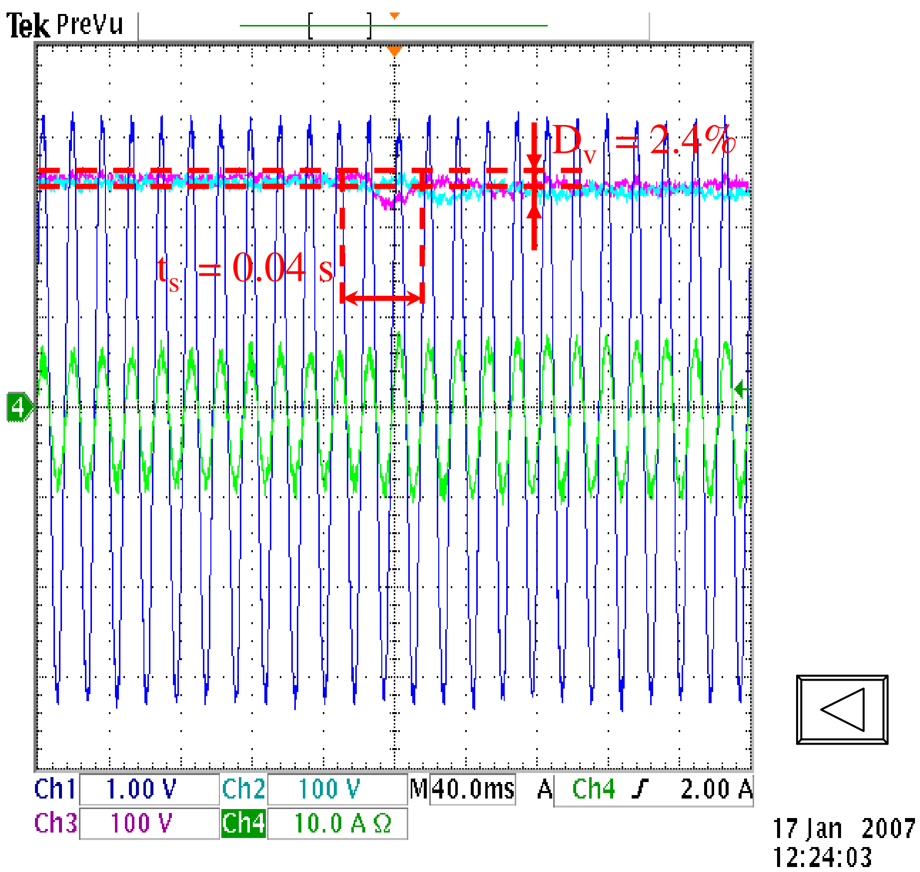

TRANSIENTS DURING A TEMPORARY LOSS OF PHASE (a)

QLC

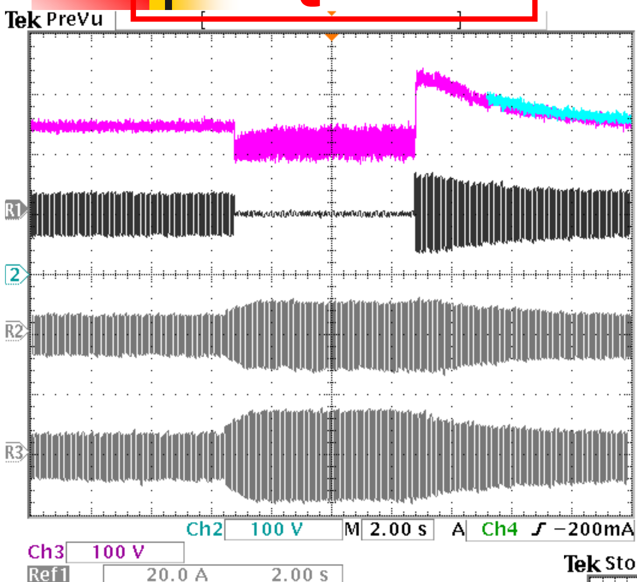

NLC

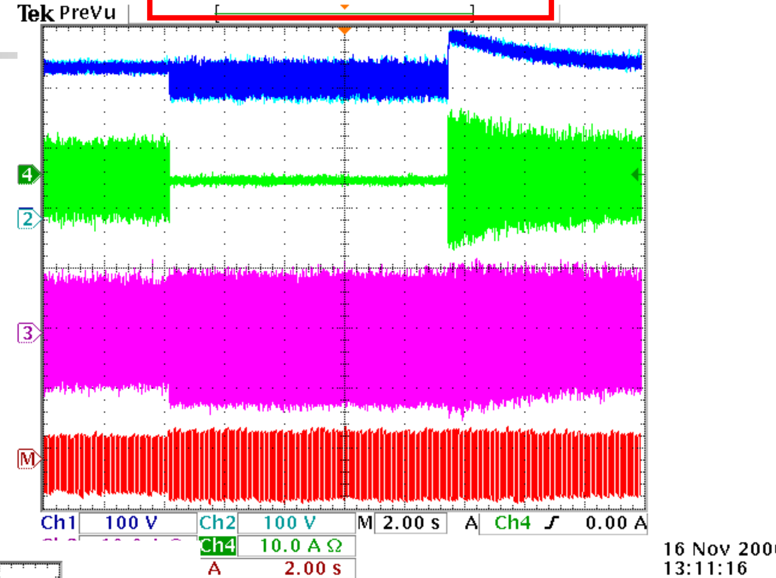

NLAC

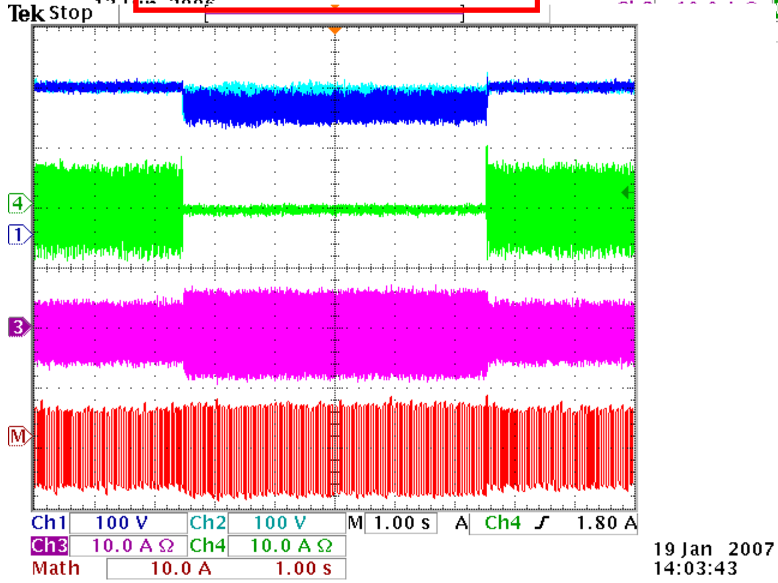

PHASE LOSS : QLC VS NLAC

QLC

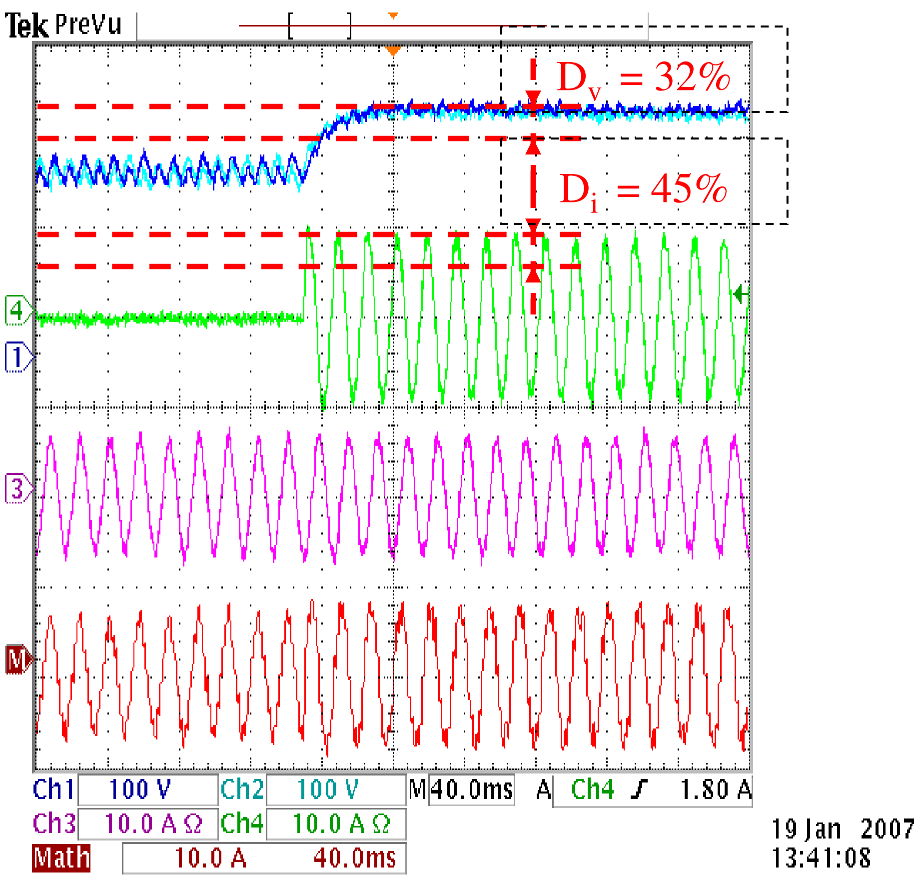

NLAC

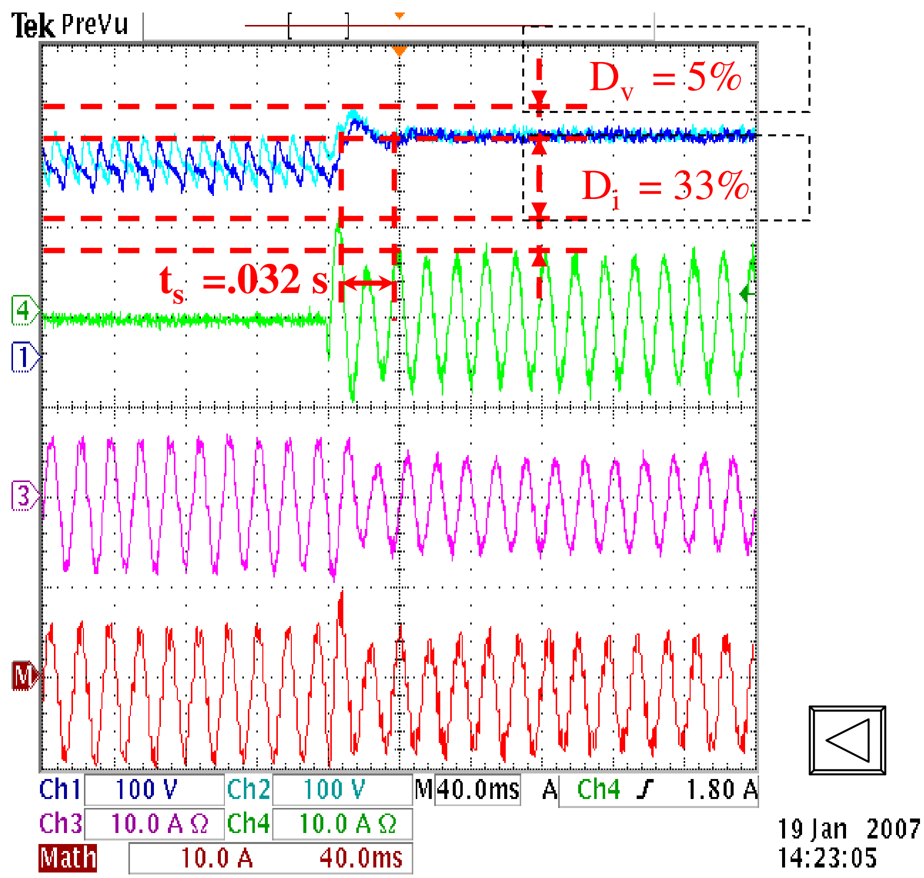

SENSORLESS CONTROL USING AN EXTENDED KALMAN FILTER

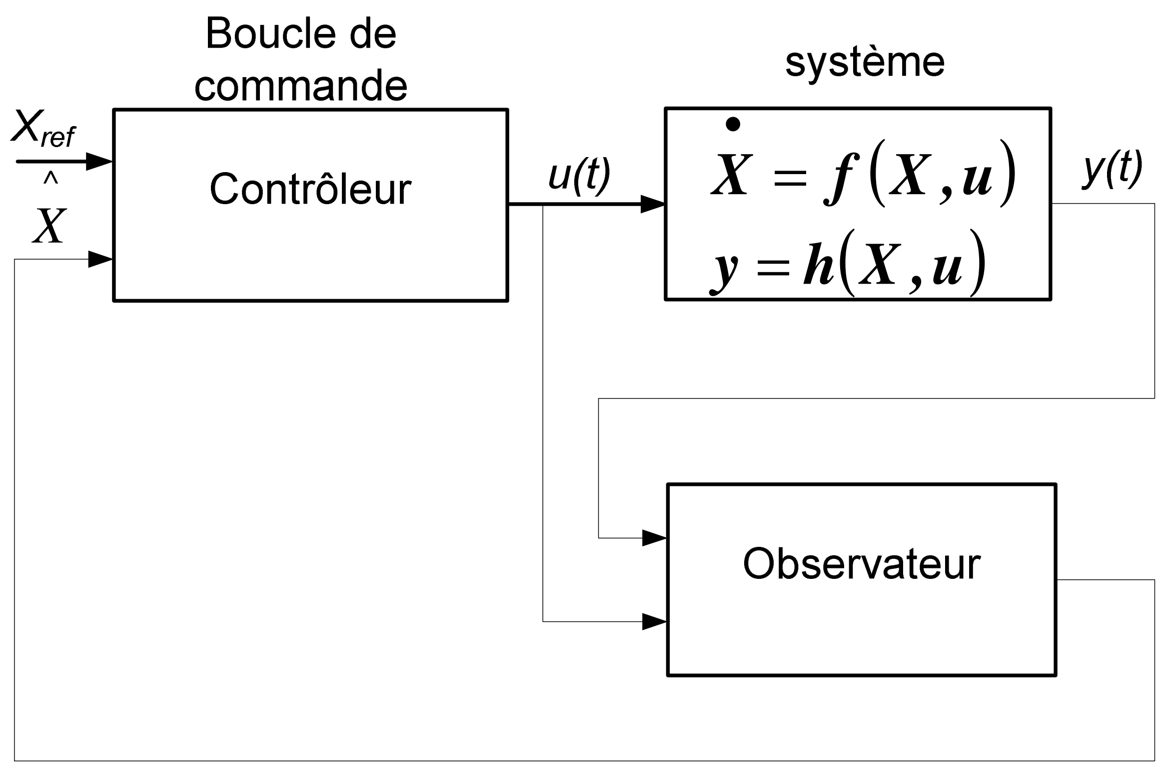

EFK EQUATIONS

$$X_e(k+1) = f_e(X_e(k), u_e(k)) + \omega_{x1}(k)$$

$$Z(k) = H_e X_e(k) + \omega_{x2}(k)$$

Extended state vector

Measure vector

Measure noise

System noise

APPLICATION TO THE VIENNA CONVERTER

$$X_e = \begin{bmatrix} i_d \\ i_q \\ \Delta v_{dc} \\ v_{dc} \\ v_d \\ v_q \end{bmatrix}$$

$$Z = \begin{bmatrix} i_d \\ i_q \end{bmatrix}$$

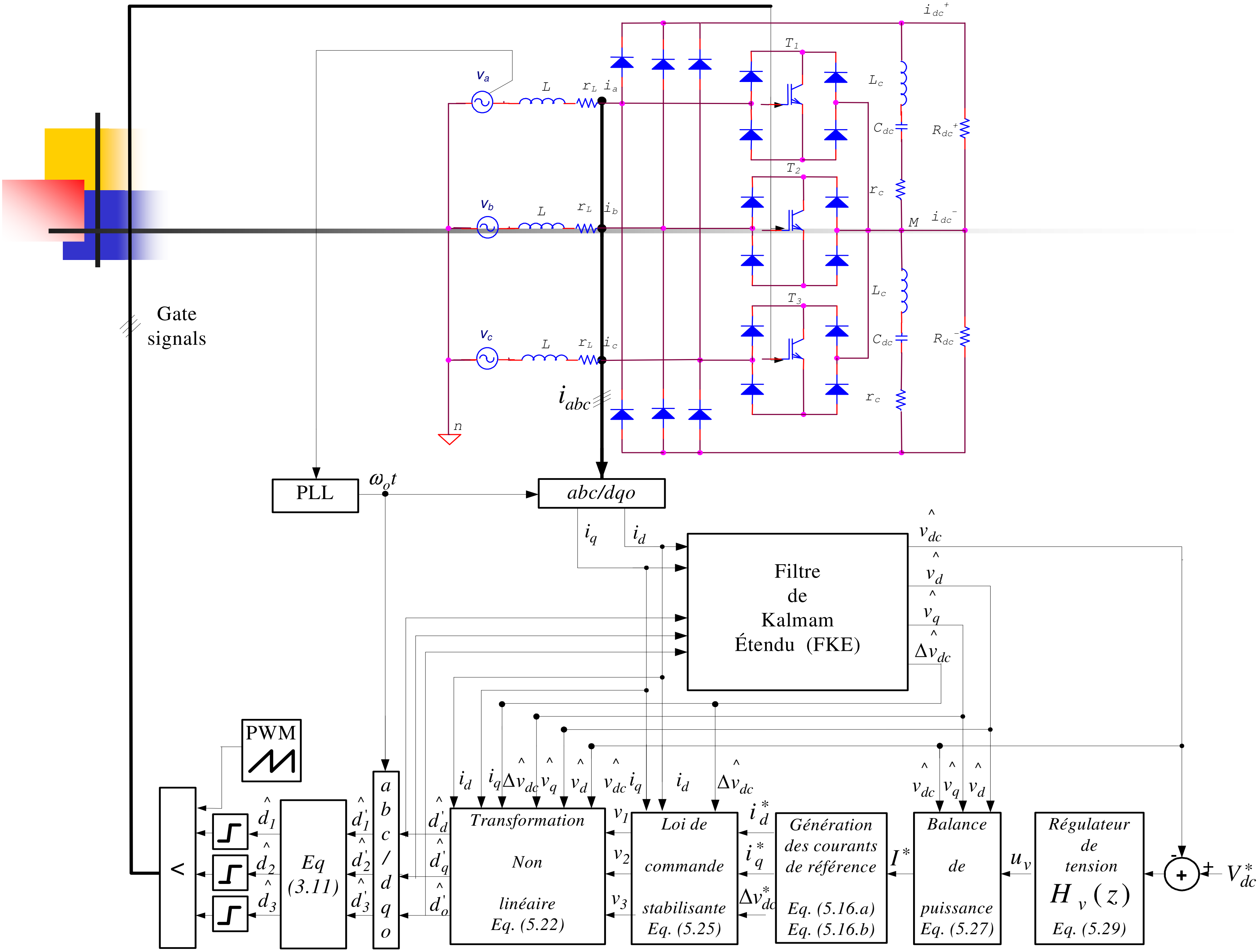

Gate
signals
PLL
$\omega_o t$
abc/dqo
i_{abc}
Filtre
de
Kalmam
Étendu (FKE)
PWM
Eq
(3.11)
a
b
c
/
d
q
o
Transformation
Non
linéaire
Eq. (5.22)
Loi de
commande
stabilisante
Eq. (5.25)
Génération
des courants
de référence
Eq. (5.16.a)
Eq. (5.16.b)
Balance
de
puissance
Eq. (5.27)
Régulateur
de
tension
$H_v(z)$
Eq. (5.29)
V_{dc}^*
u_v
I^*
i_d^*
i_q^*
Δv_{dc}^*
v_1
v_2
v_3
T_1
T_2
T_3
L_c
C_{dc}
R_{dc}^+
R_{dc}^-
r_c
M
n

ESTIMATED VARIABLES VS MEASURED VARIABLES

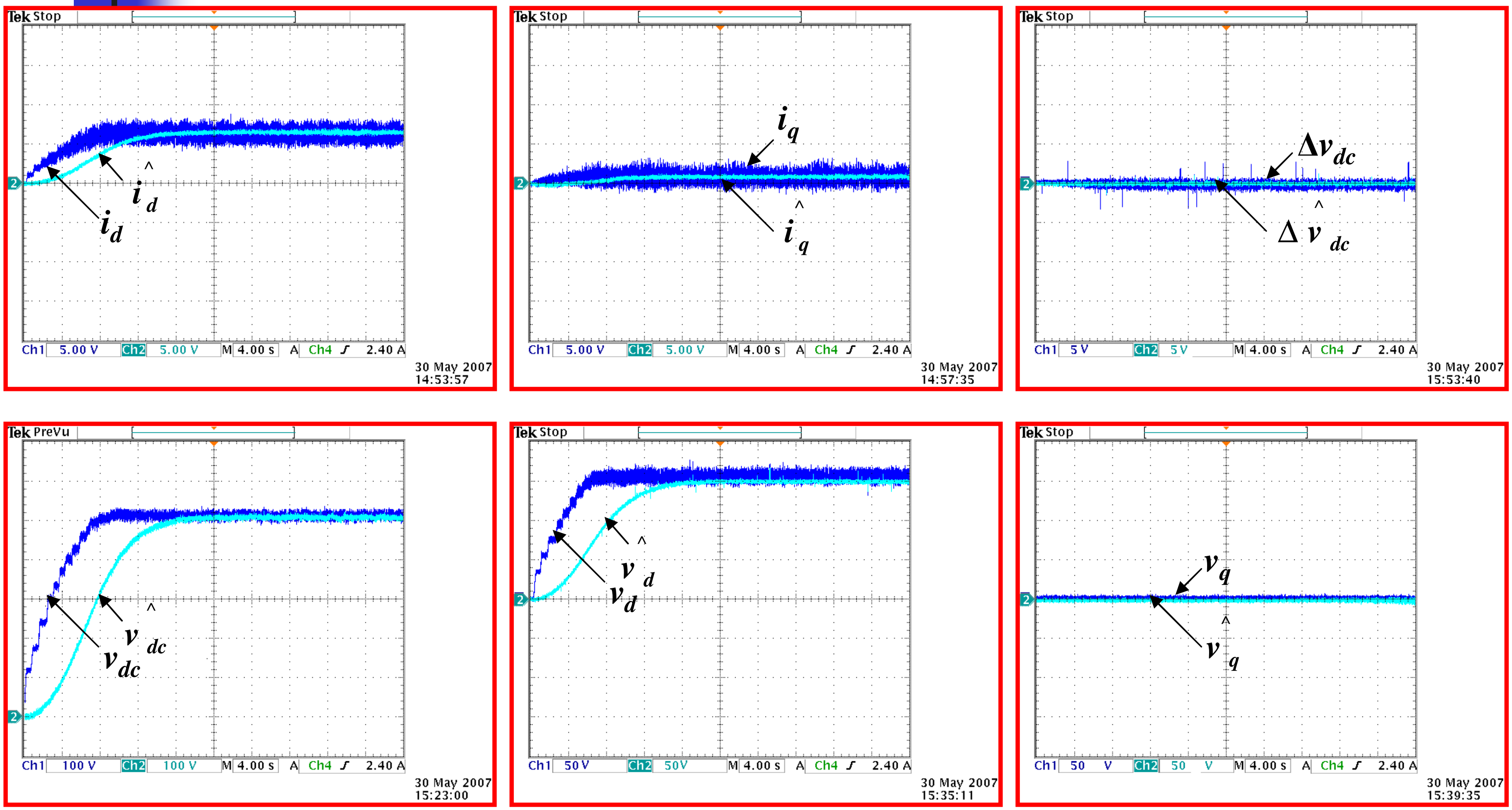

STEADY-STATE RESULTS

THD = 7%
PF = .98

⇩

THD = 9%
PF = .97

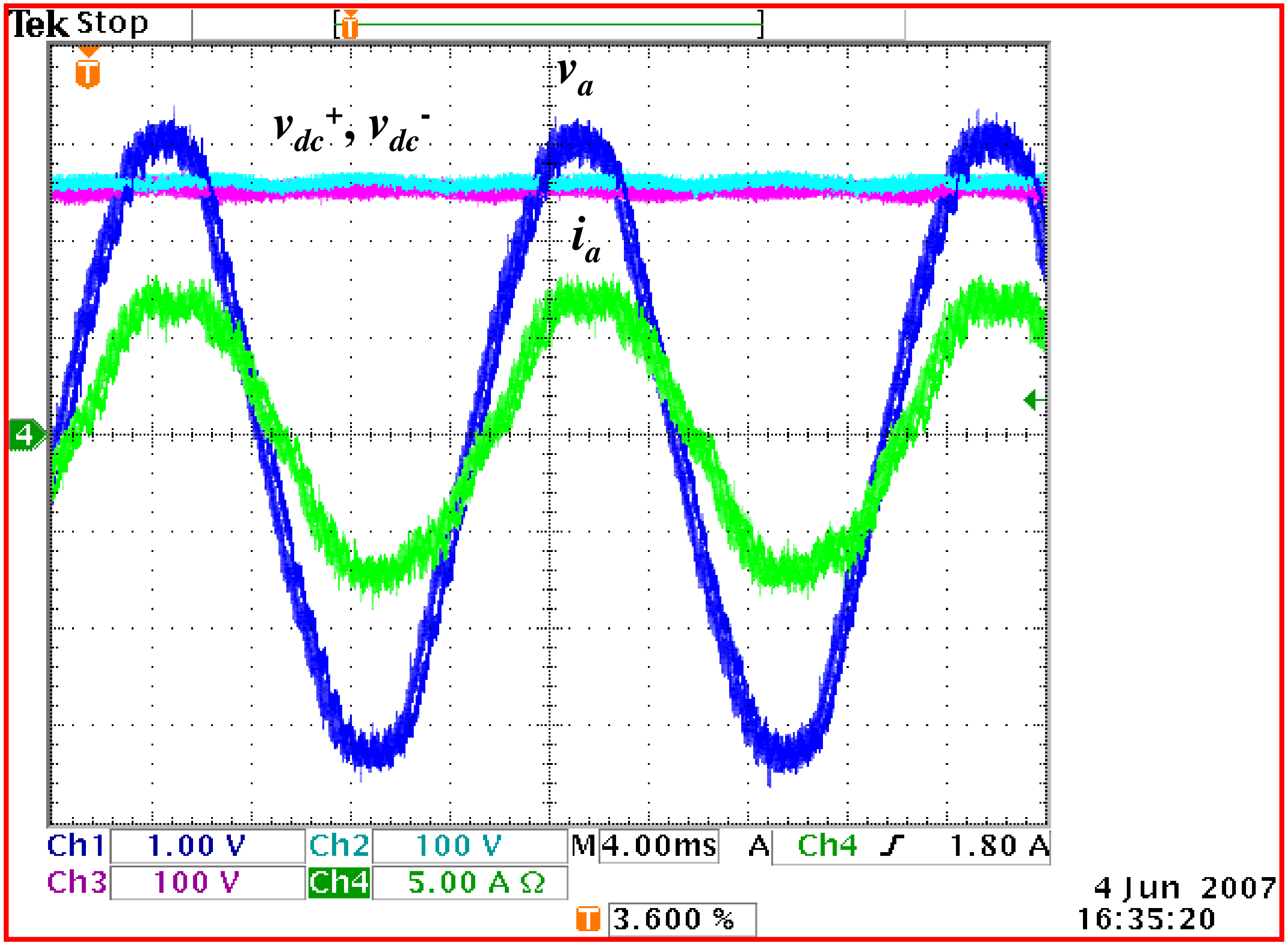

CONTRIBUTIONS (1)

1. Generalized design approach for the Vienna topology, which may be extended to different power levels and switching frequencies.

2. Complete and reliable dynamic model for the Vienna converter.

3. Identification of the converter in large and small signal regimes in the synchronous reference frame, which differs from the conventional identification procedures.

CONTRIBUTIONS (2)

4. Adaptation of the new quasi-linear control theory to the discrete systems and multi-input-multi-output systems.

5. Use of the sensorless control concept, largely used for electric machines, for the power converters.

6. Publication of 4 revue papers (IEEE transactions on Industrial Electronics (3), IEE-Electrical Power Applications (1)).

CONTRIBUTIONS (3)

6. Publication of 13 IEEE conference papers, with lecture comity (IECON (5), ELECTRIMACS (2), ISIE (2), EUROCON (1), ICIT(1), MELECON (1), IAS (1)).